Scuola Internazionale Superiore di Studi Avanzati - SISSA
International School for Advanced Studies - ISAS

Trieste, Italy

Age-dependent and tissue-related features of the cellular prion protein

Thesis submitted for the degree of "Doctor Philosophiae"

Academic Year 2009/2010

CANDIDATE
Stefano Benvegnù

SUPERVISOR
Giuseppe Legname

Declaration

The work described in this thesis has been carried out at SISSA-ISAS, Trieste, from November 2006 to October 2010.

Experiments performed in these years are included in the following publications:

Stefano Benvegnù, Ilaria Poggiolini, Giuseppe Legname (**2010**)
Neurodevelopmental expression and localization of the cellular prion protein in the central nervous system of the mouse.
*Journal of Comparative Neurology. **2010** Jun 1;518(11):1879-91.*

Stefano Benvegnù, Paola Roncaglia, Federica Agostini, Cristina Casalone, Cristiano Corona, Stefano Gustincich, Giuseppe Legname
Developmental influence of the cellular prion protein on the gene expression profile in mouse hippocampus.
*Physiological Genomics. **2011** Jun 28;43(12):711-25.*

Stefano Benvegnù, Lisa Gasperini and Giuseppe Legname
Aged PrP null mice show defective processing of neuregulins in the peripheral nervous system.
*Molecular and Cellular Neuroscience. **2011** May;47(1):28-35.*

In addition, the following publication has been published:

Benvegnù S, Franciotta D, Sussman J, Bachi A, Zardini E, Torreri P, Govaerts C, Pizzo S, Legname G. (**2009**)
Prion protein paralog doppel protein interacts with alpha-2-macroglobulin: a plausible mechanism for doppel-mediated neurodegeneration.
*PLoS One. **2009** Jun 18;4(6):e5968. PMID: 19536284*

Index

Introduction

Neurodegenerative diseases are likely to be the neurological disorders with the highest incidence in affecting the world population in the next years. Among these diseases, prion diseases are undoubtedly of prominent biological and pathological interest (Prusiner, 2001). Prion diseases are also called Transmissible Spongiform Encephalopathies, or TSEs, and they can arise with sporadic, genetic or infective etiology. The latter characteristic so far discriminates prion diseases from other neurodegenerative diseases, like Alzheimer's disease or Parkinson's disease.

Prion diseases include bovine spongiform encephalopathy (or BSE) of cattle, scrapie of sheep, chronic wasting disease (or CWD) of deer, moose and elk, and Kuru, Creutzfeldt-Jakob disease (or CJD), fatal familial insomnia (or FFI) and Gerstmann, Sträussler and Scheinker syndrome (or GSS) in humans. (Table 1, from (Aguzzi et al., 2004))

Spectrum of prion diseases of humans and animals

Prion disease	Natural host species	Etiology
sCJD	Humans	Unknown (somatic *PRNP* mutation?)
Familial Creutzfeldt-Jakob disease (fCJD)	Humans	Familial (germ line *PRNP* mutation)
Iatrogenic Creutzfeldt-Jakob disease (iCJD)	Humans	Surgical procedures (infection)
vCJD	Humans	Ingestion of BSE-contaminated food; transfusion medicine (infection)
Kuru	Humans	Ingestion, ritualistic cannibalism (infection)
Fatal Familial Insomnia (FFI)	Humans	Familial (germ line *PRNP* mutation)
Gerstmann-Sträussler-Scheinker Syndrome	Humans	Familial (germ line *PRNP* mutation)
Scrapie	Sheep, goats	Infection, natural; mode of transmission unclear
Chronic Wasting Disease (CWD)	Deer, Elk	Infection; mode of transmission unclear
BSE	Cattle	Ingestion of BSE-contaminated feed (infection)
Transmissible mink encephalopathy	Mink	Ingestion (infection); Origin unclear
Feline spongiform encephalopathy	Cats	Ingestion of BSE-contaminated feed (infection)
Spongiform encephalopathy of zoo animals	Zoologic bovids, primates	Ingestion of BSE-contaminated feed (infection)

Table 1. Spectrum of prion diseases of humans and animals (from Aguzzi et al., 2004)

Prion diseases affect primarily the nervous system. The clinical features of TSEs vary dramatically according to the different form of prion diseases affecting the individual (Collins et al., 2004). These differences regard the etiology (whether sporadic, genetic

or infective), the incidence of the disease, the region of the brain mainly affected by the deposition of replicating prions, the clinical symptoms manifested by the affected individual, the time-course of the disease (Prusiner, 1992, Prusiner and DeArmond, 1994). However, they all share common pathological traits and are characterized by a widespread spongiform neurodegeneration (which results in the "spongy", vacuolated appearance of the brain), neuronal loss and diffuse astrocytic gliosis (Figure 1) (Masters and Richardson, 1978). All prion diseases are fatal, progressive and without cure at present.

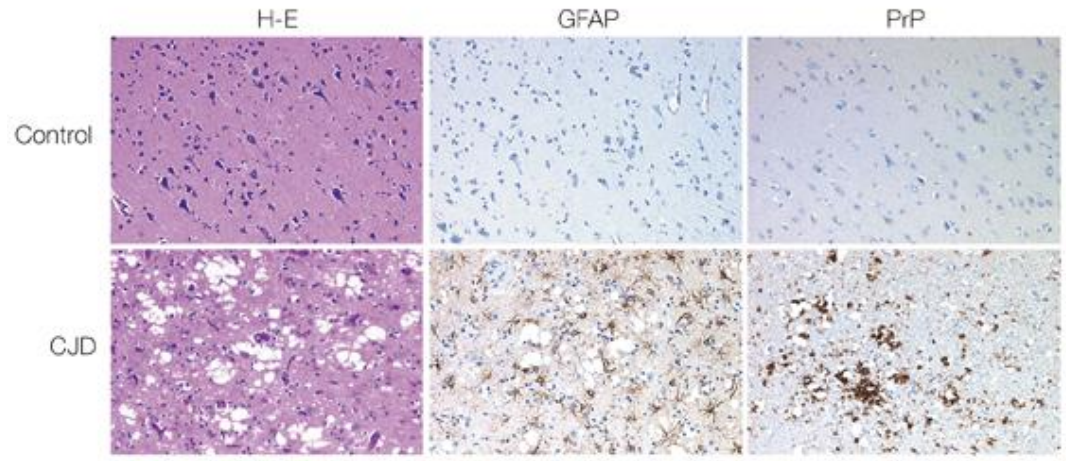

Figure 1. Neuropathological features of transmissible spongiform encephalopathies.
Histological and immunohistochemical analysis of frontal cortex samples from the brain of a patient who died of non-cerebral causes (upper row) and of a patient suffering from CJD (lower row). Brain sections were stained with hematoxylin-eosin (H-E, left panels), with antibodies against glial fibrillary acidic protein (GFAP, middle panels) and with antibodies against the prion protein (PrP, right panels). Neuronal loss and prominent spongiosis are visible in the H-E stain. Strong proliferation of reactive astrocytes (gliosis) and perivacuolar prion protein deposits are detectable in the GFAP and PrP immunostains of the CJD brain samples (from Aguzzi et al., 2001).

Prion concept

The term "prion" was coined in 1982 (Prusiner, 1982) to highlight the solely proteinaceous property of the causative, infective agent of these diseases. Indeed, the resistance to inactivation of the scrapie agent to by the most widely diffused methods against viral particles (such as ionizing radiation, UV exposure, formalin and heat

treatment) (Alper et al., 1966, Alper et al., 1967) and, on the contrary, the reduction of the infectivity of inoculated brain extracts only after proteolytic treatments, led Stanley B. Prusiner to formulate the "protein-only hypothesis" (Prusiner, 1982). According to his hypothesis, the infective particle responsible for scrapie disease is primarily composed of a protein which is capable of transmitting infection and replicating without the need of nucleic acids. This protein was identified as a protein of about 27-30 kDa (PrP^{Sc}) and is the only molecule that co-purifies with infectivity after protease digestion of brain extracts of ill hamsters (Bolton et al., 1982). The subsequent sequencing of the prion protein (PrP) allowed the identification of an endogenous cellular gene (in mice *Prnp*), whose translated product was called the cellular PrP, or PrP^{C} (Oesch et al., 1985). This finding showed that the PrP is encoded by a chromosomal gene, and not by a nucleic acid in the infectious scrapie prion particle. In humans this gene (*PRNP*) is on chromosome 20, and in mice maps on chromosome 2. According to the protein-only hypothesis, prions are formed by a posttranslational conformational remodeling event in which PrP^{C} is converted into the disease-associated infectious form (PrP^{Sc}). The cellular form and the scrapie form of the PrP show peculiar different biochemical characteristics: PrP^{C} has a high α-helix content (40% of the protein) and relatively little β-sheet (3% of the protein), while on the contrary PrP^{Sc} contains 30% α-helix and 45% of β-sheet (Caughey et al., 1991; Gasset et al., 1993). Two main models of conversion of PrP^{C} into PrP^{Sc} have been postulated: the "template-assisted" model and the "nucleation" model (Figure 2) (Aguzzi et al., 2001).

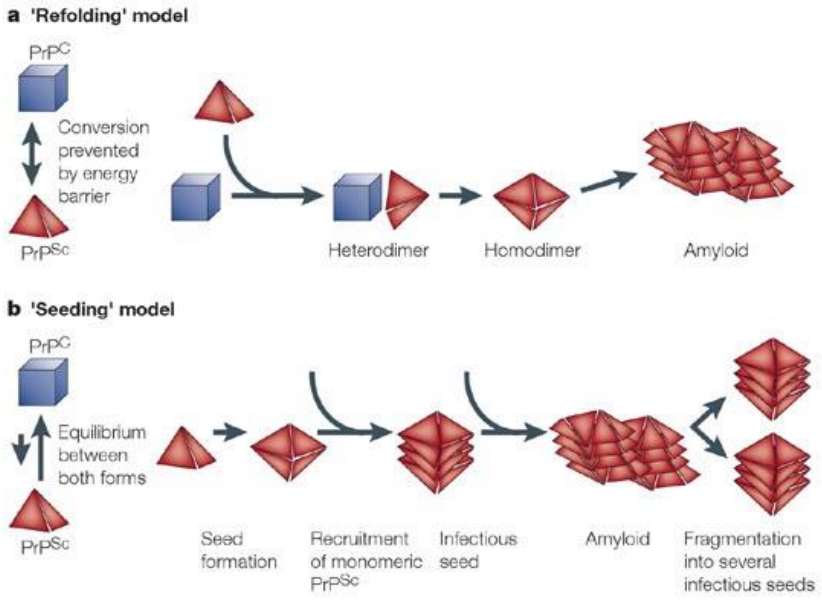

Figure 2. The 'protein-only' hypothesis and two popular models for the conformational conversion of PrP^{C} into PrP^{Sc} (from Aguzzi et al., 2001).
a. The 'refolding' or template-assistance model postulates an interaction between exogenously introduced PrP^{Sc} and endogenous PrP^{C}, which is induced to transform itself into further PrP^{Sc}. A high-energy barrier might prevent spontaneous conversion of PrP^{C} into PrP^{Sc}. b. The 'seeding' or nucleation–polymerization model proposes that PrP^{C} and PrP^{Sc} are in a reversible thermodynamic equilibrium. Only if several monomeric PrP^{Sc} molecules are mounted into a highly ordered seed can further monomeric PrP^{Sc} be recruited and eventually aggregate to amyloid. Within such a crystal-like seed, PrP^{Sc} becomes stabilized. Fragmentation of PrP^{Sc} aggregates increases the number of nuclei, which can recruit further PrP^{Sc} and thus results in apparent replication of the agent. In sporadic prion disease, fluctuations in local PrP^{C} concentration might — exceedingly rarely — trigger spontaneous seeding and self-propagating prion replication.

According to the template-assisted model (or refolding model) (Figure 2a), a high energy barrier is preventing the conversion from PrP^{C} to PrP^{Sc}, therefore the need of an exogenously introduced PrP^{Sc} molecule is necessary for the replication to start: PrP^{Sc} interacts with and converts an endogenous molecule of PrP^{C} into a newly formed, β-sheet rich PrP^{Sc} isoform. The newly formed PrP^{Sc} molecule, in turn, can convert other endogenous PrP^{C} molecules. According to the nucleation model (or polymerization model) (Figure 2b), PrP^{C} and PrP^{Sc} are in a reversible thermodynamic equilibrium, which strongly favours the cellular (PrP^{C}) conformation. Only when several molecules of PrP^{Sc} are aggregated (into oligomeric or fibril-like seeds), the replication can start. In this case, the seed recruits other monomeric PrP^{Sc} molecules and stabilizes them. The

fragmentation of the aggregates increases the number of seeds that can actively recruit new PrP^{Sc} molecules, thus accelerating the replication process, the prion accumulation, and finally giving rise to the disease. These two models are not to be considered mutually exclusive, and indeed the different etiology of prion diseases (infective, sporadic or genetical) can be fitted in both the models. In inherited prion diseases, genetic mutation of the *PRNP* gene may destabilize the tertiary structure of PrP^{C} promoting the spontaneous conversion to PrP^{Sc}, or these mutations can lower the energy barrier from PrP^{C} to PrP^{Sc}, thus facilitating and accelerating PrP^{Sc} aggregation. In infective disease, the ingestion of an already preformed PrP^{Sc} aggregate can directly convert endogenous PrP^{C} molecules, or act as an already preformed PrP^{Sc}-aggregate and recruit PrP^{Sc} molecules. In sporadic TSEs, biochemical modifications (whose characteristics are at present unknown) of PrP^{C}, or other environmental aspects, can perturb PrP^{C} tertiary structure and then favour the conversion into PrP^{Sc}. However, if and what biochemical and environmental mechanisms are at the basis of sporadic TSEs is yet to be clarified (Prusiner, 1991, 1994).

How do prions exert their neurotoxic effects?

Once PrP^{Sc} is formed, replicating and accumulating in the body and in the brain of the individual affected (Fig. 3) (Soto and Satani, 2010), the cellular pathological mechanisms by which prion exert their neurotoxic effects are still under debate.

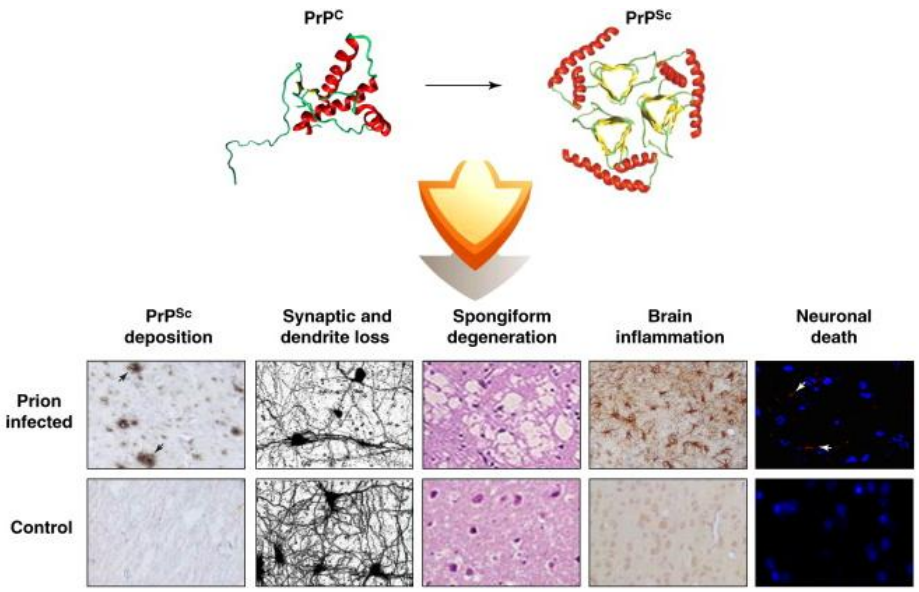

Figure 3. Multiple neurodegenerative pathways are implicated in TSEs. The conversion of the natively folded PrP^{C} to PrP^{Sc} triggers disease. The structure of PrP^{C} corresponds to the experimentally determined tridimensional conformation of the protein by nuclear magnetic resonance and the structure of PrP^{Sc} corresponds to a model based on low resolution techniques. Abnormalities in the brain of infected individuals include the accumulation of PrP^{Sc} deposits, synaptic damage and dendrite loss, spongiform degeneration, brain inflammation and neuronal death. PrP^{Sc} deposition was determined after immunohistochemical staining with anti-PrP antibodies (black arrowheads). Dendrites were labeled by Golgi–silver staining to illustrate the substantial decrease on dendrites and synaptic connections in prion-infected animals. Spongiform degeneration was evaluated after hematoxylin and eosin staining. Astrogliosis (brain inflammation) was detected by immunohistochemical staining of reactive astrocytes with an anti-GFAP (glial fibrillary acidic protein) antibody. Apoptosis was detected by staining with caspase-3 antibody (red indicated by white arrowheads) and DAPI (4′,6-diamidino-2-phenylindole, blue) staining of nucleus. For each stain, images from prion-infected animals (upper) and controls (lower) are shown (from Soto and Satani 2010).

The disease-causing PrP^{Sc} induces cell death both *in vitro* e *in vivo*, for which microglial activation and glial reactivity appear to be instrumental (Collins et al., 2004). Thus, in this perspective, prion diseases are believed to be a gain-of-(toxic)-function consequence of the formation of PrP^{Sc}. However, mice devoid of PrP are resistant to scrapie upon prion inoculation (Büeler et al., 1993), and this finding seems in favour of a loss-of-function mechanism. Indeed, further studies show that accumulation of PrP^{Sc} within PrP^{C}-expressing tissue grafted into the brains of $Prnp^{0/0}$ mice does not damage the neighboring PrP^{C}-null tissue (Brandner et al., 1996), and the accumulation of PrP^{Sc} in glial cells around PrP^{C}-null neurons does not induce cell death in the knockout

neurons, also arguing against a direct toxic effect of PrP^{Sc} *per se* (Mallucci et al., 2002, 2003; Mallucci and Collinge, 2004). However, the lack of striking phenotypes and the absence of neurodegeneration and spongiform changes in the brain of mice ablated for PrP (Büeler et al., 1992), also after postnatal depletion (Mallucci et al., 2002), is controversial with a loss-of-function mechanism. Thus, the mechanisms responsible for prion diseases are not probably to be linked to the direct loss of the cellular PrP *per se*, but to the perturbation of the neurochemical systems that are associated to PrP^{C} expression and functions. However, the physiological function(s) of PrP^{C} is (are) still unknown, and a lot of controversies surrounding the several proposed functions of PrP^{C} are still under debate.

PrP^{C}

The cellular form of the PrP, PrP^{C}, is a host-encoded protein. In humans, PrP^{C} is a 253 amino acids protein, which has a molecular weight of 35-36 kDa. It has two hexapeptides and repeated octapeptides at the N-terminus, a disulphide bond, and it is anchored at extracellular part of the cell membrane through a glycosylphosphatidyl inositol (GPI) anchor (Figure 4) (Chesebro and Caughey, 1993; Caughey and Baron, 2006).

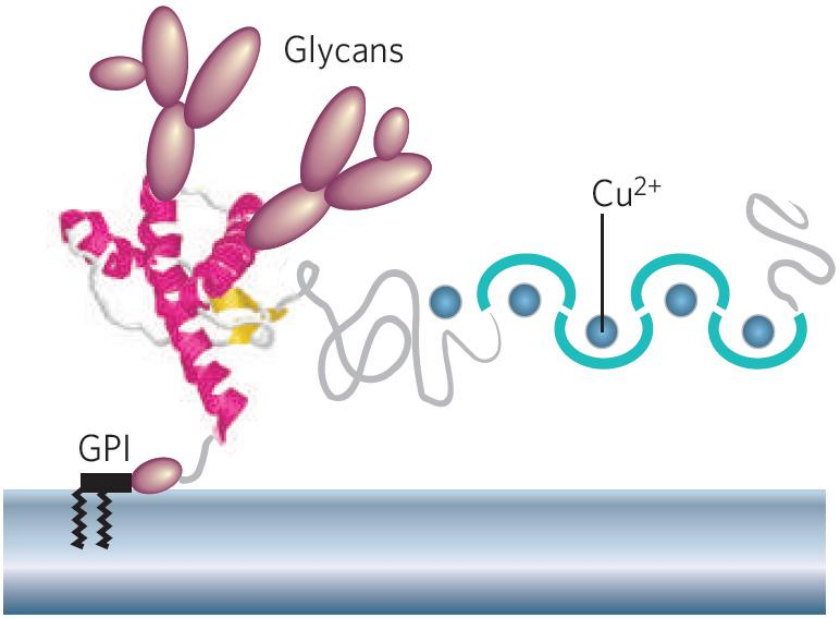

Figure 4. Mature form of the cellular prion protein, PrP^C. PrP^C is a GPI-anchored membrane protein, with a flexible, random coil N-terminus and a globular C-terminal domain. The N-terminal domain of PrP^C contains octapeptide repeats (in light blue), which can bind divalent cations such as copper ions. The C-terminal domain of PrP^C contains three alpha-helices (in pink) and an antiparallel β-pleated sheet formed by two β-strands (in yellow). PrP^C can be found non-, mono-, or diglycosylated forms (from Caughey and Baron, 2006).

The preprotein PrP^C is produced as a precursor protein of ~230 amino acids containing two signals peptides. The ~22 amino acids peptide at the N-terminus targets the protein to the endoplasmic reticulum (ER), while the ~23 amino acid sequence at the C-terminus is essential for the addition of the GPI moiety. Following the removal of the signal peptides, most of mammalian PrP^C is exported to the cell surface as a mature protein of 208-209 amino acids (Stahl et al., 1987). PrP^C contains two moieties of roughly the same length, an NH_2-terminal flexible region, and a COOH-terminal globular domain of about another 100 amino acids. The globular domain of human PrP^C is arranged in three α-helices corresponding to amino acids 144–154, 173–194, and 200–228, interspersed with an antiparallel β-pleated sheet formed by β-strands at residues 128–131 and 161–164. A single disulfide bond is found between cysteine residues 179 and 214. The N-terminal domain contains the repeated octapeptides, termed OR, preceded and followed by two positively charged charge clusters, CC_1 (amino acids 23–27) and CC_2 (amino acids 95–110).

The N- and C- domains are linked by a hydrophobic stretch of amino acids [amino acids 111–134, also termed hydrophobic core (HC)] (Figure 5) (Zahn et al., 2000; Aguzzi and Calella, 2009).

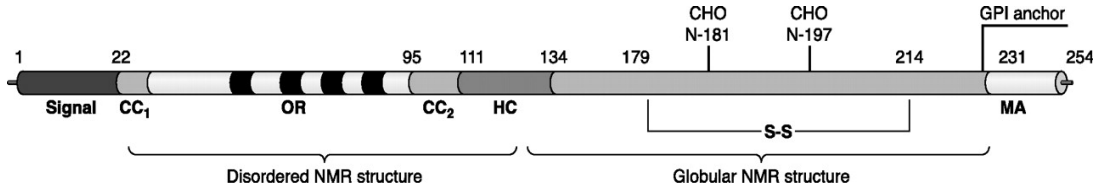

Figure 5. Outline of the primary structure of the cellular prion protein including posttranslational modifications. A secretory signal peptide resides at the extreme NH_2 terminus. CC_1 and CC_2 define the charged clusters. OR indicates the octapeptide repeat, and four are present. HC defines the hydrophobic core. MA denotes the membrane anchor region. S-S indicates the single disulfide bridge, and the glycosylation sites are designated as CHO. The numbers describe the position of the respective amino acids (from Aguzzi and Calella, 2009).

The octapeptide repeats can coordinate Cu^{2+} ions in cooperative fashion with high affinity, and display weaker binding properties towards other divalent cations, such as Zn^{2+}, Fe^{2+}, Mn^{2+} and Ni^{2+} (Stöckel et al., 1998).

The protein PrP^C is found in un-, mono-, or di-glycosylated forms, corresponding to the variable occupancy of residues Asn-181 and Asn-197 in human PrP^C and Asn-180 and Asn-196 in mice (Haraguchi et al., 1989).

PrP^C subcellular localization and trafficking

PrP^C and membrane localization

During its normal life cycle almost all PrP^C is anchored to the cell surface by a GPI-anchor (Taylor and Hooper, 2006). Similarly to other GPI-anchored proteins, PrP^C

molecules are found attached to low-density, detergent-insoluble membrane domains (DRMs or lipid rafts), rich in cholesterol and sphingolipids (Naslavsky et al., 1997; Taylor and Hooper, 2006).

The association with DRMs appears to control the distribution of mature PrP^C among very distinct regions of the plasma membrane, as shown by the extensive redistribution of PrP^C at the surface of cultured neurons upon cholesterol or sphingolipid depletion (Taraboulos et al., 1995; Galvan et al., 2005). However, controversial findings have been reported as both of the nature of PrP^C-containing rafts as well as of the distribution of PrP^C between raft and non-raft membrane domains.

PrP^C trafficking

PrP^C is translocated to the endoplasmic reticulum (ER) due to the presence of an N-terminal signal peptide that is then cleaved into the ER lumen. The GPI anchor is also added in the ER, after removal of a C-terminal peptide signal. The core GPI anchor added to the immature PrP^C is then processed (Stahl et al., 1987). Association of PrP^C to lipid rafts starts early within the ER, and the maturation of the protein proceeds along the ER-Golgi-plasma membrane pathway accompanied by association with distinct membrane rafts (Sarnataro et al., 2004; Campana et al., 2005).

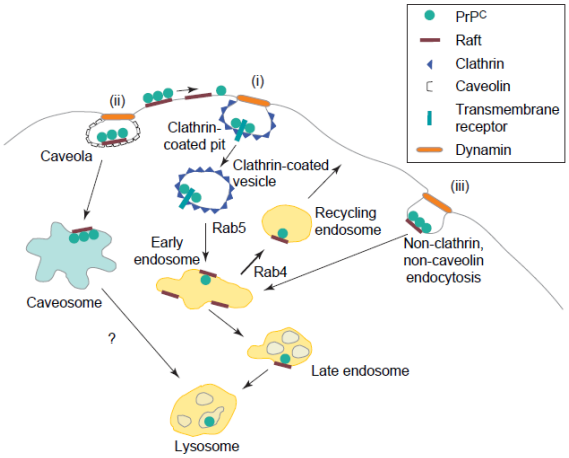

Figure 6. Pathways of PrP^C internalization. At the plasma membrane, PrP^C can be constitutively internalized and its endocytosis can be increased by extracellular copper ions (not shown). The main pathway of PrP^C internalization in neuronal cells seems to depend on clathrin-mediated endocytosis (i). Caveolin-related endocytosis and trafficking have been implicated in PrP^C transport in Chinese hamster ovary and glial cells (ii). Rab5-positive endosomes and recycling endosomes involving Rab4 have also been implicated in the endocytic transport of PrP^C. Finally, non-clathrin and non-caveolin but raft-dependent endocytosis has been proposed to participate in the internalization and conversion of prion protein (iii). (from Campana et al., 2005)

Results of cholesterol depletion also suggested that raft association is required for correct folding of PrP^C (Sarnataro et al., 2004), as well as for the export of the protein to the Golgi apparatus and for proper glycosylation (Sarnataro et al., 2004; Campana et al., 2005).

The glycosylation patterns of PrP^C may also affect protein trafficking and biophysical features (Cancellotti et al., 2005).

The mechanism of PrP^C internalization is still controversial because both raft/caveolae or caveolae-like (Vey et al., 1996; Kaneko et al., 1997; Marella et al., 2002; Peters et al., 2003) as well as clathrin-dependent endocytosis may be operative (Shyng et al., 1994; Taylor et al., 2005) (Figure 6).

PrP^C expression pattern

The protein PrP^C is highly abundant in the developing and in the mature nervous system, where it is expressed in neuronal and glial cells. Its expression content varies among distinct brain regions, among differing cell types, and among neurons with distinct neurochemical phenotypes (Linden et al., 2008). However, some controversial findings are reported, regarding the cellular localization: cell body, axonal, dendritic, synaptic compartment. Moreover, as for the latter, conflicting results were reported as to whether PrP^C resides in either or both pre- and postsynaptic components (see for reference (Linden et al., 2008)). Finally, some discrepancies between the correlation level of PrP mRNA and PrP^C protein were reported (Ford et al., 2002). Multiple technical and biological reasons may account for these controversial findings, like the usage of different monoclonal or polyclonal antibody, the different experimental tissue fixation, the continuous trafficking and turnover of PrP^C, the degree of surface exposure of PrP^C, to species differences, or to technical artefacts.

The protein PrP^C has been shown to be expressed starting from early embryonic development, and to be developmentally regulated (Mobley et al., 1988; Lazarini et al., 1991; Manson et al., 1992; Salès et al., 2002; Tremblay et al., 2007). In the brain, the levels of the PrP expression increases during the first postnatal weeks till the completion of synaptogenesis, and then remain stable at plateau during adulthood, with a slight decrease of the level of expression in aged animals (Salès et al., 2002). In particular, its levels of expression are high in the olfactory bulb and in the hippocampus, which are regions known to have ongoing neuronal renewal also during adult life (Salès et al., 2002).

PrP functions

The protein PrP^C has been linked to several cellular processes in the nervous system. These processes include neuronal survival, neurite outgrowth, synapse formation, maintenance, and function, and maintenance of myelinated fibers (reviewed in (Aguzzi et al., 2008)) (Figure 7). Table 2 (from (Caughey and Baron, 2006)) summarizes all the cellular processes in which PrP^C is demonstrated to be involved.

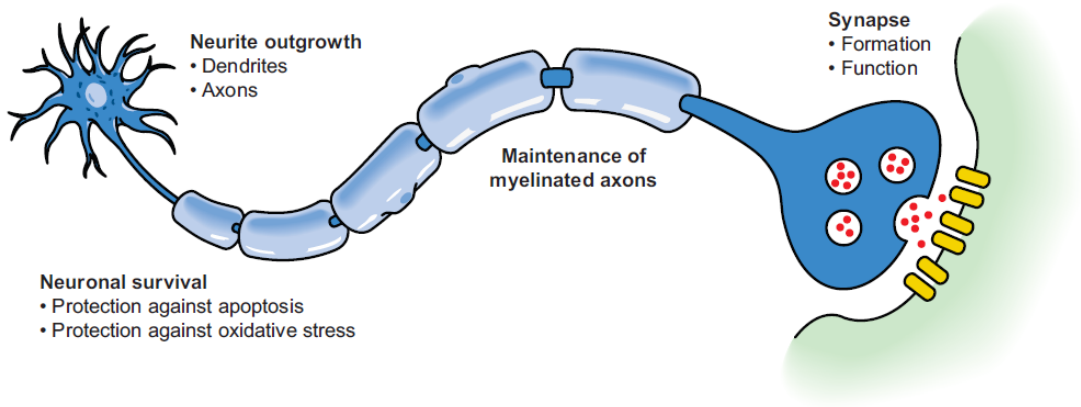

Figure 7. Physiological functions proposed for PrP^C. (from Aguzzi et al., 2008)

Cell type	Process	Function	Mechanisms, ligands and pathways
Neuron	Neuritogenesis	Adhesion, signalling	Recruits NCAM into rafts to allow it to activate Fyn kinase , which mediates intracellular signalling pathways
			STI-1 binding induces activation of mitogen-activated protein kinase
			Binds LRP/LR and HSPG by means of separate sites
			Binds laminin
	Synaptogenesis, polarization	Signalling	PrP^C acts as a growth factor, activating multiple pathways
	Survival, trophic effects	Anti-apoptotic	Interacts with BAX , STI1 and NCAM
		Pro-apoptotic	Binds to anti-apoptotic Bcl-2
			Crosslinks with anti-PrP antibody
			Increases levels of p53
	Copper binding	Copper endocytosis	Induces PrP^C to aggregate, exit from rafts and undergo clathrin-dependent endocytosis
		Copper homeostasis	Maintains appropriate copper levels at the presynaptic membrane and during conditions of oxidative stress
		SOD activity*	Copper-bound PrP^C has SOD activity
	Redox homeostasis	Signalling	Induces NADPH-oxidase dependent ROS through Fyn activation
Neural stem cells	Neurogenesis	Unknown	Increases cell proliferation in neurogenic regions
	Differentiation	Unknown	PrP^C levels positively influence differentiation
Haematopoietic stem cells	Long-term renewal	Anti-apoptotic? Homing?	Possible mechanisms: transduce cell survival signals; cell-adhesion activity targets cells to appropriate environment; or function as co-receptors for hormones affecting HSC activity
T cells	Activation	Signalling?	PrP^C upregulation upon mitogen-induced activation
	Development	Antioxidant	Copper binding in thymus
Leukocytes	Differentiation	Unknown	PrP^C expression by lymphocyte/monocyte lineage
	Phagocytosis	Unknown	PrP^C modulates phagocytosis
	Inflammatory response	Homing	PrP^C alters leukocyte recruitment to site of inflammation

Table 2. The cellular distribution and activities of PrP^C in cell types in which known or putative functions have been descrive (from Caughey and Baron, 2006)

I will focus on some of the proposed functions, which serve as a framework of my Ph.D. project and of this doctorate thesis.

PrP^C and neurite outgrouth

The analysis of the distribution of PrP^C during central nervous system (CNS) development demonstrated that *Prnp* gene expression is developmentally regulated, generally increasing during brain maturation (first postnatal weeks). Looking more in details, at the cellular level PrP^C is localized in fiber tracts early in development, then it shifts to synapses rich regions with aging (concomitantly with its increasing abundance in brain) in close spatio-temporal association with synapse formation. The appearance of a synaptic distribution for PrP^C follows and parallels the time-course of synapse formation in several brain stuctures (e.g., in the olfactory bulb, which contains synapses at birth, PrP^C has a terminal distribution already at P0) (Salès et al., 2002).

All these findings lead to speculations about a role of PrP^C in axonal development and synaptic formation and functioning.

Evidences for such an involvement can be found also in some *in vitro* studies.

In 2001, Shmitt-Ulms and colleagues demonstrated for the first time, with cross-linking experiments, that PrP^C can interact with Neuronal Cell Adhesion Molecules (NCAMs) (Schmitt-Ulms et al., 2001).

Two years later, Chen and colleagues demonstrated that the addition of PrP-Fc on primary cell cultures from p5-p7 mice cerebellar neurons stimulates neurite outgrowth (Chen et al., 2003).

Subsequently, two different groups independently demonstrated that PrP stimulates neurite outgrowth by interacting with NCAMs. Santuccione and colleagues worked on cerebellar neurons from p5-p7 mice and demonstrated that PrP-Fc acts on their surface recruiting NCAMs and stimulating neurite outgrowth (Santuccione et al., 2005). Instead, Kanaani and colleagues, using for their experiments hippocampal neurons from E18 rats, demonstrated that the overnight exposure to recombinant PrP (recPrP), folded into an an α-helical-rich conformation similar to that of PrP^C, led to a 1.9-fold increase in neurons with a differentiated axon, a 13.5-fold increase in neurons with differentiated dendrites, a 5-fold increase in axon length and the formation of extensive neuronal circuitry (Kanaani et al., 2005). The formation of synaptic-like contacts was increased by a factor of 4.6 after the exposure to recPrP for 7 days. NCAMs are the principal interactors of PrP^C in carrying out this function. The interactions between PrP and NCAMs are important for their stabilization in lipid rafts that leads to the activation of Fyn kinase via receptor-type protein phosphatase-α (RPTPα). The activation of Fyn stimulates neurite outgrowth (Figure 8).

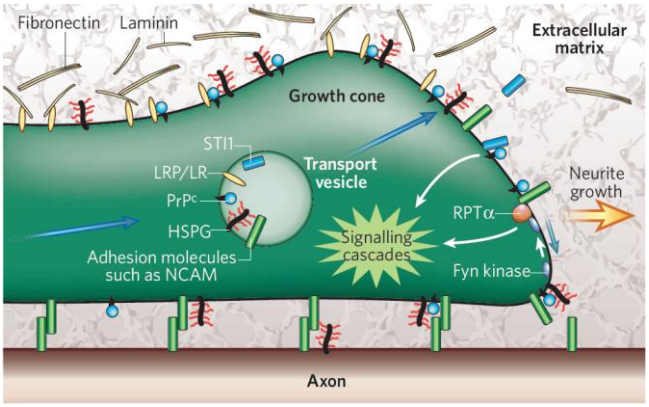

Figure 8. Model of potential PrP^C interactions associated with axonal growth. PrP^C seems to be important for neurite (nascent axon and dendrite) growth and synapse formation in neurons. Neurite outgrowth is modulated by PrP^C interactions with NCAM and STI-1, which can lead to activation of intracellular signalling pathways. In the case of NCAM, this signalling pathway is mediated by activation of Fyn kinase, presumably through RTPTα. PrP^C binds HSPG, laminin and the laminin receptor (LR) and its precursor (LRP), which, along with NCAM, are known to mediate contacts between neurons, other cells and the extracellular matrix. Various adhesion and extracellular-matrix molecules help to guide growing neurites to their appropriate destinations. These molecules are presumably delivered to the growing tips (growth cones) of neurites through transport vesicles, perhaps as preformed complexes (from Baron and Caughey, 2006).

Axon or dendrite outgrowth was also associated with other PrP^C-dependent activation of signal transduction pathways including cAMP/protein kinase A (PKA) (Chen et al., 2003; Lopes et al., 2005), protein kinase C (PKC) (Kanaani et al., 2005), and MAP kinase activation (Chen et al., 2003).

PrP^C and neuroprotection

Neuroprotection is probably the best-supported function attributed to PrP^C. This arises from several *in vitro* and *in vivo* findings mainly linked to anti-apoptotic and anti-oxidative stress effects exerted by the presence of the protein. The *Prnp*$^{0/0}$ mice display a higher susceptibility to stroke (McLennan et al., 2004) and to kainic acid-induced seizures (Rangel et al., 2007). Moreover, PrP^C was shown to wield neuroprotective function in mouse models of amyotrophic lateral sclerosis (Steinacker et al., 2010) and of experimental autoimmune encephalomyelitis (Tsutsui et al., 2008). Oxidative damage to proteins and lipids is higher in the brain lysates derived from *Prnp*$^{0/0}$ compared to their wildtype counterpart (Wong et al., 2001; Klamt et al., 2001). The

protein PrP^C may also exert a neuroprotective function by decreasing the rate of apoptosis after particular apoptotic stimuli, as for example Bax overexpression (Bounhar et al., 2001). Notably, PrP^C lacking the octarepeats could not reverse the Bax-mediated induction of apoptosis, thus hinting at the octapeptide domain as a potential neurotrophic/neuroprotective domain of PrP^C. This finding is supported by the finding that brain ectopic expression of Doppel (Dpl), a PrP paralog (see next chapter), triggers cerebellar Purkinje cells death, and that only full length PrP^C, but not N-terminally truncated PrP^C, can suppress the Dpl-mediated neurotoxicity and rescue the pathological phenotype (Atarashi et al., 2003).

PrP knockout and transgenic mice

Several knockout and transgenic mice lines for the *Prnp* gene have been created in order to address the crucial question of the physiological function of PrP^C. Indeed, the first generation of knockout mice, namely $Prnp^{0/0}$ (Zurich I) and $Prnp^{-/-}$ (Edimburgh) (Büeler et al., 1992; Manson et al., 1994) showed normal development and no spongiform change or any sign of pathology later in life. Later, other three PrP^C knockout mice line were created, namely $Prnp^{-/-}$ [Nagasaki], Rcm0, and $Prnp^{-/-}$ [Zurich II] (Sakaguchi et al., 1996; Moore et al., 1999; Rossi et al., 2001), and revealed loss of Purkinje cells and cerebellar degeneration. This finding, in contradiction with the previous reports on the absence on phenotypical variations in Zurich I and Edimburgh PrP knockout mice, was solved by the discovery of a novel gene, *Prnd*, located 16kb downstream of the *Prnp* gene. The *Prnd* gene encodes for the protein Dpl. The protein is overexpressed in Ngsk, Rcm0, and Zurich II mice, but not in Zurich I or Edimburgh PrP knockout mice (Moore et al., 1999). The protein Dpl is usually not expressed in the brain. However, in the second generation of PrP knockout mice, the transgenesis procedure introduced a deletion in *Prnp*, extended to the third exon of the gene, thus provoking the deletion of

the splice acceptor site. This led to an exon skipping phenomenon, and in turn the generation of a chimeric *Prnp-Prnd* mRNA containing the Dpl-coding exon. Thus Dpl becomes controlled by the *Prnp* promoter and therefore highly expressed in brain. The ectopic expression of Dpl in the brain causes ataxia and degeneration of cerebellar granule and Purkinje cells, and its levels can be inversely correlated with the onset of disease (Moore et al., 2001). However, the reintroduction of the *Prnp* gene in mice overexpressing Dpl in the brain rescues the phenotype (Nishida et al., 1999; Moore et al., 2001). Thus Dpl neurotoxicity is counteracted by PrP^C, but the mechanisms underlying this antagonism remain elusive. The molecular basis of Dpl-PrP^C antagonism may be hypothesized only with some models. For example, PrP^C and Dpl may compete for a common ligand, the binding of this latter with Dpl triggers neurodegeneration. Thus, the search for specific Dpl ligands in the brain could be key information for the mechanisms of Dpl-mediated neurodegeneration. However, Dpl-deficient mice are sterile (Behrens et al., 2002), suggesting that the primary physiological function of Dpl is related to sperm maturation. Other transgenic mice have been created in order to study the function of PrP^C. Mice carrying deletion mutants of PrP^C have been created to identify possible functional domains of PrP^C (Figure 9). For example an initial report of $Prnp^{0/0}$ mice expressing PrP^C lacking amino acid residues 32-121 or 32-134 (PrPΔ32-121 and PrPΔ32-134) revealed how the expression of these truncated PrPs caused severe ataxia and neuronal death limited to the granular layer of the cerebellum, and a widespread cerebellar leukoencephalopathy, similar to the one elicited by Dpl ectopic expression (Shmerling et al., 1998). The leukodystrophy, but not the cerebellar granule cell degeneration, can be rescued by oligodendrocyte-specific expression of PrP^C. On the other hand, neuron-specific expression of PrP^C can partially rescue cerebellar granule cell degeneration but not demyelination (Radovanovic et al., 2005). Thus white matter disease and cerebellar granule cell degeneration in these mice

are distinct, and the endogenous expression of PrP^C in both neurons and glia is required for complete reversion of the degenerative phenotype. Therefore, neurodegeneration and myelin damage may reflect two distinct pathological phenotypes elicited by different cellular types expressing PrP mutants. *Prnp*$^{0/0}$ mice expressing PrP lacking amino acid residues 32-93 (PrPΔ32-93) within the octapeptide region do not display any pathological phenotype, thus hinting at the central domain (CD, residues 94-134) of PrP^C as a key functional domain for signal transudction. The central domain comprises a charge cluster (CC_2, residues 95–110) and a hydrophobic core (HC, residues 112–134) (Figure 5, 9).

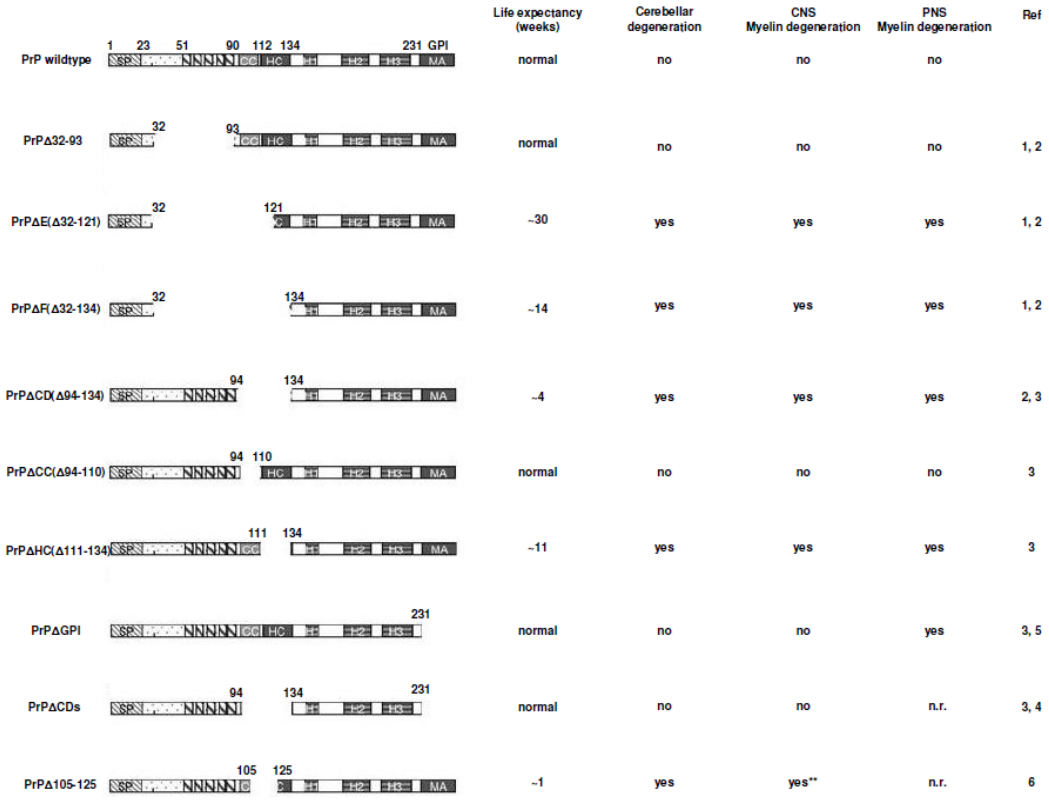

Figure 9. Murine PrP^C protein and transgenic mutant PrP. Schematic drawing of full-length murine PrP^C, with sequence for the signal peptide (SP) and for the GPI anchor (MA). The left column denotes the individual mutants described in this thesis. The right columns indicate life expectancy of the animals, presence of cerebellar neurodegeneration, central nervous system demyelination, peripheral nervous system demyelination, and references. All the mutants are to be intended as expressed in a *Prnp*$^{0\backslash0}$ genetic background. n.r. = not reported; ** = CNS demyelination of PrPΔ105-125 mice was revealed in a *Prnp*$^{+\backslash0}$ genetic background, due to the neonatal lethality of the mice expressing the transgene in a *Prnp*$^{0\backslash0}$ genetic background.
1 = Shmerling et al., 1998; 2 = Bremer et al., 2010; 3 = Baumann et al., 2007; 4 = Baumann et al., 2009; 5 = Chesebro et al., 2005; 6 = Li et al., 2007 (modified from Baumann et al., 2007).

In order to analyze the different contributions of these two domains to the pathological phenotype, other *Prnp* transgenic mice have been created lacking the entire central domain (PrPΔ94-134) (Baumann et al., 2007). Mice lacking the entire central domain (CD), i.e. expressing PrPΔ94-134, revealed a drastic neuropathological phenotype, characterized by vacuolar degeneration and astrogliosis with extensive central and peripheral myelin degeneration, and death within 20–30 days (Baumann et al., 2007). However, these mice lack the extensive cerebellar granule cell degeneration found in mice expressing PrPΔ32-121 and PrPΔ32-134 (Shmerling et al., 1998), despite the similarity of the myelin damage between the transgenic mice. In such scenario, the N-terminal octarepeat domain of PrP^C seems to be involved in transducing a neuroprotective effect on neurons (at least in the cerebellum), while the CD of PrP^C seems to transduce myelin-maintenance signals. Mice lacking the region spanning the residues 105-125 (PrPΔ105-125) display an even more dramatic phenotype, by developing a severe neurodegenerative illness that becomes lethal within 1 week of birth (Li et al., 2007).

Each of these pathologies can be counteracted by coexpression of wildtype PrP^C, in a dose-dependent fashion according to the level of expression of the mutant PrP transgene and the severity of the illness elicited by the mutant PrPs (Baumann et al., 2007; Li et al., 2007). According to the model in Figure 10, PrP^C and its deletion mutants can compete for a common ligand, maybe a receptor that regulate signal transduction (Baumann et al., 2007).

Moreover, a recent report highlights again the involvement of PrP^C in myelin homeostasis. Bremer et al. (Bremer et al., 2010) showed that $Prnp^{0/0}$ mice display a late-onset chronic demyelinating polyneuropathy (CDP) in their peripheral nervous system (PNS). Interestingly, the CDP is triggered by the specific ablation of PrP from neurons,

whereas PrP depletion from Scwhann cells did not elicit the disease. Accordingly, CDP was suppressed by PrP^C expression limited to neurons but not to Schwann cells. Thus, PrP^C expression by Schwann cells is not required for peripheral myelin maintenance, but PrP^C needs to be neuronal expressed to elicit its myelin-protective function. Bremer and colleagues showed that *Prnp*$^{0/0}$ nerve fibers had thinned myelin sheaths despite normal axonal morphology, thus suggesting a proper Schwann cells defect rather than an axonal one. Their finding frames up a scenario where axonal PrP^C regulates *in trans* a direct molecular communication from axons to Schwann cells. Moreover, mice expressing mutant PrP lacking the CC_2 domain (PrPΔ94-110) did not develop CDP, while on the contrary mice expressing mutant PrP lacking the hydrophobic core (PrPΔHC) (Figure 9) showed a reduced life expectancy (survival 80 ± 3.5 days), white-matter vacuolation and astrogliosis in cerebellum, brain stem and corpus callosum, and showed CDP (Bremer et al., 2010). Thus, the hydrophobic core (HC), but not the charge cluster (CC_2), of the central domain (CD) of PrP^C is essential for myelin maintenance.

However, the demyelinating phenotype in *Prnp*$^{0/0}$ mice is mild and less severe than the demyelination-affecting mice expressing PrP mutants lacking the central domain (CD). Indeed, *Prnp*$^{0/0}$ mice show only demyelination in their PNS, which is not lethal and does not prevent to the animal a correct development and behaviour (Büeler et al., 1992), and clinical manifestations of the polyneuropathy are limited to reduced grip strength and nociception (Bremer et al., 2010). On the contrary, *Prnp*$^{0/0}$ mice expressing deletion mutant of the central domain of PrP, *i.e.* PrPΔHC, PrPΔ32-121, PrPΔ32-134, show a more dramatic and lethal demyelinating phenotype, with both central and peripheral demyelination, clinical manifestations ranging from partial hind limb paresis to ataxia, full tetraplegia, and reduced life expectancy of the transgenic animals (Figure 9) (Shmerling et al., 1998; Baumann et al., 2007; Bremer et al., 2010).

Also *Prnp*$^{0/0}$ mice expressing Dpl show central and peripheral demyelination (Baumann et al., 2009). Thus, Dpl resembles the neurotoxic ΔPrP mutants lacking the central domain. Indeed, the addition of the domain containing the CD region of PrP^{C} was shown to detoxify Dpl (Baumann et al., 2009).

According to the scenario where full length PrP^{C} and PrP mutants compete for the same putative receptor, this great phenotypical difference between demyelination in *Prnp*$^{0/0}$ and PrPΔCD-expressing mice may be explained by a residual, basal activity of this receptor in *Prnp*$^{0/0}$ mice, whereas disruption of the CD may sequester the receptor in a dominant-negative state (Figure 10) (Steele et al., 2007).

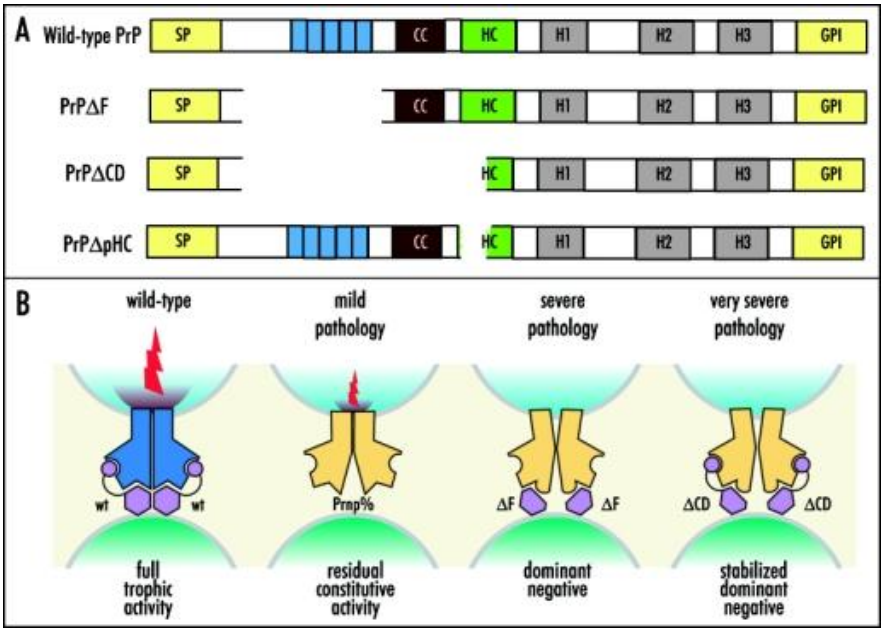

Figure 10. A model showing the effects of PrP^{C} deletion mutants. (A) Schematic diagram of wildtype PrP^{C} and its several deletion mutants. SP, signal peptide; octapeptide repeats are indicated in blue; CC, charge cluster; HC, hydrophobic core; H1, H2, H3 Helix 1, 2 and 3, respectively; GFP, GPI-anchor addition sequence (B). PrP (purple) consists of a globular C-terminal domain (hexagon) and a N-terminal flexible tail (arch) encompassing the octapeptide repeats (circle). The model rests on the following assumptions: (1) PrP activates a hitherto unidentified receptor (PrP_R) which transmits myelin maintenance signals (flashes); (2) in the absence of PrP, PrP_R exerts some residual activity, either constitutively or by recruiting a surrogate ligand; (3) the activity of PrP and its mutants requires homo- or heterodimerization, and induces dimerization of PrP_R; and (4) PrP dimers containing PrPΔCD or PrPΔCD trap PrP_R in an inactive dominant-negative state (from Steele et al., 2007).

The authors suggest that the cleavage of PrP^{C} appears to be linked to its myelinotrophic function. PrP^{C} is subjected to regulated proteolysis in late secretory compartments

(Sunyach et al., 2007), and its proteolysis generate two distinct fragments, namely C1 and C2. C1 is generated by α-cleavage at amino acids 110–112, whereas C2 is derived by β-cleavage in the octarepeat region at position 96 (Mangé et al., 2004; Watt and Hooper, 2005).

Bremer and colleagues (Bremer et al., 2010) evidence an association between the presence of CDP and lack of the C1 fragment in sciatic nerves. Indeed, all transgenic mice showing CDP lack C1 fragment, whereas all PrP mutants, in which the CDP was rescued, produce abundant C1. This suggests that alpha-cleavage is important for PrP^{C} function on myelin physiology. The alpha-cleavage activity seems to be dependent on the size of the central region of PrP, rather than on the sequence specificity (Oliveira-Martins et al., 2010).

Interestingly, mice expressing the toxic mutant PrPΔ94-134 but lacking the GPI anchor (namely, PrPΔCDs) do not display any sign of pathology irrespectively of the presence or absence of wt PrP^{C} (Baumann et al., 2009). Moreover, the expression of this transgene failed to influence the survival of mice expressing PrPΔ94-134 mice irrespectively of the presence or absence of full length PrP^{C}. This suggests that proper anchoring of PrP^{C} and of PrP mutants to lipid rafts is necessary for exerting their beneficial and/or toxic functions. This is in agreement, in turn, with the discovery that mice expressing anchorless PrP^{C} accumulate prions, protease-resistant PrP and amyloid plaques when infected with scrapie, but they develop only minimal subtle pathologies (Chesebro et al., 2005). Prion replication and neurotoxicity thus appear to be two distinct phenomena, the first requiring the coexpression and interaction of PrP^{Sc} with PrP^{C}, the latter requiring the correct GPI-anchoring of PrP^{C} to the cell membrane. Thus both for PrP mutants and for prion diseases, GPI-anchored PrPs are necessary for transducing the neurotoxic effect. Notably, also mice expressing anchorless PrP show the same CDP as $Prnp^{0/0}$ mice (Bremer et al., 2010), thus suggesting that proper

expression and anchoring of PrP^C to lipid rafts is also necessary for PrP^C to elicit its myelin-protective function. Thus, GPI membrane anchoring is necessary for both beneficial and deleterious effects elicited by PrP^C and its variants, including the neurodegenerative effect of PrP^{Sc}. Anchorless PrP is not physiologically processed and thus it does not give rise to C1 and C2 fragment (Bremer et al., 2010), thus enforcing the hypothesis of the cleaved fragments of PrP^C as the bioactive species for myelin maintenance.

In summary, a preponderant role for PrP^C in neuroprotection and myelin maintenance is described, yet with some peculiarities:

- Neuroprotection and myelin maintenance are probably two distinct phenomena, the former requiring neuronal expression of PrP^C, the latter requiring oligodendrocytes-specific full length PrP^C expression in the CNS, while axonal-specific full length PrP^C expression in the PNS (Radovanovic et al., 2005; Bremer et al., 2010).
- The N-terminal domain seems to mediate the neuroprotective function of PrP^C (Baumann et al., 2009).
- Mutants of PrP lacking the CD are highly myelinotoxic, with deleterious effects both on the CNS and in the PNS (Baumann et al., 2007; Bremer et al., 2010). This myelinotoxic effect can be counteracted by concomitant expression of full-length PrP^C.
- Proper GPI-anchoring of PrP^C and of PrP mutants is necessary for the transduction both of the physiological and of the pathological effects of the different PrPs, including also PrP^{Sc} elicited neurotoxicity (Chesebro et al., 2005; Baumann et al., 2009).
- Specific cell types (neurons, oligodendrocytes, astrocytes, Schwann cells) expression of full length PrP^C, anchorless PrP or PrP deletion mutants can differently

influence neurodegeneration and/or myelin damage (Radovanovic et al., 2005; Race et al., 2009; Bremer et al., 2010).

The GPI anchor localizes PrP^C to the outer part of the cellular membrane, and enriches PrP^C in the lipid rafts. Lipid rafts thus appear as the key functional site for PrP^C physiological function, and also for triggering the neurodegenerative effect of PrP^{Sc} - PrP^C interaction.

PrP^C and Alzheimer's disease

Alzheimer disease (AD) is the most common form of dementia, affecting at present more than 37 million people worldwide (Mount and Downton, 2006; Burns and Iliffe, 2009). The neurodegenerative disorder AD is characterized pathologically by the formation of senile plaques composed of amyloid-β (Aβ) peptides and distinctive neurofibrillary tangles composed of hyperphosphorylated Tau (Haass and Selkoe, 2007). The peptides Aβ are derived from the amyloidogenic-processing pathway of the amyloid precursor protein (APP) (Figure 11) (Aguzzi and O'Connor, 2010).

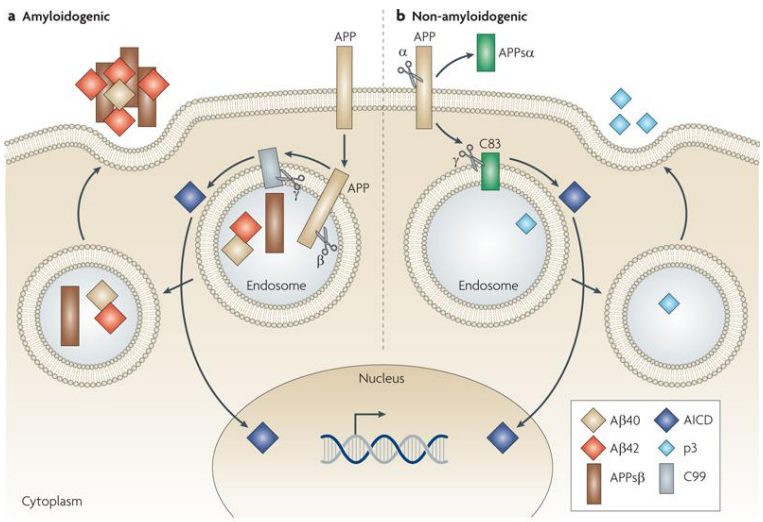

Figure 11. APP processing and amyloid-β formation. Amyloid precursor protein (APP) undergoes a series of proteolytic cleavages in neurons to form the amyloid-β (Aβ) peptides that are associated with senile plaques in AD. In the amyloidogenic pathway (a), internalized APP is initially cleaved at its amino terminus by endocytic β-secretase (β) to form secreted APPsβ and C99. C99 then becomes a substrate for intramembraneous cleavage by the γ-secretase complex, leading to the release of $A\beta_{40}$ (or $A\beta_{42}$ at low frequency) and the APP intracellular domain (AICD), which may regulate gene expression. In a competing, non-amyloidogenic pathway (b), α-secretase cleaves cell surface APP to liberate secreted APPsα and C83. C83 is then cleaved by γ-secretase to form the soluble p3 peptide and the AICD. The majority of Aβ and N-terminal APP cleavage fragments are eliminated from the neuron by the secretory pathway (from Aguzzi and O'Connor, 2010).

Several neuropathological similarities and genetic links between AD and prion diseases have been reported. The coexistence of AD pathology in CJD has been reported (Hainfellner et al., 1998) and PrP^C has been shown to colocalise with Aβ peptides in plaques (Voigtländer et al., 2001). These composite PrP-Aβ plaques were shown to be present in most CJD patients with associated AD-type pathology (Del Bo et al., 2006) and it has been proposed that PrP^C may promote Aβ plaque formation (Schwarze-Eicker et al., 2005). A genetic correlation between PrP^C and AD has also been reported. A systematic meta-analysis of AD genetic association studies revealed that the gene encoding PrP^C, *PRNP*, is a potential AD susceptibility gene (Bertram et al., 2007) and the Met/Val 129 polymorphism in *PRNP* has been reported to be a risk factor for early-onset AD (Dermaut et al., 2003). More recently, other reports strongly suggest a direct link between prion biology and AD.

Vincent et al. (Vincent et al., 2009) reported a link between PrP^C expression and regulation by the presenilins, the catalytic subunits of the γ-secretase complex. The authors of this study determined that the amyloid intracellular domain (AICD), resulting from the γ-secretase cleavage of APP (Figure 11), plays a role in the regulation of PrP^C expression. AICD, in association with Tip60 and Fe65, translocates to the nucleus and acts as a transcription factor to regulate p53 expression. The protein p53 was shown to regulate PrP^C at the transcriptional level by interacting with its promoter, resulting in changes in PrP^C mRNA and protein expression.

More recently, the group of Strittmatter (Laurén et al., 2009) proposed that PrP^C acts as receptor for $A\beta_{42}$ oligomers, which are the Aβ specie mainly responsible for neuronal dysfunction and degeneration (Walsh et al., 2002; Lesné et al., 2006; Selkoe, 2008). The authors state that soluble $A\beta_{42}$ oligomers reduce long-term potentiation (LTP) in wildtype mice but not in $Prnp^{0/0}$ mice, indicating that PrP^C is required to mediate one of the toxic effects of Aβ. This study concluded that there is a direct interaction between PrP^C and $A\beta_{42}$ oligomers and that this interaction affects synaptic plasticity. This suggests, therefore, that PrP^C mediates a toxic effect of the $A\beta_{42}$ oligomers and thereby plays an important role in the neurodegeneration associated with AD (Kellett and Hooper, 2009). However, Strittmatter group's findings are now under contention as other researchers in repeating some of the reported experiments had conflicting results, and thus challenge Strittmatter's conclusions (Balducci et al., 2010; Calella et al., 2010; Kessels et al., 2010).

In 2007, Parkin et al. (Parkin et al., 2007) reported that PrP^C decreased the amyloidogenic processing of APP thereby decreasing Aβ levels. This effect of PrP^C on the lowering of Aβ levels was elicited by a direct inhibition of PrP^C on the rate-limiting enzyme in the production of Aβ, the β-secretase BACE1 (Vassar, 2004). In fact, PrP^C depletion by siRNA in a murine neuroblastoma (N2a) cell line or PrP^C absence in

Prnp$^{0/0}$ mice resulted in increased Aβ levels. Aβ levels were significantly increased also in the brains of scrapie-infected mice, thus showing that during prion diseases the inhibitory effect of PrP^C on the β-cleavage of APP may be lost. Moreover, this study shows how the interaction between PrP^C and BACE1 requires the correct localisation of PrP^C to cholesterol-rich lipid rafts, where BACE1 cleavage of APP preferentially occurs (Ehehalt et al., 2003; Cordy et al., 2003).

Moreover, the authors found that the charged cluster, the CC_1 region at the extreme N-terminus of mature PrP^C possibly through interactions with glycosaminoglycans is critical for the interaction with and inhibition of BACE1 (Parkin et al., 2007). Thus, PrP^C has a crucial effect in suppressing the production of the Aβ peptide, and further studies are required to determine whether PrP^C could play a functional role in preventing AD.

Despite being a fascinating point of investigation for AD, PrP^C interaction with BACE1 could also be interesting for myelin physiology. I have previously described how the role of PrP^C in myelin homeostasis appears to be complex, with distinct influences in CNS and PNS myelin development and maintenance. Myelination and myelin maintenance are different physiological processes which require distinct axonal molecular signals acting on glial cells and supporting them at different developmental stages. One of the most studied molecular signals is mediated by neuregulin-1 (NRG1) (Newbern and Birchmeier, 2010). The protein NRG1 is a trophic factor containing an epidermal growth factor (EGF)-like domain that signals through the binding of ErbB receptor tyrosine kinases (Mei and Xiong, 2008). The best-defined function of NRG1 is the control of myelination in the PNS, where NRG1 is essential for neuronal and glial survival (Garratt et al., 2000b; Jessen e Mirsky, 2005; Nave e Salzer, 2006). On the other hand, NRG1 role in the myelination of the CNS has not yet been established and,

despite *in vitro* data, NRG signaling seems to be dispensable for CNS myelination *in vivo*, at least during postnatal stages (Brinkmann et al., 2008). This suggests that NRG1 may function differently in the PNS and CNS.

The protein NRG1 is synthesized as a membrane-anchored protein, which undergoes proteolytic cleavage that releases mature (EGF)-like domain-containing NRG1 ectodomain. This cleavage is catalyzed by different membrane proteases, including members of the ADAM proteases family, like ADAM17/TACE (Loeb et al., 1998; Montero et al., 2007) and ADAM19 (Yokozeki et al., 2007), and by BACE1 (Willem et al., 2006; Hu et al., 2006). The BACE1 knockout mice show a deficit in NRG1 processing in their nervous system, and display a peripheral neuropathy similar to that observed in mice lacking NRG1/ErbB signaling (Garratt et al., 2000b; Michailov et al., 2004; Taveggia et al., 2005). Thus, the physiological BACE1-mediated processing of NRG1 seems to be a key trophic instruction for the normal development and maintenance of myelin physiology, at least in the peripheral nervous system. As PrP^{C} interacts and regulates BACE1 activity (Parkin et al., 2007), a potential influence of PrP^{C} on BACE1-mediated NRG1 cleavage is intriguing. Indeed, Bremer and colleagues (Bremer et al., 2010) reported no PrP^{C} influence on NRG1 processing in sciatic nerves from P11 and P35 mice.

Aim of the thesis

Despite years of intense research, the physiological functions of the cellular PrP, PrP^C, are still unknown. The protein PrP^C has been shown to be involved in several cellular and physiological processes (Aguzzi et al., 2008). Indeed, the involvement of PrP^C on these several physiological functions seems to be time- and tissue- dependent. The early embryonic expression of PrP^C (Manson et al., 1992) and its functional role for neuritic outgrowth (Santuccione et al., 2005; Kanaani et al., 2005) are suggestive of a developmental function for the PrP. On the contrary, its role for myelin maintenance seems to be physiologically required only in adult and aged animals, and not for the early phases of myelination. Myelin in the PNS is affected by the lack of PrP or by expression of PrP deletion mutants. On the contrary, myelin homeostasis in the CNS is not affected by the lack of PrP^C but it is severely compromised by the expression of some PrP deletion mutants (Radovanovic et al., 2005; Baumann et al., 2007, 2009; Bremer et al., 2010). Therefore, PrP^C seems to fulfil different functions between CNS and PNS at different time point during the life of the animal. During my Ph.D. studies I focused on some of the biological problems concerning PrP^C functions at different developmental stages, from embryonic to aged animals.

At first, I undertook a spatio-temporal analysis of PrP^C expression and distribution during embryonic and early postnatal development in the brain of the mouse, by *in situ* hybridization and immunofluorescence techniques, to identify brain region and structures expressing PrP^C during the first developmental stages of the animal.

Then I focused on potential transcriptional effect mediated by PrP^C expression or absence. I took advantage of microarray platform to analyze the gene expression profile

in the hippocampus of newborn and adult wildtype and *Prnp*$^{0/0}$ mice in order to unravel differentially regulated genetic pathways during development.

Finally, I investigated both in the CNS and in the PNS the potential influence of PrP^C on neuregulin cleavage to shed new light on the possible mechanisms linking PrP^C to myelin homeostasis.

Materials and methods

Animals

All experiments were carried out in accordance with European regulations [European Community Council Directive, November 24, 1986 (86/609/EEC)], and were approved by the local authority veterinary service. For microarray and realtime RT-PCR experiments, inbred FVB/N *Prnp*$^{+/+}$ and FVB *Prnp*$^{0/0}$ mice were used in these experiments. The FVB *Prnp*$^{0/0}$ mice were obtained by backcrossing the original *Prnp*$^{0/0}$ mice (Büeler et al., 1992) to FVB/N inbred mice for more than 20 generations.

For immunofluorescence, *in situ* hybridization, western blotting experiments, C57/B6 wildtype, mixed B6/129 wildtype, B6/129 *Prnp*$^{0/0}$ (Büeler et al., 1992), FVB wildtype and FVB *Prnp*$^{0/0}$ (Lledo et al., 1996) mice were used.

Immunohistochemistry

Embryonic and newborn animals were sacrificed and brains immediately collected and washed several times in cold PBS 1x glucose 0.6% w/v. Then brains were fixed by complete immersion in freshly prepared PBS 1x paraformaldehyde (PFA) 4% with very gentle shaking over night at 4°C. The day after, the samples were washed in PBS 1x and cryopreserved by complete immersion in PBS 1x sucrose 30% with gentle shaking overnight at 4°C. Then brains were washed several times in PBS 1x to remove excess of glucose, included in OCT and stored at -80°C. Two-weeks old and older animals were deeply anesthetized, then perfused with PBS 1x and PBS 1x PFA 4%. After perfusion, animals were decapitated and brains were collected, fixed and cryopreserved as previously described.

10 micrometer thick sections were cut with a cryostat and mounted onto Superfrost Plus coated slides (Menzel-Gläser). Slides were thawed at room temperature (RT), then washed with TBS + Triton X-100 0.3% (TBS+T). Sections then were blocked with blocking solution: TBS+T + Normal Goat Serum (NGS) 10% and Bovine Serum Albumine (BSA) 5% for 1h at RT Then slides were incubated with primary antibodies diluted in blocking solution for 2h at RT with gentle shaking. After washing, appropriate secondaries antibodies diluted in blocking solution were added for 1h at RT with gentle shaking. Slides then were extensively washed with TBS+T, mounted with Vectashield and analyzed under Leica fluorescence microscope. All data are representative of at least three independent experiments.

- **Antibodies**

Recombinant anti-PrP^{C} humanized (HuM) Fab D18 was purchased from InPro Biotechnology (South San Francisco, CA; ABR-0D18) and used to a final concentration of 1 µg/mL. HuM-D18 is a recombinant Fab with human constant moiety, first raised by immunizing *Prnp*$^{0/0}$ mice against the protease-resistant core of Syrian hamster (SHa) PrP^{Sc} (Peretz et al., 1997). It showed high affinity for the region spanning the residues 133–152 incorporated in the first alpha-helix of PrP^{C} (Williamson et al., 1998), and proved to have a large accessibility to its specific epitope and to bind the largest fraction of the cell surface PrP^{C} population, as revealed by cross-competition experiments (Leclerc et al., 2003). Moreover, it was able to inhibit prion propagation and clear cell cultures of prion infectivity (Peretz et al., 2001).

Anti-neurofilament 200 antibody was purchased from Sigma (St. Louis, MO; N-4142) and used at dilution 1:800. This antibody is developed in rabbit using purified neurofilament 200 from bovine spinal cord as the immunogen. It localizes only the 200-kDa neurofilament polypeptide in immunoblotting from mouse brain homogenate.

- ***In situ* hybridization**

Twenty-µm-thick cryosections were cut and collected on slides (Menzel-Gläser SuperFrost Plus) and then stored at -80°C. Sections were dried at RT for 2 hours and fixed in 4% PFA in PBS 1x at room temperature for 10 min, washed in PBS 1x, treated with 18 mg/mL Proteinase K (Roche, Nutley, NJ) at 30°C for 15 min, washed in glycine 4 mg/mL, PBS 1x, and fixed once more in 4% PFA for 10 min, washed, incubated in 0.1 M thriethanolamine pH 8.0 with acetic anhydride (0.03%), and washed again. Slides were then dried at RT and hybridized overnight at 55°C with 1.5 µg/mL digoxigenin (DIG)-labeled probe in hybridization solution: 50% formamide, salts 10x pH 7.2 (NaCl 3M, Tris HCl 0.1M, NaH_2PO_4 0.1M, 2% Ficoll 400 (Sigma), 2% polyvinyl pyrrolidone (Sigma)), DTT 2M (Sigma) in 10 mM sodium acetate pH 5.2, polyadenilic acid (Sigma) 10 mg/mL, ribonucleic acid (Sigma) 9.2 mg/mL, transfer type x–SA (Sigma) 7 mg/mL, 10% dextran sulfate (Sigma).

After hybridization, slides were washed in 5x SSC – β-mercaptoethanol at RT for 30 min. Then they were washed in 50% formamide-1x SSC – β-mercaptoethanol at 65°C for 30 min, several times in the NTE solution (5M NaCl, 1M Tris-HCl pH 8.0, 0.5 M EDTA pH 8.0) at RT, then in 2x SSC and 0.2x SSC. Slides were put in a humidified chamber with buffer B1 (1M Tris-HCl pH 7.5, 5 M NaCl), blocked in HI-FBS (heat-inactivated fetal bovine serum)-B1 (10÷90) for 60 min. Each slide was treated with 1:1,000 anti-DIG (Roche) in HI-FBS-B1, covered with a parafilm coverslip, and incubated overnight at 4°C.

Chromogenic-stained slides were washed several times with buffer B1 and with buffer B2 (0.1 M Tris-HCl pH 7.5, 0.1 M NaCl, 50 mM $MgCl_2$ pH 9.5) and stained with NBT 3.5 µL (Roche)-BCIP 3.5 µL (Roche) in 4 mL B2. After 10 min the reaction was observed under the microscope and stopped when the transcript signal level was

detectable. Slides were then washed several times in buffer B1, then in PBS 1x. Slides were mounted with one 20 µL drop of PBS 1x 30% glycerol solution and a glass coverslip, sealed with enamel, and stored at 4°C.

Microarray analysis

Hippocampi from postnatal day 4.5 (P4.5) and 3-month-old males were investigated. For each developmental stage, hippocampi of 3 or 4 animals were dissected immediately after animal sacrifice and promptly processed for RNA extraction and purification.

Total RNA from each pair of hippocampi was extracted using the TRIzol reagent (Invitrogen) following the manufacturer's instructions, and purified using the RNeasy mini kit (Qiagen). The quality of total RNA was assessed using a bioanalyzer (Agilent 2100; Agilent Technologies) and RNA was quantified using an ND-1000 Nanodrop spectrophotometer. Ten µg of each total RNA sample were labeled according to the standard one-cycle amplification and labeling protocol developed by Affymetrix (Santa Clara, CA). Labeled cRNA was hybridized on Affymetrix GeneChip Mouse Genome 430A 2.0 Arrays, containing 22,690 probesets corresponding to approximately 14,000 well-characterized mouse genes. Hybridized arrays were stained, washed (GeneChip Fluidics Station 450) and scanned (GeneChip Scanner 3000 7G). Cell intensity values and probe detection calls were computed using the Affymetrix GeneChip Operating Software (GCOS). Further data processing was performed in the R computing environment (http://www.r-project.org/) version 2.8.0 with BioConductor packages (http://www.bioconductor.org/).

Robust Multi-Array Average (RMA) normalization was applied (Irizarry et al., 2003). Data were then filtered based on Affymetrix detection call and probeset intensity, so

that only probesets that had a present call and intensity value >100 in at least one of the arrays were retained.

Statistical analysis was performed with limma (Smyth, 2004). P-values were adjusted for multiple testing using Benjamini and Hochberg's method to control the false discovery rate (Hochberg and Benjamini, 1990). Genes with adjusted P values below 0.05 were considered differentially expressed. Data were analyzed through the use of Ingenuity Pathways Analysis (Ingenuity Systems®, www.ingenuity.com) and DAVID Bioinformatics Resources (Dennis et al., 2003; Huang et al., 2009). For Alzheimer's disease (AD)-related genetic analysis, we took advantage of GeneCards® GeneALaCart Beta software (http://www.genecards.org/). Microarray data are deposited in the GEO database with Accession Number GSE21718.

Quantitative real-time RT-PCR

Total RNA was extracted as described above and purified using the RNeasy mini kit (Qiagen). Single strand cDNA was obtained from 1 µg of purified RNA using the iSCRIPT™ cDNA Synthesis Kit (Bio-Rad) according to manufacturer's instructions. Quantitative RT-PCR was performed using SYBR-Green PCR Master Mix (Applied Biosystem) and an iCycler IQ Real Time PCR System (Bio-Rad). Expression of the gene of interest was normalized to house-keeping gene *β-actin*, and the initial amount of the template of each sample was determined as relative expression versus *β-actin* sample chosen as reference. The relative expression of each sample was calculated by the formula $2\ \exp^{-\Delta\Delta Ct}$ (User Bulletin 2 of the ABI Prism 7700 Sequence Detection System). *β-actin* expression is not modified under the present experimental conditions (data not shown).

Western Blotting

Mouse hippocampi and sciatic nerves were dissected and immediately frozen in ice-cold lysis buffer (50 mM Tris-HCl pH 7.5, 150 mM NaCl, 1 mM EDTA, 0.5% CHAPS, 10% glycerol) containing proteases inhibitors (Inhibitor complete mini, Roche Diagnostics Corp., Mannheim, Germany) and stored at -80°C or immediately homogenized. Hippocampal samples were further cleared by centrifugation at +4°C, 2000 g, 10 min. For sciatic nerves of P15 and P30 wildtype and *Prnp*$^{0/0}$ mice, nerves from 2 animals were pooled together in each sample, while for older mice each sample included sciatic nerves from a single animal. Total protein content was determined by the bicinchoninic acid (BCA) assay (Pierce), and the same amount of proteins for each sample (50 μg) was separated either on gradient SDS-PAGE gels (NuPAGE® Novex 4-12%, Invitrogen) or on 8% homemade SDS-PAGE gels, and transferred to PVDF membrane.

Antibodies

We used the following primary antibodies: for total Tau, Tau-5 antibody (Pharmingen, BD Biosciences, California, USA); for phospho-Tau, AD2 antibody (Bio-Rad, California, USA); NRG1 C-Terminal epitope, C-20 (sc-348, Santa Cruz Biotechnology); NRG1 N-terminal epitope, H-210 (sc-28916, Santa Cruz Biotechnology); NRG3, H-70 (sc-67002, Santa Cruz Biotechnology); Anti-PrP antibody HRP-conjugated Fab D13 (Williamson et al., 1998); anti total non-phosphorylated Fyn, phosphorylated Fyn and phosphorylated ERK kinases [Src Family Antibody #2109, phospho-Src Family (Tyr416) antibody #2101, and phospho-p44/42 Map Kinase (Thr202/Tyr204) Ab #9101, Cell Signaling Technology]. The appropriate horseradish peroxidase-coupled secondary antibodies (Pierce, Rockford, USA) were used.

Cell Culture

N2a and N2a-CL3 cells, stably transfected with and overexpressing full-length mouse PrP^C, were cultured as previously described (Ghaemmaghami et al., 2010). Briefly, all cell lines were maintained in Modified Eagle's Medium (MEM) supplemented with 10% v/v fetal bovine serum, 1% penicillin-streptomycin, and 1% GlutaMAX (Invitrogen) at 37°C in a humidified atmosphere with 5% CO_2.

Preparation of cytosolic extracts and conditioned medium proteins

Cells were grown almost to confluency in 10-cm diameter tissue culture plates (Corning). Cells were then washed with PBS (3X), and maintained in serum-depleted MEM for 40h. Conditioned medium was then removed, spun at 10000g, 10 min, 4ºC to remove cell debris, and then precipitated with 5 volumes of cold acetone. Samples were incubated at least 2 hours at -20ºC, and then spun at 5000g, 20 min, 4ºC. Protein pellets were then air dried and resuspended in Laemmli buffer.

The cell layer remaining in the plate after the incubation period in serum-free MEM was washed with PBS (3X) and lysed with 500 µL of cold lysis buffer (10 mm Tris-HCl, pH 8.0, 150 mm NaCl, 0.5% sodium deoxycholate, 0.5% Nonidet P-40). Cell lysates were then centrifuged at 10000g, 5 min, 4ºC to remove cell debris. The supernatant was collected and the total protein concentration was measured by using the bicinchoninic acid assay (Pierce). The conditioned medium and cell lysates were normalized for total protein based on the cell lysate protein concentrations, boiled for 5 min, electrophoresed on gradient SDS-PAGE gels (NuPAGE® Novex 4-12%, Invitrogen) and transferred to PVDF membrane.

Results

Prnp gene expression detected throughout the developmental mouse brain

To investigate *Prnp* gene expression, PrP-encoding mRNA expression was analyzed in several regions of the mouse brain during pre- and postnatal development. *In situ* hybridizations were performed on 20-µm-thick coronal cryosections of mouse brains. *Prnp* gene expression in the brain was analyzed in 14.5- and 16.5-day-old embryos (E14.5, E16.5), in 1- (P1) and 7- (P7) day-old mice, and in adult mice. As negative control, sections from $Prnp^{0/0}$ mice were hybridized with the PrP riboprobes (data not shown).

Between E14.5 and E16.5 noticeable labeling was detected in brain regions known to have a highly active cellular proliferation, such as the ventricular zone (VZ) of the neocortex of the lateral ventricles (Figure 12 A, B) and the neuroepithelia of the third ventricle (IIIv) (Figure 12 I–L). In addition, *Prnp* signal was detected underneath the marginal zone (MZ) in the superficial cortical plate (CP), where newborn neurons were. At P1 the signal spanned the entire CP (Figure 12 C, D), whereas at P7 it was mainly restricted to the superficial CP, where the youngest neurons were (Figure 12 E, F). At P7 it was possible to observe a decrease of the signal in the subventricular/ependymal zone (SVZ/E) and in the subplate zone (SP), while it increased in the outer layers of the cortex (layers 6-2) (Figure 12 E, F).

At P7 it was possible to observe strong *Prnp* gene expression in other brain areas, such as the CA1 and the DG fields of the hippocampus (Figure 13). Moreover, during postnatal development and in the adult the expression pattern of PrP mRNA was constantly detectable in the olfactory bulbs.

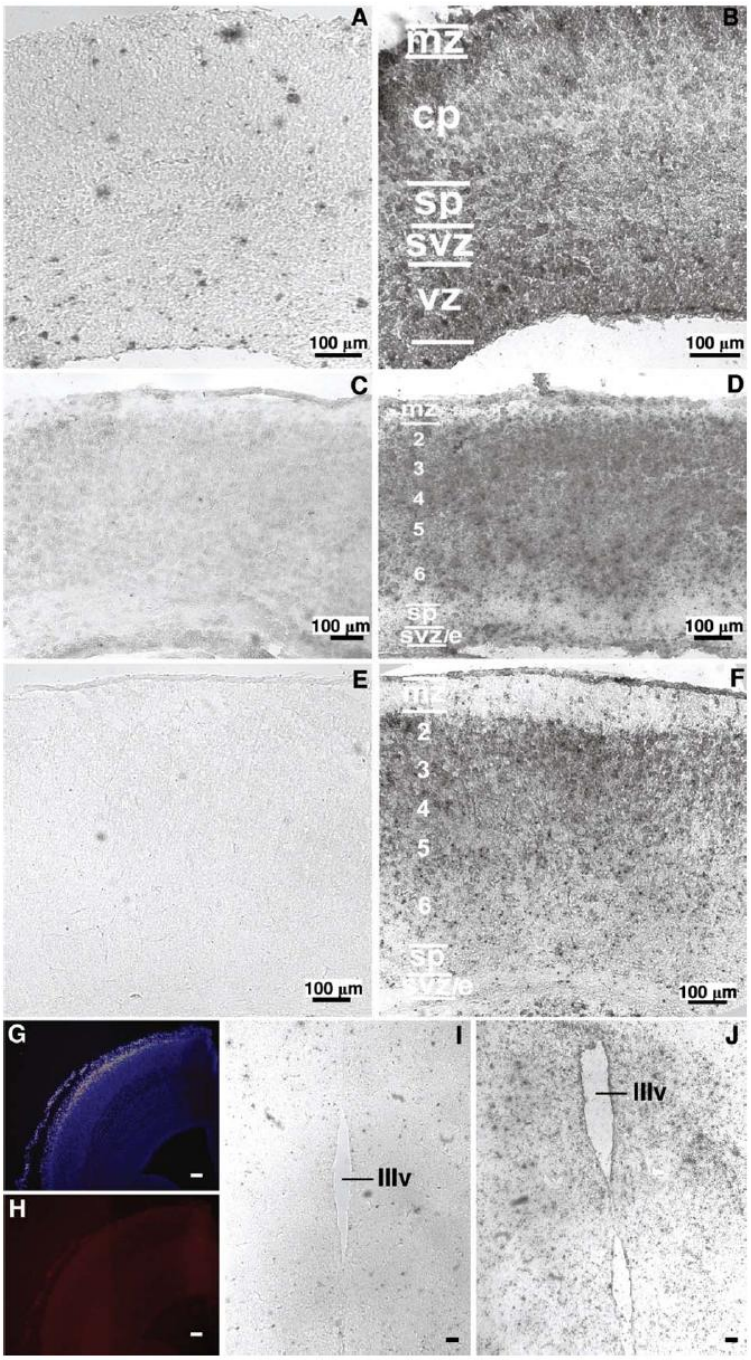

Figure 12. *Prnp* shows a patterned developmental expression in mouse brain. A, B: In situ hybridization of E14.5 brain coronal section. A: No positive cell was detected in the neocortex area using negative sense probe. B: Positive antisense probe shows that *Prnp* was detected in the ventricular zone (VZ). In addition, *Prnp* signal seems to be underneath the marginal zone (MZ) and in the superficial cortical plate (CP). Less intense signal was detected in the subventricular zone (SVZ) and in the subplate zone (SP). C, D: In situ hybridization of P1 brain coronal section. The antisense probe (D) shows signal for *Prnp* spanning the entire CP (layer 6-2). Negative control sense probe shows specificity of the signal in (C). E, F: Expression pattern of *Prnp* gene in the cortex layers of P7 postnatal stage. The positive signal of *Prnp* (F) is mainly concentrated to the superficial CP, whereas it progressively decreases in the subventricular/ependymal zone (SVZ/E) and in the subplate zone (SP). No signal was detected with the negative probe (E). G, H: Immunohistochemical staining of E14.5 mouse brain shows no expression of the mature PrP^C in the neocortex. PrP^C (in H) and nuclei (blue, in G) were stained, and no PrP^C immunoreactivity was detected. I, J: The expression of *Prnp* was detected in the neuroepithelia of the third ventricle (IIIv) at E14.5 using antisense probe (J), whereas no signal was detected using negative sense probe (I). Scale bars = 100 μm in G,H; 25 μm in I,J.

Hybridization signals were found in the mitral cells layer (Mi), along the wall of the olfactory bulb ventricle, and in the glomerular layer (GL) at P7 (Figure 14 A, B); this expression pattern remained constant until adult life (data not shown). These results are in agreement with previous descriptions (Le Pichon and Firestein, 2008). As expected, a signal was also detected in the frontal cortex.

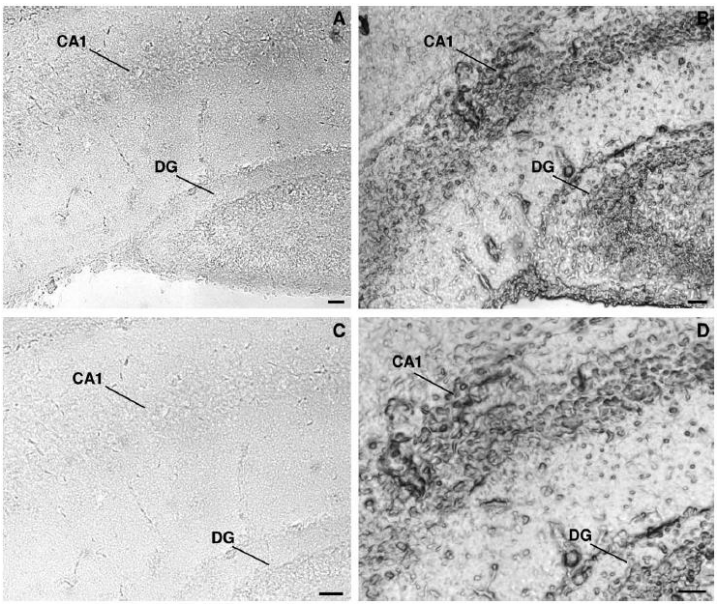

Figure 13. Expression of *Prnp* in the postnatal hippocampus. A–D: In situ hybridization of P7 hippocampal coronal section. A, B: *Prnp* signal was detected in the CA1 and in the DG cells in the hippocampus (B); no signal was detected with the control probe (A). C, D: Higher magnification of the CA1 pyramidal cells, indicating a clear perinuclear staining of *Prnp* expression (D). No signal was detected when using the negative sense probe (C). Scale bars = 50 μm.

By E16.5, intense expression was also found in nonneuronal tissue, such as the choroid plexus (ChP) of the ventricles, both at the mRNA and protein level (Figure 14 C–F). Specifically, PrP^{C} immunoreactivity was detected in the apical surface of the epithelial cells, on the side facing the ventricle (Figure 14 F).

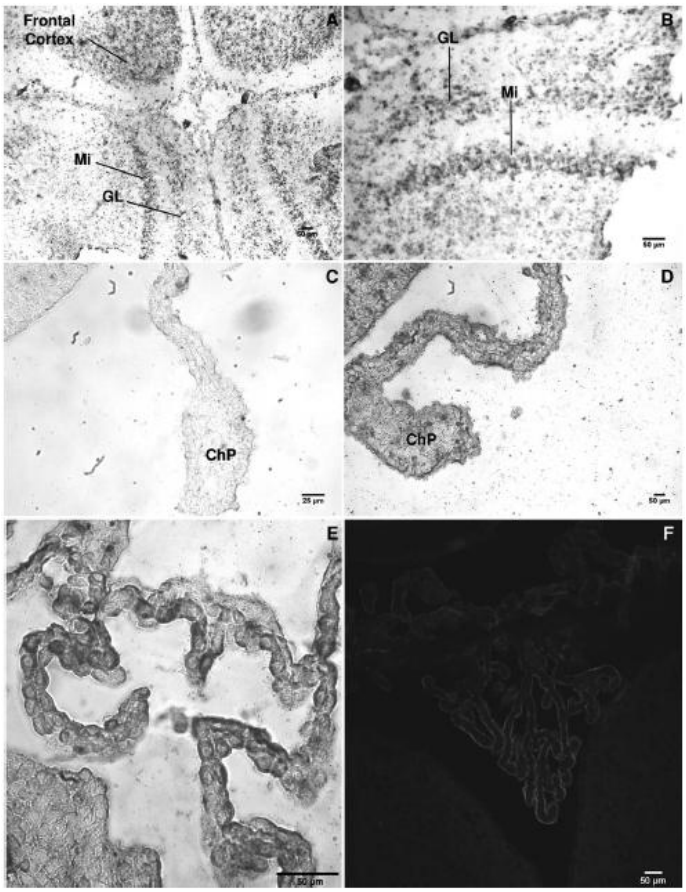

Figure 14. *Prnp* is expressed in the olfactory bulb and in the choroid plexus during development and in adult life. A: At P7 the expression of *Prnp* is widespread in the olfactory bulb, with an increased expression in mitral cells layer (Mi) and in the glomerular layer (GL). B: Higher magnification of the different layers. C–F: PrP is expressed also by the choroid plexus. C–E: Epithelial cells of the choroid plexus show an intense *Prnp* signal starting at E16.5 (D) until adult life (E). No signal is detected using the control probe (C). F: At P7 PrP^C is detected in the epithelial cells of the choroid plexus, specifically at the apical surface of the cells toward the ventricle.

Dynamics of PrP^C expression in the developmental mouse brain

The overall distribution of PrP^C in the developmental mouse brain was also examined by immunohistochemistry technique. The dynamics of PrP^C expression during prenatal and postnatal development were examined in coronal and longitudinal brain sections of E14.5, E18.5, P1, P4, P7, P9, and adult mice. The hippocampus was the region with the earliest and highest PrP^C immunoreactivity. Starting from E18.5 to adult life the hippocampus was labeled by Fab D18 in all parenchyma, with a net increase in PrP^C

immunoreactivity in the stratum lacunosum moleculare (str l m) (Figure 15 A, B). This layer of the hippocampus contains a high number of synapses from hippocampal internal interneurons and from external inputs, such as the enthorinal cortex (Deng et al., 2006a). Strong PrP^C immunoreactivity was also observed in the fimbria (Fi) of the hippocampus (Fig. 15 C–L). In this structure, PrP^C-immunoreactivity was first observed at E18.5 and progressively increased during development (Figure 15 E–H). Next to the fimbria of the hippocampus, the stria terminalis (St) also showed a high level of PrP^C immunoreactivity (Figure 15 C–L), and paralleled the developmental expression of PrP^C of the fimbria (Figure 15 E–H). The stria terminalis is the main nervous output of the amygdala up to thalamic nuclei (Lee and Davis, 1997). The immunostaining clearly highlighted that PrP^C expression in these white matter fiber bundles is very high and well defined (Figure 15 I–L). The thalamus was another region showing basal PrP^C expression during neurodevelopment (Figure 16). Within the thalamus the fornix, the anatomical continuation of the hippocampal fimbria, showed an intense and definite PrP^C-immunoreactivity (Figure 16 A). The specificity of PrP^C expression for particular brain white matter tracts could be appreciated by the complete lack of PrP^C staining of the mammillothalamic tract (Figure 16 A–C). Moreover, the fasciculus retroflexus (Fr) specifically showed a high staining for the mature protein during development (Figure 16 D–H). As for the fimbria of the hippocampus and the stria terminalis, PrP^C immunoreactivity was first observed at E18.5 and progressively increased during development both for the fornix (Figure 16 I–M) and for the fasciculus retroflexus (Figure 16 N–P).

However, we did not observe any dramatic alterations in the size or in the morphology of any of these structures in *Prnp*$^{0/0}$ animals.

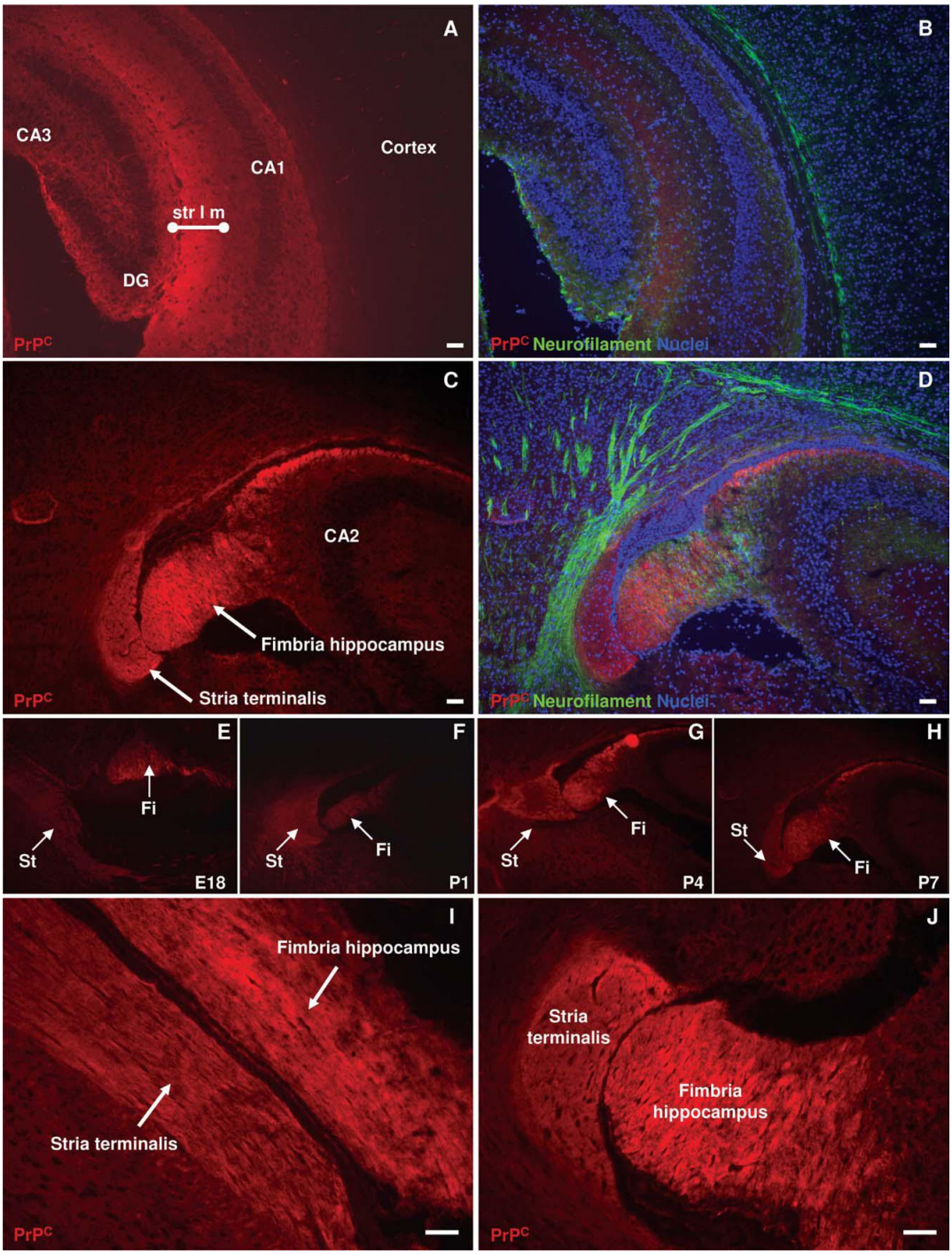

Figure 15. PrP^C expression in the hippocampus during development. A, B: At P7 PrP^C (in red; A) is detected throughout the hippocampus, and in particular at high levels in the stratum lacunosum-molecolare (str l m), a synapse-dense region. No signal for PrP^C is yet detected in the cortex. A merged image is shown in B (PrP^C, in red; neurofilament, in green; nuclei signals in blue). C–H: PrP^C is specifically and highly expressed by the fimbria of the hippocampus and the stria terminalis at P7 (C, D). The fimbria of the hippocampus (Fi) and the stria terminalis (St) express high level of PrP^C also at embryonic stages (E18.5), and progressively increase the level of expression during postnatal development: P1 (F), P4 (G), and P7 (H). I, J: Higher magnification of longitudinal (I) and coronal (J) section of the fimbria of the hippocampus and the stria terminalis, highlighting the net boundaries of PrP^C-expression between other brain regions and these structures. Scale bars = 50 μm.

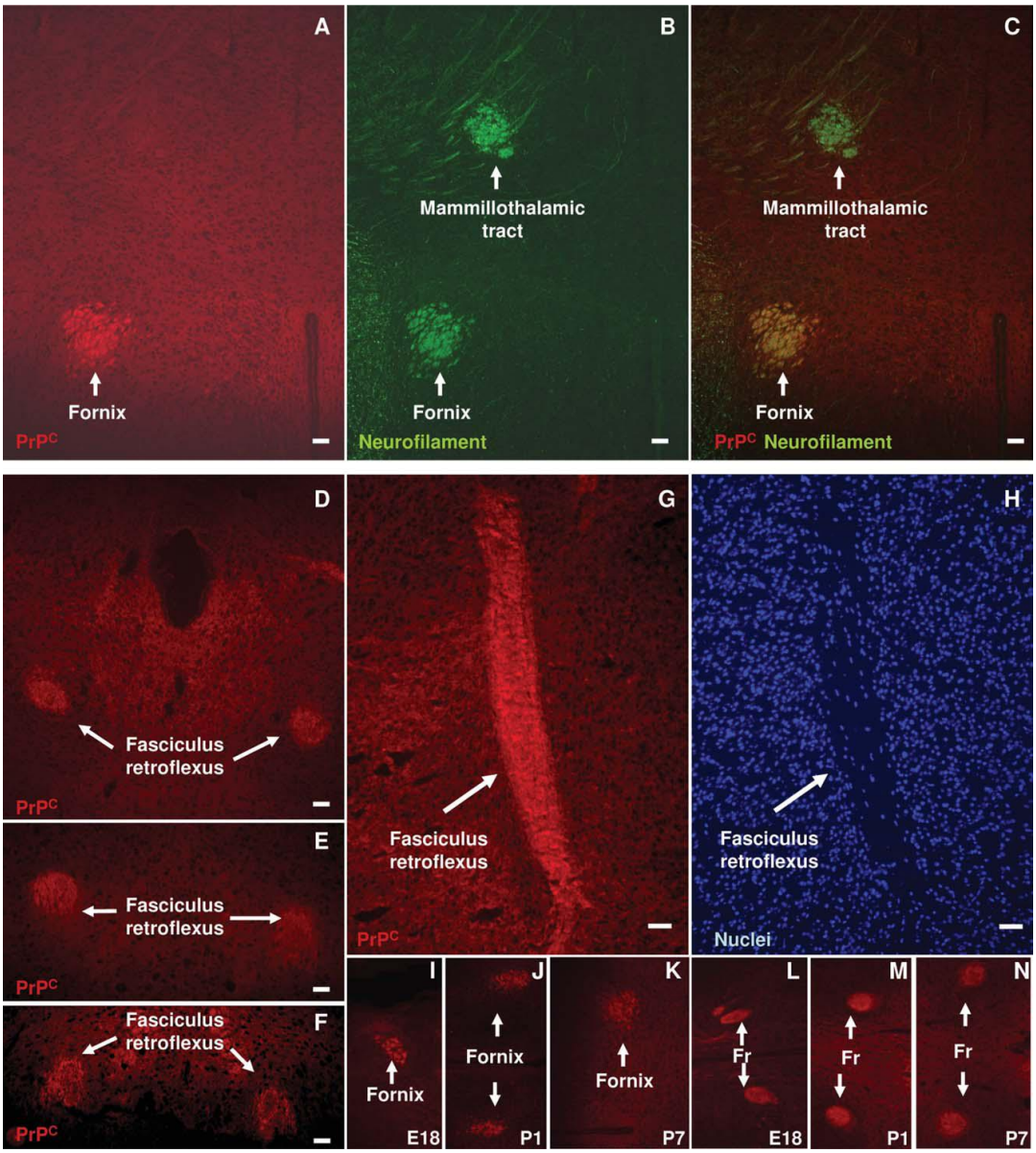

Figure 16. Thalamic expression of PrP^C during development. Immunohistochemical staining for PrP^C (in red; A, C, D–G, I–N) and neurofilament (in green; B, C). A merged image is shown in (C). A–C: At P7 PrP^C is detected in the thalamus, with abundant and specific expression in fornix (A). The specificity of PrP^C expression by this structure is highlighted by the counterstaining of neurofilaments, which labels both the mammillothalamic tract and the fornix (B). Only the fornix shows colocalization of PrP^C and neurofilament signals (in yellow; C). D–H: P7: PrP^C expression is detected also specifically in the fasciculus retroflexus (or habenulointerpeduncular tract). The fasciculus retroflexus expresses PrP^C all along its length, with clear boundaries, highlighted by coronal (D–F) or longitudinal (G) PrP^C staining. Counterstaining of nuclei (in blue; H) underlines the low number of nuclei in this white matter structure. I–N: Developmental PrP^C expression by the fornix and the fasciculus retroflexus (Fr). Both these structures show a progressively increasing level of expression of the protein during development, starting from E18.5 (fornix and Fr, respectively; I, L), to P1 (respectively, J, M), until P7 (respectively, K, N). Scale bars = 50 μm.

Microarray analysis of gene expression during development in *Prnp*$^{+/+}$ and *Prnp*$^{0/0}$ mice

The *Prnp*$^{0/0}$ mice used in our study revealed no overt phenotype (Büeler et al., 1992; Manson et al., 1994), thus PrP^{C} proved not to be essential for the normal development and survival of the animal. However, phenomena of developmental plasticity and genetic compensation may mask the phenotype of PrP^{C} deficient mice (Steele et al., 2007). In order to analyze the potential influence of PrP^{C} on the CNS gene expression profile during neuronal postnatal development, a microarray analysis was performed with cDNA transcribed from total RNA obtained from hippocampi of *Prnp*$^{+/+}$ and *Prnp*$^{0/0}$ mice. I focused this analysis on the hippocampus, in the perspective that the deficiency of PrP^{C}, such as in *Prnp*$^{0/0}$ animals, may be more detrimental in brain regions requiring high levels of expression of the protein during development (*i.e.*, the hippocampus), rather than in regions with a lower physiological expression.

To this purpose, the analysis was performed at two different developmental stages: in newborn animals (day 4 of postnatal development) and in adult mice (3-month-old mice). *Prnp*$^{+/+}$ wildtype mice used were inbred FVB/N mice, whereas *Prnp*$^{0/0}$ mice used were created by backcrossing the original Zurich I mice (Büeler et al., 1992), which were created in a mixed C57Bl6/129 genetic background, to recipient inbred FVB/N mice, thus raising the concern of the transcriptome comparison between mixed genetic backgrounds. Despite the several generations of backcrossing process, it cannot be ruled out that possible genetic differences highlighted by microarray analysis between *Prnp*$^{+/+}$ and *Prnp*$^{0/0}$ mice may be due to the presence of residual C57Bl6/129 alleles, rather than to a direct influence of PrP^{C} presence or absence on the mouse transcriptome. Indeed, although the backcrossing breeding system leads to extensive replacement of unwanted donor strain alleles (C57Bl6/129 in this case) by desired recipient strain genes (FVB/N

in this case), the final congenic strain may still harbour residual genetic contamination of donor strain origin (Krinke, 2000). This genetic contamination may be revealed by very senstitve techniques, such as microarray analysis, and potentially be misinterpreted as differences owed to the differentially expressed PrP^{C}. In order to minimize, at our best, this potential genetic bias, the analysis was performed in two different steps:

- First, by comparing separately the transcriptome profiles of *Prnp*$^{+/+}$ adult and newborn animals, and of *Prnp*$^{0/0}$ adult and newborn animals. This allowed the comparison of the transcriptomes of animals whose genome variability (*Prnp*$^{+/+}$ adult compared to *Prnp*$^{+/+}$ newborn, and *Prnp*$^{0/0}$ adult compared to *Prnp*$^{0/0}$ newborn) may be considered as much fixed as possible. However, other potentially interfering phenomena of genetic drift or variability (*i.e.*, mutations, or residual heterozigosity) cannot be ruled out. This comparison allowed to trace a dynamic frame of gene regulation, from young to adult animals, independently both for *Prnp*$^{+/+}$ and *Prnp*$^{0/0}$ mice. These patterns of expression could be subdivided into two main categories: genes that were up-regulated ("UP") during neuronal development (from newborn to adult animals), and genes that were down-regulated ("DOWN") during the same developmental stage.

- Then the comparison was made between the two differential dynamic frames of *Prnp*$^{+/+}$ and *Prnp*$^{0/0}$ mice. Comparing these two differential dynamic patterns of expression allowed to identify genes that were commonly co-regulated (up- or down-regulated) both in *Prnp*$^{+/+}$ and in *Prnp*$^{0/0}$ mice during development, and genes that showed a differential and unique developmental regulation either in *Prnp*$^{+/+}$ mice or in *Prnp*$^{0/0}$ mice (Figure 17).

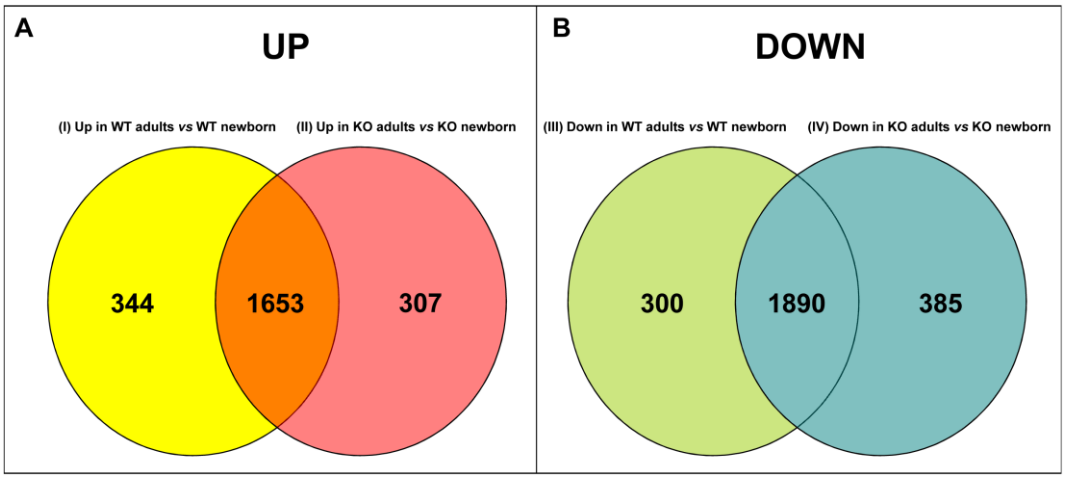

Figure 17. Venn diagrams with gene lists of wildtype (WT) and *Prnp*$^{0/0}$ mice. Venn diagram A (up-regulated genes in WT adults *vs* WT newborn [I] are compared with up-regulated genes in KO adults *vs* KO newborn [II]), and Venn diagram B (down-regulated genes in WT adults *vs* WT newborn [III] are compared with down-regulated genes in KO adults *vs* KO newborn [IV]) show the effect of PrP^{C} expression or deficiency during hippocampal development. The numbers in the space of overlapping circles represent the number of transcripts that show a dynamic developmental expression profile common both to WT and to *Prnp*$^{0/0}$ mice.

To this aim, the following procedure was applied.

Given the large extent of differential expression when comparing the two developmental stages in both genetic backgrounds, and based on the scarce phenotypical variation between *Prnp*$^{+/+}$ and *Prnp*$^{0/0}$ mice, this analysis aimed at establishing proper conditions able to identify genes and pathways whose dynamic behavior (induction or repression during hippocampal development) is altered following PrP^{C} deficiency. Therefore, a fold-change threshold was set, considering only differentially expressed genes whose transcript levels differed at least 1.5 times between newborn and adult mice, whether they were up- or down-regulated. Then, the following four gene lists were drawn:

1. Genes uniquely up-regulated in *Prnp*$^{+/+}$ mice during development ("UP IN WT")

2. Genes uniquely up-regulated in *Prnp*$^{0/0}$ mice during development ("UP IN KO")

3. Genes uniquely down-regulated in *Prnp*$^{+/+}$ mice during development ("DOWN IN WT")

4. Genes uniquely down-regulated in *Prnp*$^{0/0}$ mice during development ("DOWN IN KO")

Finally, the four gene lists above were filtered by excluding genes whose level of induction or repression during hippocampal development was too similar between *Prnp*$^{+/+}$ and *Prnp*$^{0/0}$ mice, *i.e.* the fold changes above was required to differ by at least 10%.

The comparison analysis of the different samples revealed that 344 genes were significantly and uniquely up-regulated in *Prnp*$^{+/+}$ mice, 307 genes were uniquely up-regulated in *Prnp*$^{0/0}$ mice, 300 genes were uniquely down-regulated in *Prnp*$^{+/+}$ mice, and 385 genes were uniquely down-regulated in *Prnp*$^{0/0}$ mice (Figure 17).

Biological pathways regulated by PrP during hippocampal development

To assess the functional role of the above genes, we applied Ingenuity™ Pathways Analysis (IPA) (Ingenuity Systems®, www.ingenuity.com), and DAVID Bioinformatics Resources. For AD-related genetic analysis, we took advantage of GeneCards® GeneALaCart Beta software (http://www.genecards.org/). Detailed below are the results of such functional analyses. The tables of reference in the following sections are combined and listed in the "Appendix" section of this thesis.

1) Genes that are up-regulated during hippocampal development in *Prnp*$^{+/+}$ mice.

Among the genes that are uniquely up-regulated in *Prnp*$^{+/+}$ mice (UP IN WT gene list), the vast majority are related to cell signaling events *via* second messengers. In particular, the most represented pathways are cAMP mediated signaling, retinoic acid

receptor (RAR) activation, NRF2-mediated oxidative stress response and calcium signaling (Table 3). These findings show that among the common developmentally-regulated genes, PrP^C can specifically influence the expression of genes involved in signal transduction. PrP^C has indeed shown to be involved in cell signaling events (Mouillet-Richard et al., 2000) through the activation of different enzymes and amplification of the signal.

Moreover, genes belonging to the Ras/Rab family and protein kinases are up-regulated in *Prnp*$^{+/+}$ mice (Table 4). The former are small GTPases that mediate signal transduction *via* GTP-binding, whereas the latter are kinases involved in signal transduction through phosphorylation of different substrates.

In adult life, PrP^C is shown to have a mainly synaptic localization (Fournier et al., 1995; Herms et al., 1999; Moya et al., 2000a), and to be involved in synaptic transmission (Collinge et al., 1994; Carleton et al., 2001; Curtis et al., 2003). Thus, I also looked at the gene expression of transcripts belonging to the synaptic compartment, and was able to identify several genes involved in synaptic transmission that were up-regulated in *Prnp*$^{+/+}$ mice, among which ionic channels and ionic transporters (Table 5). These genes affect the transmembrane potential of the neuronal membrane, and also affect some synaptic properties, such as long-term potentiation. The positive regulation of these genes mediated by PrP^C during development is suggestive of a potential role for PrP^C in mediating the correct structuring and functioning of neuronal connections during CNS development.

Since PrP^C undergoes conformational changes that cause prion disease, I was also interested in identifying the biological correlation between PrP^C expression and the genes, so-called chaperones, involved in protein folding and unfolding. The performed

analyses revealed that a cluster of genes involved in chaperone-mediated protein folding is up-regulated in *Prnp*$^{+/+}$ mice (Table 6). This finding is particularly intriguing as it may establish a direct correlation between PrP^{C} expression and chaperone genes expression.

Another important factor in the biology of prion disease is the clearance of prion aggregates from the cellular membrane; in general the ubiquitin-proteasomal system (UPS) is a key point for this function in all major protein-aggregation neurodegenerative diseases (Moore et al., 2003; Lim and Tan, 2007; Upadhya and Hegde, 2007; Whatley et al., 2008). The microarray analysis revealed an up-regulation of genes involved in the ubiquitin-proteasomal system in *Prnp*$^{+/+}$ mice (Table 7), and a concomitant down-regulation of genes involved in the ubiquitin-proteasomal system in *Prnp*$^{0/0}$ mice (see Table 19). This finding points at PrP^{C} as a positive regulator of the ubiquitin-proteasomal system, and may shed additional light on the central role of PrP^{C} in the biology of prion disease and other neurodegenerative disorders.

2) Genes that are up-regulated during hippocampal development in *Prnp*$^{0/0}$ mice.

In general, among the genes that are uniquely up-regulated in *Prnp*$^{0/0}$ mice (UP IN KO gene list), I could find an up-regulation of cytosolic signaling pathway genes (Table 8) and of genes related to cell death signaling, in particular neuronal cell death (Table 9). This finding may explain the increased susceptibility of *Prnp*$^{0/0}$ mice to neuronal damage, such as ischemic brain injury (McLennan et al., 2004), serum deprivation (Kim et al., 2004), seizures (Walz et al., 1999) and oxidative stress (Brown et al., 1997b; White et al., 1999). Up-regulation of genes involved in neuronal cell death can make neurons more susceptible to toxic stimuli from the external environment.

Genes that are uniquely regulated in *Prnp*$^{0/0}$ mice during development are the most intriguing. In fact, an up-regulation of genes involved in neuregulin signaling is found in these mice (Table 10). Neuregulins are members of the epidermal growth factor family, and are ligands for the ErbB receptors (Falls, 2003; Birchmeier, 2009). Binding of neuregulins to ErbB receptors stimulate the dimerization of the receptors, their autophosphorylation and in turn the activation of intracellular signaling cascades involved in development, maintenance and repair of the nervous system (Holbro and Hynes, 2004). Indeed, both PrP^{C} and neuregulins can trigger intracellular signaling cascades mediated by kinases such as Src kinases. In *Prnp*$^{0/0}$ mice the up-regulation of genes belonging to signaling pathways involved in neuronal development and function may suggest a potential role for PrP^{C} in controlling the expression of neurodevelopment signaling pathways, such as the neuregulin one.

The *Prnp*$^{0/0}$ mice have been reported to carry defects in synaptic plasticity (Colling et al., 1996; Herms et al., 2001; Carleton et al., 2001; Mallucci et al., 2002), thus this analysis focused also on genes related to synaptic activity, and it was possible to identify genes affecting this process (Table 11); in particular, a voltage-gated chloride channel-related gene group was found to be up-regulated in *Prnp*$^{0/0}$ mice (Table 12) compared to their wildtype counterpart. Thus PrP^{C} can act not only as direct modulator of synaptic events, but also in an indirect way by modulating the expression of other synaptic and membrane components.

Since PrP^{C} interacts with adhesion molecules and can mediate cell-cell adhesion, I searched for up-regulated genes involved in cell-to-cell interaction, and indeed detected genes involved in cell adhesion (Table 13). Moreover, up-regulated genes involved in neurite outgrowth, axon guidance and lamellipodia formation were found (Table 13).

In *Prnp*$^{0/0}$ mice, developmentally up-regulated genes related to calcium homeostasis were also detected (Table 14).

3) Genes that are down-regulated during hippocampal development in *Prnp*$^{+/+}$ mice. This category (DOWN IN WT gene list) represents genes that are uniquely down-regulated during neuronal development in *Prnp*$^{+/+}$ mice, but do not display the same dynamic changes in *Prnp*$^{0/0}$ mice. Bioinformatics analysis detected weak functional clusterization among the different members belonging to this gene list. These findings hint at PrP^{C} as a positive gene expression regulator, rather than a negative regulator during neuronal development. Indeed, genes belonging to the metabolism of carbohydrate and of small molecules (such as nucleotides) were identified as a functional cluster by bioinformatics analysis (Table 15). Interestingly, genes belonging to the Notch signaling pathway (*Notch4*, *Dll3*, *Mnfg* and *Rbpj*) were down-regulated during hippocampal development in wildtype mice. Notch signaling is an evolutionarily conserved mechanism for cell-cell interaction, is involved in cell fate choices (Talora et al., 2008), and recent findings report a strict correlation between prion-mediated neurodegeneration and *Notch1* increased expression and signaling (Ishikura et al., 2005; Spilman et al., 2008). Thus, this finding suggests that a physiological expression of PrP^{C} seems to reduce Notch-related signaling pathway genes expression, whereas in prion diseases, or in *Prnp*$^{0/0}$ mice, where a lack of PrP^{C} function can occur, the genetic expression of these genes is stimulated.

4) Genes that are down-regulated during hippocampal development in *Prnp*$^{0/0}$ mice. This genes group (DOWN IN KO gene list) contains transcripts down-regulated exclusively in *Prnp*$^{0/0}$ mice during neuronal development, whereas not in *Prnp*$^{+/+}$ mice. PrP^{C} deficiency negatively influences the regulation of genes involved in embryonic

development and differentiation, and nervous system development and function (Table 16). PrP^C possesses an embryonic and postnatal pattern of expression which is developmentally regulated (Mobley et al., 1988; Lazarini et al., 1991; Manson et al., 1992; Salès et al., 2002; Tremblay et al., 2007), and potentially acts as a neurotrophic factor during CNS development. The lack of PrP^C, as in *Prnp*$^{0/0}$ mice, may in turn be a regulatory step for the expression of other genes involved in CNS development. Considering that PrP^C is a protein anchored to the cell membrane and is known to interact with different cell adhesion molecules (Rieger et al., 1997; Graner et al., 2000; Gauczynski et al., 2001; Schmitt-Ulms et al., 2001), a possible involvement of PrP^C expression on the regulation of expression of other cell membrane adhesion proteins is of interest. Indeed, a correlation between the lack of PrP^C and the down-regulation of cadherins could be found (Table 17). Cadherins are adhesion molecules playing an important role in calcium-mediated cell adhesion (Nelson, 2008). Interestingly, a recent work (Málaga-Trillo et al., 2009) shows how PrP^C can regulate embryonic cell adhesion during gastrulation, as well as E-cadherin function by modulating its processing or its transport to the cell membrane, possibly *via* the activation of fyn-mediated signaling. Thus, it would be tempting to affirm that PrP^C acts as an adhesion and signaling protein, and that these properties also influence the function and the expression of other adhesion molecules.

PrP^C is able to bind divalent ions such as copper and zinc (Brown et al., 1997a; Walter et al., 2007). Therefore a possible correlation between PrP^C expression and the regulation of other genes involved in ion homeostasis was considered in this analysis. A large cluster (Table 18) of functionally-related genes involved in transition metal ion binding was found. This finding shows how the expression of PrP^C may in turn influence the expression of genes involved in metal ion homeostasis.

Another functional cluster of genes down-regulated in *Prnp*$^{0/0}$ during development is related to the ubiquitin system (Table 19). Ubiquitination occurs when a moiety of ubiquitin is attached to a protein, most prominently for proteasomal degradation. Increasing evidence suggests a role for the ubiquitin-proteasome system (UPS) in prion disease. Both WT PrP^{C} and disease-associated PrP isoforms accumulate in cells after proteasome inhibition leading to increased cell death, and abnormal beta-sheet-rich PrP isoforms have been shown to inhibit the catalytic activity of the proteasome (reviewed in (Deriziotis and Tabrizi, 2008)). The finding that *Prnp*$^{0/0}$ mice show a developmentally deregulated UPS pathway points at PrP^{C} as a potential regulator of this system. Indeed, the loss of PrP^{C} function when converted to PrP^{Sc}, or its lack in *Prnp*$^{0/0}$ mice, can alter the expression of genes involved in the UPS, and thus alter the correct physiological expression and function of this system.

Comparative analysis of adult *Prnp*$^{+/+}$ and adult *Prnp*$^{0/0}$ mice. A recent study (Rangel et al., 2007) reports a microarray analysis on the comparison of hippocampal RNA among wildtype, *Prnp*$^{0/0}$ and PrP^{C}-overexpressing adult mice. Then, an analysis to identify genes that are differentially expressed in adult *Prnp*$^{0/0}$ mice, by comparing them with adult *Prnp*$^{+/+}$ specimens, was carried out. 83 significantly up-regulated genes and 62 significantly down-regulated genes were identified (Table 20).

In the up-regulated genes group an enrichment in genes related to cell-cell adhesion (like lymphocyte antigen 6 complex locus A, junction adhesion molecule 3, lymphocyte antigen 6 complex, locus C2; lymphocyte antigen 6 complex locus C1, CD14 antigen); in the down-regulated genes group we identified an enrichment in genes related to metal ion binding (like tripartite motif-containing 39; RNA binding motif protein 26; zinc finger CCCH type containing 11A; mitogen-activated protein kinase kinase kinase 7 interacting protein 2) and to protein kinase activity (like Rho-associated coiled-coil

containing protein kinase 1; cell division cycle 7 *S. cerevisiae*; conserved helix-loop-helix ubiquitous kinase; protein kinase, cGMP-dependent, type I 1) could be highlighted. These final results differed from those reported in the cited paper. It cannot be ruled out that this may be due to dissimilar experimental procedures, to variations in the age of the animals, or to the different genetic background of the animals used in the two studies (FVB/N in this study, C57Bl/6 in their study).

AD-related genes regulated by PrP^C during hippocampal development and effects on Tau phosphorylation. Recent findings point at an involvement of the cellular PrP in the etiology of AD (Checler and Vincent, 2002; Laurén et al., 2009; Parkin et al., 2007; Spilman et al., 2008; Vincent et al., 2009). *Prnp*$^{0/0}$ adult gene expression profile was compared to *Prnp*$^{0/0}$ young animals profile, and significantly deregulated genes were subjected to GeneCards® GeneALaCart Beta software (http://www.genecards.org/), in order to identify potential regulation of AD-related gene mediated by the absence of PrP. 18 up-regulated genes and 12 down-regulated AD-related genes were found, among which *Ch25h*, *S100a9*, *Kcnip3*, *Grin2b*, *Cdk5r1*, *Cdk5*, *Psen1* and *Sod2* to be up-regulated, whereas genes such as *Gsk3β* to be down-regulated in *Prnp*$^{0/0}$ mice (Table 21). Bioinformatics analysis revealed how the amyloid processing pathway comprises part of the most-known AD-related genes, and in particular genes affecting tau phosphorylation (Figure 18).

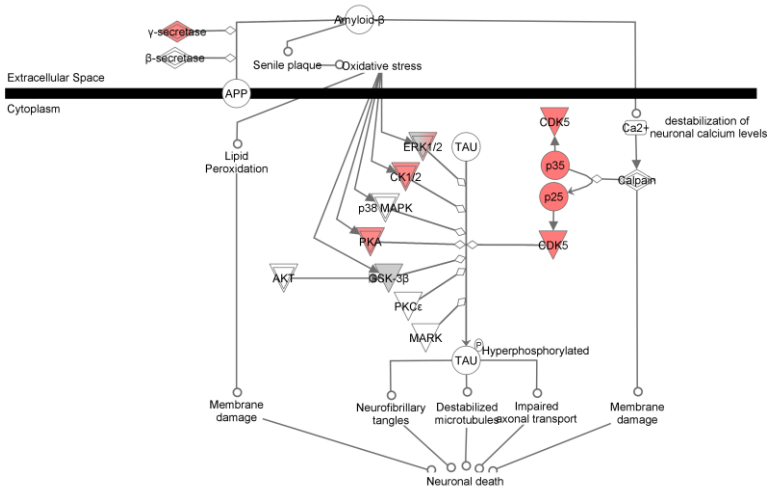

Figure 18. Tau phosphorylation genes affected by PrP^C expression during hippocampal development. Genes affecting APP processing and Tau phosphorylation (in pink and grey) are found to be differentially regulated by PrP^C expression during hippocampal development. Adapted from Ingenuity Pathways Analysis (Ingenuity Systems®, www.ingenuity.com).

Hyperphosphorylated tau protein is the main component of the paired helical filaments (PHF), the structural constituents of neurofibrillary tangles in AD (Bretteville and Planel, 2008). An explanation of the biological mechanisms through which tau becomes abnormally phosphorylated in AD is still missing (Hanger et al., 2009), and the relationship between amyloid deposition and neurofibrillary tangle formation is a central issue in the pathogenesis of AD. Due to the differences in the expression levels of genes affecting tau phosphorylation between wildtype and *Prnp*$^{0/0}$ mice (Figure 18), we next investigated whether the levels of total-tau and phosphorylated-tau were affected in our animal models at the different experimental ages (Figure 19). Total tau protein is known to decrease from young to adult animals (Charrière-Bertrand and Nunez, 1992). Accordingly, we could highlight a similar decrease in the total expression of tau proteins, from newborn to adult animals, both in wildtype and in *Prnp*$^{0/0}$ hippocampus (Figure 19 A). However, while the levels of phosphorylated tau were similar in adult wildtype and in adult *Prnp*$^{0/0}$ mice, the levels of phosphorylated tau

were significantly higher in newborn *Prnp*$^{0/0}$ mice if compared to newborn wildtype animals (Figure 19 B, 19 C).

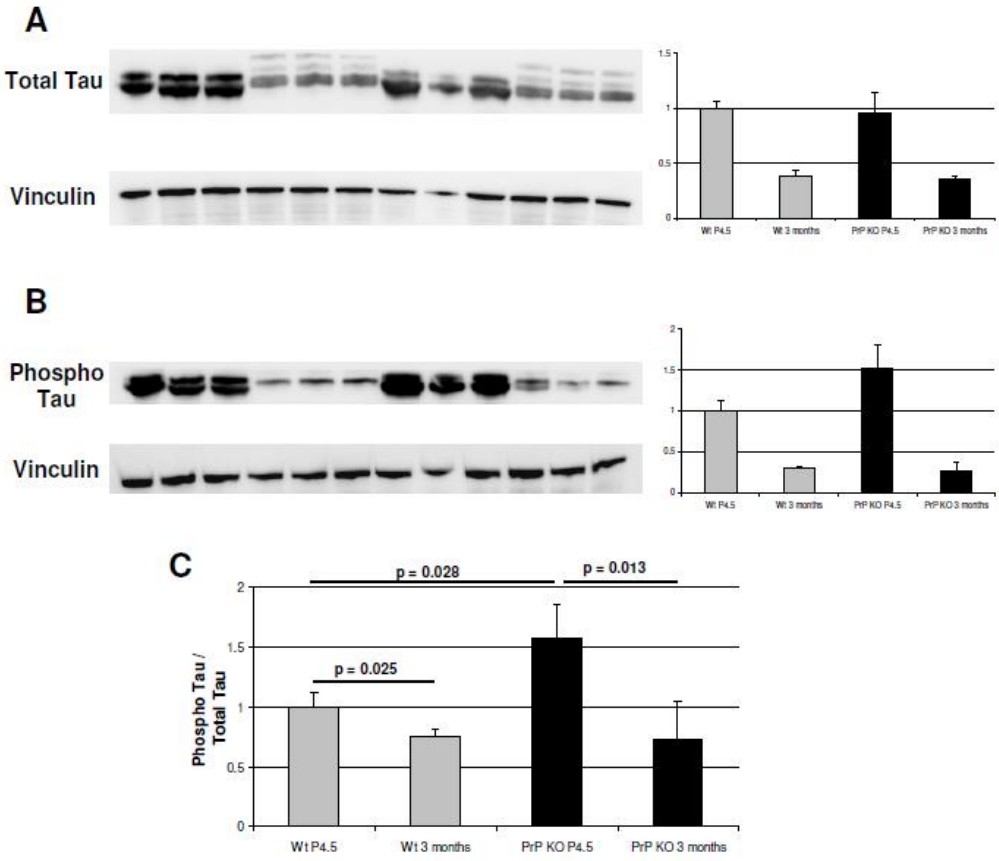

Figure 19. Tau phosphorylation levels in young and adult, wildtype and *Prnp*$^{0/0}$ mice.
The levels of total Tau protein and its phosphorylated form were analyzed in wildtype and *Prnp*$^{0/0}$ mice. (A) Total Tau protein in young (P4.5) and adult (3 months), wildtype (Wt) and *Prnp*$^{0/0}$ (PrP KO) mice (n=3 for each genotype and age). The quantification of the western blot revealed the same trend of decreasing levels of total tau protein from young to adult animals, both for wildtype and *Prnp*$^{0/0}$ mice. (B) Phosphorylated form of Tau protein in young and adult, wildtype and *Prnp*$^{0/0}$ mice (n=3 for each genotype and age). The quantification revealed a decreasing level of phospho-tau protein from young to adult animals, yet in PrP KO young animals (P4.5) a higher level of the phosphorylated form of the protein was found, compared to their wildtype littermates. (C) The levels of phosphorylated tau were significantly ($p = 0.028$) higher in newborn *Prnp*$^{0/0}$ mice if compared to newborn wildtype animals. The levels of phosphorylated-tau protein were normalized on the levels of total-tau protein. Values presented: mean ± SD of three animals.

Besides being highly phosphorylated in AD brain, tau is also highly phosphorylated in normal developing brain, in the window of age of neurite outgrowth (Kenessey and Yen, 1993; Yu et al., 2009), probably for its function in keeping a high dynamics of microtubule assembly-disassembly during brain development. These results indicate that PrP^{C} negatively influences the phosphorylation levels of tau during the first

postnatal brain development, while it has no effect on tau phosphorylation in adult brain, when phosphorylation of tau is physiologically at a steady-state. This finding may in part shed new light on the developmental functions linked to PrP^C. Moreover, an involvement of PrP^C on the regulation of tau phosphorylation could imply a novel correlation between AD and prion biology.

Confirmation of microarray data

For validation of the results obtained by microarray analysis, real-time RT-PCR was carried out on the original RNA samples. Changes in gene expression levels of the selected transcripts were normalized to the gene expression of beta-Actin.

Among the selected transcripts, however, we could confirm by real-time RT-PCR only some of them (Figure 20). Most of the genes whose expression is negatively influenced by the deficiency of PrP^C are involved in embryonic development and differentiation, and nervous system development and function (Table 16). One example is *Tbx18*, a gene affecting limb development (Kraus et al., 2001). Downregulation during postnatal development was observed for $Prnp^{0/0}$ mice, while for wildtype mice our microarray analysis did not reveal any statistical change. This different gene regulation was confirmed by real-time RT-PCR (Figure 20 A).

An unpregulation, in wildtype mice, of the adenylate cyclase 8 gene (*adcy8*) as observed by our microarray study was confirmed by real-time RT-PCR: while there is an increase in adcy8 gene expression levels during post-natal development in wildtype mice, in $Prnp^{0/0}$ mice we could not detect any significant variation in gene expression level between newborn and adult animals (Figure 20 B). The same trend of regulation, identified by our microarray anaylsis, for the ionotropic glutamate receptor subunit NMDA2B (*grin2b*) was confirmed by real-time RT-PCR (Figure 20 C).

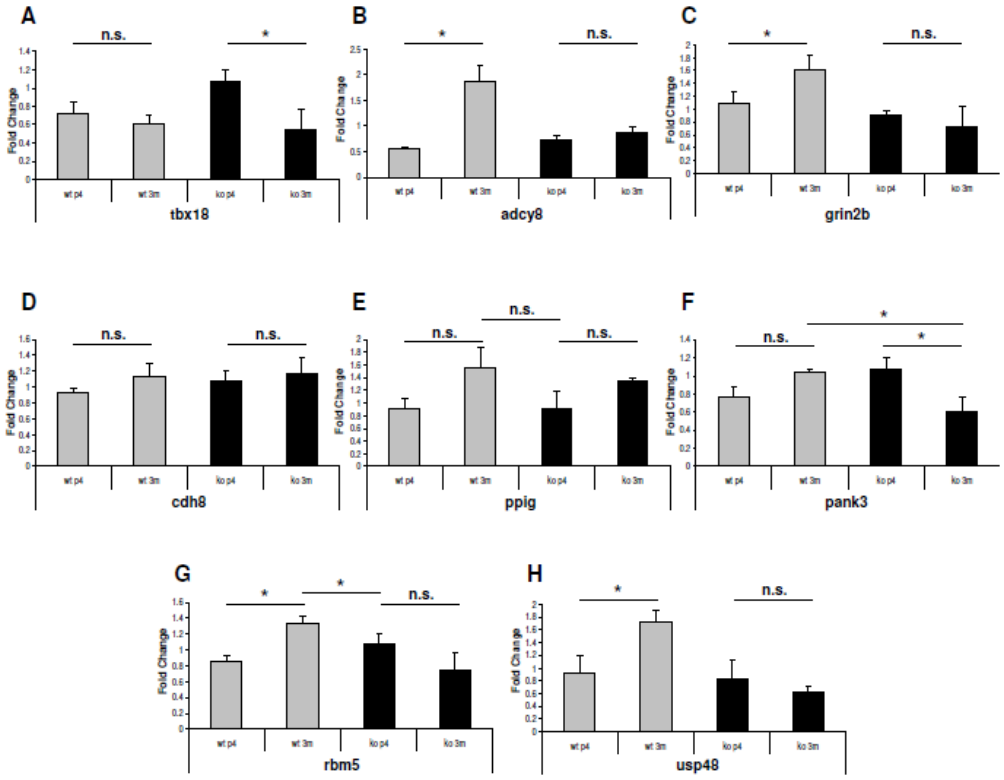

Figure 20. Analyses of gene expression of selected candidate genes by real-time RT-PCR. Expression levels of individual transcripts. Shown are the results from RT-PCR analysis of young (P4.5) and adult (3 months), wildtype (Wt, in grey) and *Prnp*$^{0/0}$ (PrP KO, in black) mice. Values presented: mean of fold changes ± SD of three animals. A: tbx18; B: adcy8; C: grin2b; D: cdh8; E: ppig; F: pank3; G: rbm5; H: usp48. Statistical significance was determined by using Student's t-test analysis; * = $p \leq 0.05$. n.s. = not statistically significant.

However, for other genes like *cdh8* and *ppig*, we could not confirm our microarray data by real-time RT-PCR (Figure 20 D, E). This discrepancy between the microarray and the real-time RT-PCR results could be explained by the relatively low differences of the fold change ratios between wildtype and *Prnp*$^{0/0}$ mice. Moreover, genes like *pank3*, *rbm5* and *usp48* show different trends of regulation after microarray and real-time RT-PCR analysis (Figure 20 F, G and H): *pank3* gene was found to be downregulated in adult wildtype mice compared to young wildtype mice by microarray analysis (DOWN IN KO gene list), whereas real-time RT-PCR showed the opposite trend, i.e. an increase in the gene expression level during postnatal development, although without reaching significance (Figure 20 F); *rbm5* gene was found to be downregulated in adult wildtype

mice compared to young wildtype mice by microarray analysis (DOWN IN KO gene list), whereas by real-time RT-PCR analysis we could find a significant increase in the gene expression level (Figure 20 G); finally, *usp48* gene was found to be downregulated in adult *Prnp*$^{0/0}$ mice compared to young *Prnp*$^{0/0}$ mice by microarray analysis while its level of expression in adult wildtype mice compared to young wildtype did not significantly change (DOWN IN KO gene list), whereas by real-time RT-PCR we could identify a significant increase in the gene expression level during wildtype postnatal development, and no significant change during postnatal development in *Prnp*$^{0/0}$ mice (Figure 20 H).

Generally, our real-time RT-PCR data for these selected genes support the stability of the transcriptome in the hippocampus of *Prnp*$^{0/0}$ mice, and point at possible influences due to the deficiency of PrP^{C} in cellular mechanisms other than gene transcription modification. Moreover, as *Prnp*$^{0/0}$ mice show no gross phenotypical differences in physiological conditions, but reveal stronger phenotypes in stressful or challenging conditions (Criado et al., 2005; Sánchez-Alavez et al., 2007; Sanchez-Alavez et al., 2008; Lobão-Soares et al., 2008), we could also argue that in physiological conditions PrP^{C} is in a resting/silent state, and that only in a challenging environment PrP^{C} actual function can be switched on. Thus, it would be interesting to perform new gene expression studies in such conditions, in order to unveil possible influences of PrP^{C} on the cellular transcriptome.

NRG1 processing is developmentally regulated in the sciatic nerves.

Recently, mice lacking the PrP (*Prnp*$^{0/0}$ mice) were shown to manifest a late-onset chronic demyelinating polyneuropathy (Bremer et al., 2010). Interestingly, this phenotype was evident only in the PNS of aged *Prnp*$^{0/0}$ mice. This suggests an essential role for PrP^{C} in peripheral myelin maintenance during aging of the individual. The protein NRG1 is one of the major axonal cues acting as myelination-promoting factor during PNS development (Garratt et al., 2000a; Jessen e Mirsky, 2005; Nave e Salzer, 2006; Newbern e Birchmeier, 2010). Alteration in the processing of NRG1 has been linked to deficit in correct myelination mechanisms (Willem et al., 2006; Hu et al., 2006), thus showing that the resulting cleaved fragments, rather than the full length protein itself, are the active key instruction for a physiological myelination process. In order to analyze the processing of NRG1 during PNS development and maturation, a time-course analysis of NRG1 expression was performed in total protein extracts from mouse sciatic nerves at different ages (postnatal days P15, P30, P90 and P120) (Figure 21 A). During this time course, the levels of full length NRG1 (NRG1-FL) significantly decreases with age, while the levels of the cleaved C-terminal fragment of NRG1 (NRG1-CTF) significantly increases up to stage P90, reaching then a steady-state level (Figure 21 B). Similar results were obtained with the anti NRG1 - N-terminal fragment antibody (data not shown). This finding suggests that active processing of NRG1 is taking place and increasing during postnatal development and, once the PNS reaches full maturation, NRG1 is subjected to a stable and continuous cleavage during adulthood.

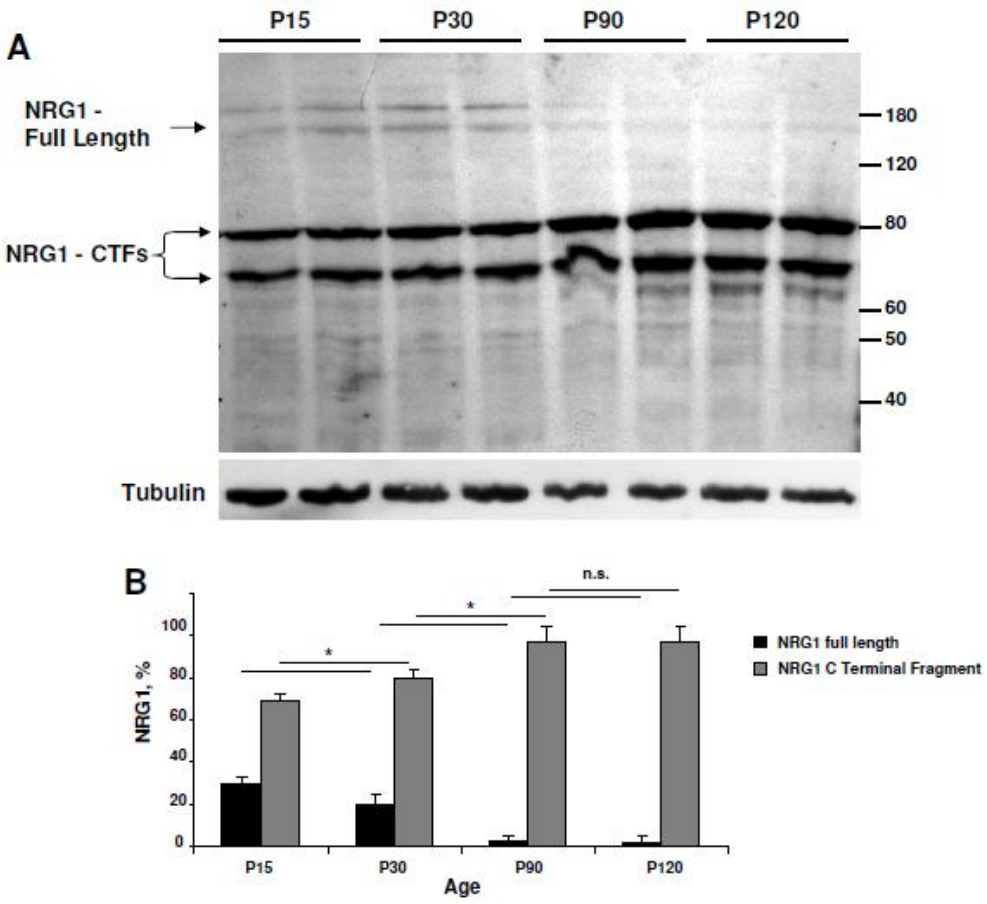

Figure 21. The processing of NRG1 is developmentally regulated in the sciatic nerve. (A) Sciatic nerves were excised from mice at different developmental stage (n = 4, for each age) and protein extract (50 µg/lane) was analyzed for NRG1 content. We used an anti-NRG1 - C-terminal antibody, by which we can recognize full length NRG1 and the NRG1 - C-terminal fragments after cleavage (NRG1-CTFs). (B) Quantification of the western blot; values of NRG1 full length and of NRG1 - C-terminal fragment were normalized on beta-tubulin levels, and expressed as percentage of total neuregulin protein. Values are expressed as mean ± SD; * = $p \leq 0.05$; n.s. = not statistically significant.

NRG1 cleavage is altered in the PNS of aged, but not young, *Prnp*$^{0/0}$ mice.

In order to verify whether the cleavage of NRG1 could be defective in *Prnp*$^{0/0}$ mice, the levels of NRG1-FL and NRG1-CTF in the sciatic nerves of wildtype mice and of their *Prnp*$^{0/0}$ littermates at different ages were compared. According to the authors of this work (Bremer et al., 2010), no significant difference in the levels of NRG1-FL and NRG1-CTF could be detected during early postnatal development, at P15 (Figure 22 A)

and at P30 (Figure 22 B). However, by increasing the age of the animals under investigation, a decreasing level of NRG1-CTF at 5 months of age (P150) in *Prnp*$^{0/0}$ mice was highlighted, yet not reaching statistical significance (Figure 22 C). Finally, by analyzing 1-year-old mice sciatic nerves, a significant lower level of the NRG1-CTF in *Prnp*$^{0/0}$ mice was detected compared to their wildtype counterpart (Figure 22 D).

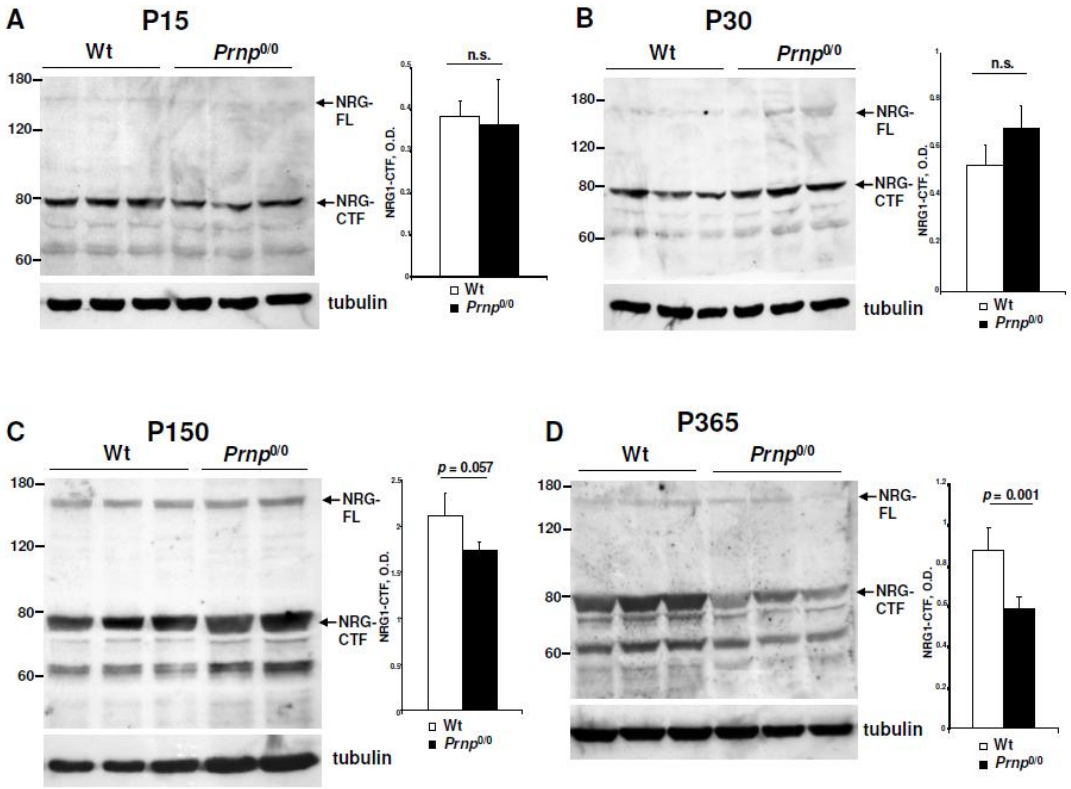

Figure 22. The proteolytic cleavage of NRG1 is affected in aged, but not young, *Prnp*$^{0/0}$ mice sciatic nerves. Comparison between protein extracts of sciatic nerves of P15 (A), P30 (B), P150 (C), and P365 mice (D) from wildtype (Wt) and *Prnp*$^{0/0}$ mice. (A) Western blot of sciatic nerve protein extracts of P15 *Prnp*$^{0/0}$ (n=3) and Wt (n=5) mice using an antibody recognizing the full length (NRG-FL) and the C-terminal fragment after cleavage (NRG-CTF) of NRG1. Quantification of the NRG-CTF was normalized to the expression levels of beta-tubulin (right panel). (B) Western blot of sciatic nerve protein extracts of P30 *Prnp*$^{0/0}$ (n=3) and Wt (n=3) mice using an antibody recognizing the full length (NRG-FL) and the C-terminal fragment after cleavage (NRG-CTF) of NRG1. Quantification of the NRG-CTF was normalized to the expression levels of beta-tubulin (right panel). (C) Western blot of sciatic nerve protein extract of P150 *Prnp*$^{0/0}$ (n=3) and Wt (n=4) mice using an antibody recognizing the full length (NRG-FL) and the C-terminal fragment after cleavage (NRG-CTF) of NRG1. Quantification of the NRG-CTF was normalized to the expression levels of beta-tubulin (right panel). (D) Western blot of sciatic nerve protein extract of P365 *Prnp*$^{0/0}$ (n=5) and Wt (n=9) mice using an antibody recognizing the full length (NRG-FL) and the C-terminal fragment after cleavage (NRG-CTF) of NRG1. Quantification of the NRG-CTF was normalized to the expression levels of beta-tubulin (right panel). Values are expressed as mean ± SD; n.s. = not statistically significant.

Thus, during early postnatal PNS development *Prnp*$^{0/0}$ and wildtype mice show no differences in NRG1 processing; in contrast, with aging, *Prnp*$^{0/0}$ mice show a chronically defective processing of NRG1 protein.

PrP^{C} stimulates ectodomain shedding of NRG1 in cell cultures.

The lack of PrP^{C} in sciatic nerves reduces the levels of NRG1-cleaved fragments. In order to verify whether high levels of PrP^{C}, on the contrary, could enhance NRG1 processing, I took advantage of N2a and N2a-CL3 cell lines. N2a-CL3 cell line consists of N2a cells stably transfected with full-length mouse PrP^{C} (Ghaemmaghami et al., 2010) to express higher level of PrP^{C} than normal N2a cells. The higher levels of PrP^{C} in cell lysates of N2a-CL3 cells compared to N2a cells was confirmed (Figure 23 A). Then, NRG1 levels in cell lysates were searched. In N2a-CL3 cell lysates, compared to N2a cell lysates, there was a significant lower amount of total NRG1-FL, in contrast to a higher amount of the NRG1 - N-terminal fragment (NRG1-NTF) (Figure 23 A, B). I then checked in the CM of N2a and N2a-CL3 cells the presence of NRG1-NTF and could identify a significant higher amount of NRG1-NTF in the CM of N2a-CL3 cells compared to the CM of N2a cells (Figure 23 A, C). These results suggest that high levels of PrP^{C} potentiate NRG1 cleavage in intracellular compartments and that, after this processing, the NRG1-cleaved fragment is released in the extracellular environment.

Prnp$^{0/0}$ mice show a defective cleavage also of NRG3.

PrP^{C} was previously demonstrated to regulate BACE1-mediated cleavage of APP, a molecule that plays a central role in the pathogenesis of Alzheimer's disease (AD) (Parkin et al., 2007). As BACE1 is known to cleave other different substrates, I was prompted to verify whether PrP^{C} could regulate the cleavage of other BACE1 substrates. The protein NRG3 is another member of the neuregulins family (Zhang et al., 1997), and was shown to share the same BACE1 cleavage site of NRG1, and to be directly processed by BACE1 (Hu et al., 2008). Thus, I investigated whether the levels of NRG3 could also change between wildtype and *Prnp*$^{0/0}$ mice sciatic nerves. Similarly to the brains of BACE1 null mice (Hu et al., 2008), a significant accumulation of unprocessed full length NRG3 in the sciatic nerves of *Prnp*$^{0/0}$ mice was detected, when compared to their wildtype counterpart (Figure 24). Thus, also NRG3 processing is affected in the PNS of mice lacking PrP.

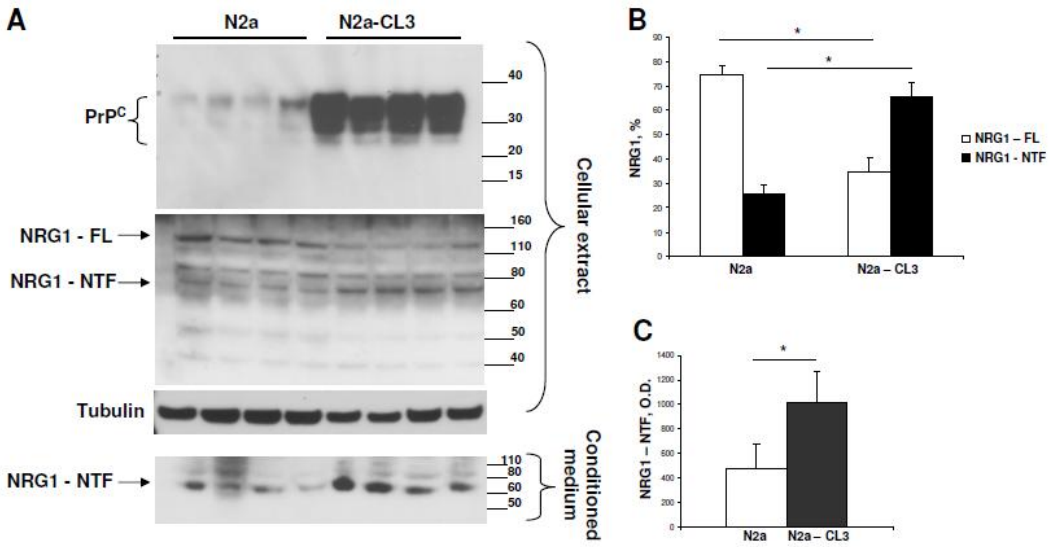

Figure 23. The shedding of NRG1 ectodomain is enhanced by overexpression of PrP^C in cell lines. N2a and N2a-CL3 cells stably overexpressing PrP^C were cultured in serum-free medium, and cellular extract and conditioned medium were prepared and analyzed for the levels of NRG1 using an antibody recognizing full length (NRG1-FL) and the N-terminal fragment on NRG1 after cleavage (NRG1-NTF). (A) Western blots of cell lysates and conditioned medium from N2a and N2a-CL3. We confirmed the overexpression of PrP^C in N2a-CL3 cell lysates, compared to N2a cell lysates (upper panel). Cell lysates of N2a-CL3 cells show a reduced level of NRG1-FL and a concomitant increased level of NRG1-NTF, if compared to N2a cell lysates (central panel). Conditioned media were also analyzed for the levels of NRG1-NTF (lower panel). (B) Quantification of NRG1-FL and NRG1-NTF in the cell lysates of N2a (left) and N2a-CL3 (right) cells. Values were normalized to the levels of beta-tubulin, and expressed as percentage of total NRG1 protein. (C) Quantification of the NRG1-NTF in the conditioned medium of N2a (white) and N2a-CL3 (black) cells. Values are expressed as mean ± SD; * = $p \leq 0.05$.

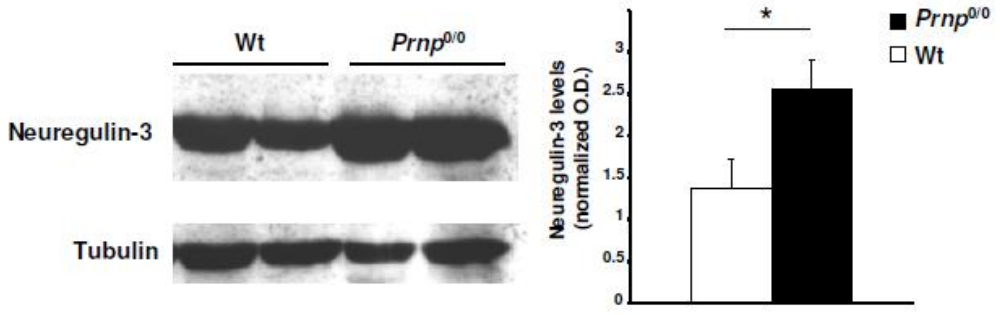

Figure 24. Unprocessed NRG3 accumulates in the sciatic nerves of *Prnp*$^{0/0}$ mice. Sciatic nerve protein extracts of 1-year-old wildtype (Wt) (n=9) and *Prnp*$^{0/0}$ (n=5) mice were investigated for the levels of full length NRG3. The amount of full length NRG3 was analyzed quantitatively and normalized to the expression level of beta-tubulin (right panel). Values are expressed as mean ± SD; * = $p \leq 0.05$.

Fyn and ERK kinases signaling pathways are not affected in *Prnp*$^{0/0}$ mice sciatic nerves.

In neuregulin canonical signaling pathways, mature cleaved NRG1 binds to and induces dimerization of ErbB receptors, which in turn activate auto-phosphorylation of the receptors themselves and the subsequent downstream activation of intracellular signaling pathways (Mei and Xiong, 2008). Among these, the extracellular signal-regulated kinase (ERK) (Tansey et al., 1996; Si et al., 1996) and Fyn kinase (Bjarnadottir et al., 2007) pathways can be activated. Moreover, PrP^{C} was also shown to signal through the same signaling pathways (Mouillet-Richard et al., 2000; Toni et al., 2006). In addition, Fyn kinase is known to regulate CNS (Umemori et al., 1994) and, recently, also PNS myelination (Hossain et al., 2010). Nevertheless, Bremer *et al.* (Bremer et al., 2010) could not detect any alteration of Akt and ERK kinases phosphorylation during PNS myelination (age P10 and P30). The convergence of these signaling pathways led me anyway to investigate whether there could be an aberrant activation of Fyn or ERK kinases in aged *Prnp*$^{0/0}$ mice compared to their wildtype counterpart. However, no alteration of ERK or Fyn kinases activation in the sciatic nerves between aged wildtype and *Prnp*$^{0/0}$ mice could be detected (Figure 25). This finding suggests that these signaling pathways are still active in aged *Prnp*$^{0/0}$ mice as in physiologically myelinated nerves, and thus are not influenced by the lack of PrP^{C} or by a deficit in NRG1 processing.

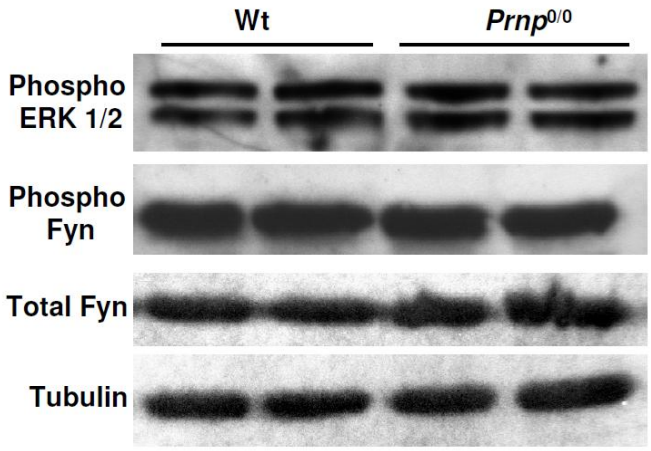

Figure 25. ERK and Fyn kinases signaling pathways are not altered in the sciatic nerves of *Prnp*$^{0/0}$ mice. Western blot of protein extracts from sciatic nerves of 1-year-old wildtype (Wt) (n=9) and *Prnp*$^{0/0}$ (n=5) mice. The levels of total Fyn protein, of phosphorylated Fyn and phosphorylated ERK proteins do not significantly change between wildtype and *Prnp*$^{0/0}$ mice.

Neuregulins processing is not altered in the CNS of *Prnp*$^{0/0}$ mice.

A correlation between the lack of PrP^{C} and a defective processing of NRG1 and NRG3 in the PNS (sciatic nerves) of aged animals was found. In order to verify whether this processing was defective also in the CNS, the levels of NRG1 and NRG3 in hippocampal homogenate from 1-year-old wildtype and *Prnp*$^{0/0}$ mice were analyzed. No difference was detected in the expression and processing of NRG1 and NRG3 in the hippocampus between wildtype and *Prnp*$^{0/0}$ mice (Figure 26). Thus, the lack of PrP^{C} influences neuregulins processing only in the PNS of aged mice, whereas in the CNS this influence is not effective.

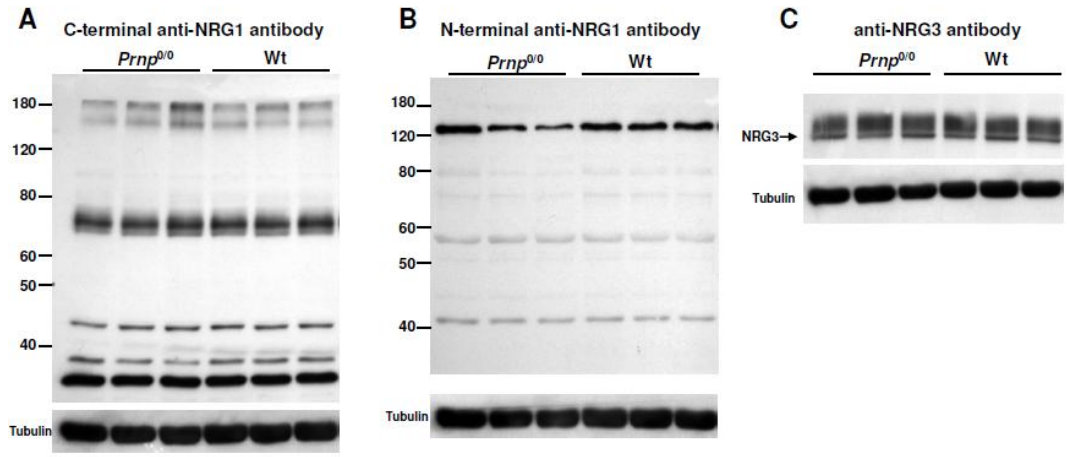

Figure 26. Processing of NRG1 and NRG3 is not altered in the hippocampus of *Prnp*$^{0/0}$ mice. Hippocampal homogenates from 1-year-old wildtype (Wt) (n=3) and *Prnp*$^{0/0}$ (n=3) mice were analyzed for the levels of NRG1 using antibody against the C-terminus of NRG1 (A), against the N-terminus of NRG1 (B), or against full length NRG3 (C). The western blot showed no difference in expression or processing of both NRG1 and NRG3 between wildtype and *Prnp*$^{0/0}$ mice hippocampi.

Discussion

Almost thirty years have passed since the postulation of the "protein-only hypothesis" by Stanley B. Prusiner. To date, the vast majority of the scientific community has accepted the revolutionary concept of a protein able to adopt different tertiary structures and transmit its conformation to other proteins. In all these years many steps have been taken towards a fuller understanding of the prion phenomenon and, although several aspects of the nature of prions are now clear, many others remain elusive. Especially, a clarified view of the physiological function of the cellular form of the PrP, PrP^C, is still missing.

The aim of my Ph.D. was to explore some of the biological features of PrP^C in the perspective of investigating a cellular protein whose widespread expression and proposed functions suggest an influence on several physiological aspects of the individual at different stages of development, from embryonic to aging animals.

At first, I investigated the expression pattern of PrP^C in the CNS on the mouse during embryonic and early post natal development. I identified a restricted PrP^C expression in specific brain areas during prenatal and postnatal brain development. By *in situ* hybridization *Prnp* gene expression was detected at E14.5 in the VZ, which is known to be a proliferative brain area, in the superficial CP, underneath the MZ where newborn neurons are, and in the neuroepithelia of the third ventricle (Figure 12). The developing choroid plexus epithelium of the ventricular zone is known to contain multipotent neural stem cells (Tramontin et al., 2003). The MZ is the outermost layer of the cerebral cortex. Cells of the MZ are known to play key roles during development such as orchestrating the development of the cortical layers and contributing to the GABAergic interneurons in the cerebral cortex (Meyer et al., 1998). MZ cells have also been shown

to guide cortical afferents to their targets (Marin-Padilla, 1978; McConnell et al., 1989) and develop a transient neuronal circuit of crucial importance for setting up the mature circuitry among CP neurons (Friauf and Shatz, 1991; Ghosh and Shatz, 1992; Schwartz et al., 1998). In the neocortex of P1 mouse, *Prnp* gene expression was detected in the SVZ/E, located adjacent to the VZ along the lateral ventricle wall. Importantly, neurogenesis persists in this part of the brain throughout the animal's adult life.

The expression pattern of *Prnp* in the VZ and SVZ/E suggests that the *Prnp* gene could be involved in the cellular proliferation control along development. Indeed, one report suggests that PrP^C positively regulates neuronal precursor proliferation in the SVZ/E during development and adult neurogenesis (Steele et al., 2006). At P1 *Prnp* gene is expressed throughout the cortical layers 6-2. At P7 the signal could still be detected in the cortical layers 6-2, with the strongest signal in layer 2 and progressively decreasing down to layer 6 (Figure 12). Premature neural cells proliferate in the ventricular side and migrate toward the cortical layers in the developing cerebral cortex. Neuronal precursors generated in the ventricular/ependymal zone migrate outwards along the glial processes to form the CP at the outer surface of the brain. Since the *Prnp* expression pattern during neurodevelopment seems to parallel such a time course of neuronal differentiation, it is possible to argue that *Prnp* expression could be implicated in neuronal proliferation and maturation: *Prnp* signal detected in neurons of layers 2 to 6 at P7 could be due to the same neurons that were previously described to express PrP mRNA in the VZ and in the SVZ/E zones at E14.5 and at P1. However, since PrP^C immunoreactivity in the cortical layers was not observed during prenatal development, it is possible to hypothesize that in the cortex PrP mRNA is not translated in PrP^C, or, if translated, the protein is quickly degraded during this developmental stage.

During brain early postnatal development PrP^C was found strongly expressed in the hippocampus. Differently from the cortex, in the hippocampus the expression of PrP^C

was concomitant with the presence of *Prnp* mRNA (Figs. 13, 15). Indeed, among all brain areas the hippocampus exhibited the earliest and the highest PrP^C expression. Within hippocampus, the stratum lacunosum-moleculare (str l m) revealed the highest PrP^C expression. As this is a synapse-rich region where hippocampal interneurons (Bertrand and Lacaille, 2001) and afferent neuronal inputs (Deng et al., 2006b) make connections (Fig. 27), the relatively high expression of PrP^C in this region could possibly be necessary to the correct development of synapses and, in turn, to a correct synaptic activity. Several studies suggest that the synaptic compartment could be the critical site of functional PrP^C expression (Herms et al., 1999; Carleton et al., 2001), and that loss of PrP^C function, such as in $Prnp^{0/0}$ mice, may interfere with the correct, physiological connections between neurons. Indeed, many of the abnormalities identified in $Prnp^{0/0}$ mice are related to a hippocampal synaptic dysfunction [(Collinge et al., 1994; Carleton et al., 2001; Curtis et al., 2003; Maglio et al., 2004) but also see (Lledo et al., 1996)]. Interestingly, some reports point to central synapses as primary dysfunctional victims also in prion diseases, before neurodegeneration occurs (Jeffrey et al., 2000; Cunningham et al., 2003).

Another phenotype of $Prnp^{0/0}$ mice is their increased susceptibility to epileptic seizures (Walz et al., 1999). The core of many forms of seizures is large and synchronized bursts of activity originated, among all the brain structures, peculiarly in the hippocampus and the neocortex (McCormick and Contreras, 2001). Indeed, increasing evidence suggests that an altered neurodevelopment, leading to either brain malformations or injuries, may be involved in the generation of epilepsy (Hermann et al., 2008). The strong developmental regulation and expression of PrP^C in the hippocampus and in the neocortex is intriguing, as it may account for the increased susceptibility of $Prnp^{0/0}$ mice to epileptic seizures.

The lack of PrP^C, in fact, may alter the physiological development of these brain structures, and in turn provoke changes in interneuronal connections and neural network properties.

Strong PrP^C immunoreactivity was also observed in brain structure involved in the regulation of the thalamolimbic system, such as the fimbria/fornix, the fasciculus retroflexus, and the stria terminalis (Figure 15, 16). The thalamolimbic system is involved in the regulation of circadian, autonomic, and hormonal functions, as well as stress response behaviors (Herman et al., 2003, 2005; Saper, 2006; Ulrich-Lai and Herman, 2009). The fimbria/fornix provides the major afferent and efferent projections of the hippocampus to basal forebrain (Olton et al., 1978); the fasciculus retroflexus connects the habenular nucleus to the interpeduncular nucleus and it is known to be integrated in the processing of various subsystems involved in the sleep–wake mechanisms (Valjakka et al., 1998); the stria terminalis is a limbic forebrain structure that receives heavy projections from, among other areas, the basolateral amygdala, and projects in turn to hypothalamic and brainstem target areas that mediate many of the autonomic and behavioral responses to aversive or threatening stimuli (Walker et al., 2003) (Fig. 27).

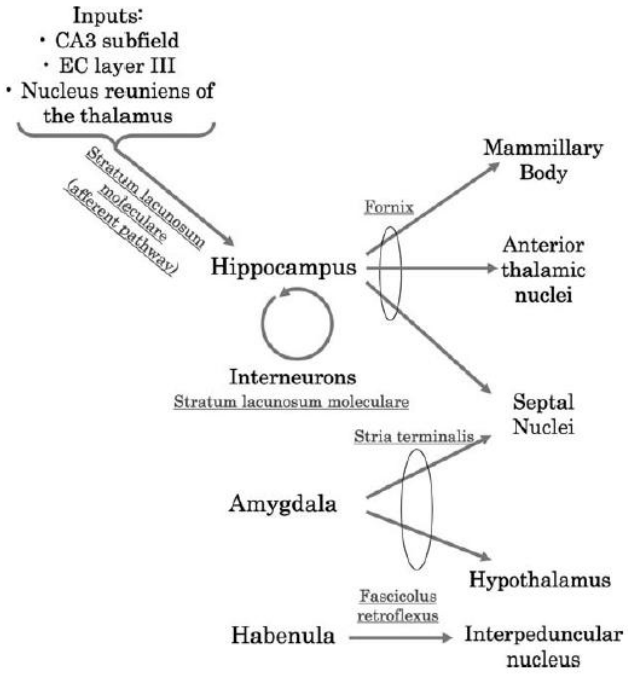

Figure 27. Brain limbic system circuits expressing PrP^C during development. Gray lines indicate the neural connections (*i.e.*, the hippocampal fimbria, the stria terminalis, and the fasciculus retroflexus) and the synapses-rich region (*i.e.*, stratum lacunosum-moleculare of the hippocampus) expressing high levels of PrP^C in neurodevelopment.

Thus, the high developmental expression of PrP^C in brain fiber bundles participating in the regulation of the thalamolimbic circuitry may reveal a potential role for PrP^C in the correct development, structuring, and functioning of this complex neural system. Interestingly, the lack of PrP^C in *Prnp*$^{0/0}$ mice was proved to be responsible for alterations that can be related to incorrect performance of this neural system. These alterations include altered circadian activity rhythms and sleep activities (Tobler et al., 1996), deficits in hippocampal-dependent spatial learning (Criado et al., 2005), altered stress response and neuroendocrine stress functions (Sánchez-Alavez et al., 2007), altered fear-induced behavior (Lobão-Soares et al., 2008), and disregulation of the hypothalamic-pituitary-adrenal axis, the ‘‘stress’’ axis (Sanchez-Alavez et al., 2008). Intriguingly, pathological alterations that can be related to a dysfunction of the thalamolimbic system have been described also in some cases of prion diseases, such as corticosteroid disturbance (Gayrard et al., 2000; Voigtländer et al., 2006). Moreover,

patients suffering the genetic prion disease FFI show predominant sleep, neuroendocrine, and autonomic dysfunction (Montagna et al., 2003). Hence, the absence of PrP^{C} in *Prnp*$^{0/0}$ mice, or its possibly altered physiological functioning in certain cases of prion diseases, gives rise to pathological alterations associated with incorrect neural information processing by brain structures contributing to the regulation of the thalamolimbic neurocircuitry.

In summary, PrP^{C} expression was identified to be highly regulated during neurodevelopment, and in particular a high level of expression of PrP^{C} was detected in specific nerve fiber bundles involved in the thalamolimbic system regulation. The high developmental expression of PrP^{C} in these white matter tracts might reflect an active axonal transport of the PrP through these fiber bundles; indeed, PrP^{C} can be transported along axons (Borchelt et al., 1994; Moya et al., 2004), and in particular, in the case of the fimbria/fornix, PrP^{C} expression in these tracts could be due to axonal transport from the hippocampus.

This strong developmental regulation and the main synaptic localization of PrP^{C} in adult neurons (Herms et al., 1999; Moya et al., 2000b) could implicate PrP^{C} in the correct structuring and functioning of specific brain circuits. The lack of PrP^{C}, such as in *Prnp*$^{0/0}$ animals, could be more detrimental for brain regions requiring high levels of expression of the protein during development than in regions with a lower physiological expression. In turn, these regions would not be able to form and/or operate properly, and when challenged by the proper external stimulus they would respond with a nonphysiological nervous output, if compared to wildtype situations. In this perspective, this may also be true for the aberrant function of PrP^{C} once converted into PrP^{Sc}.

Despite PrP^{C} synaptic localization (Moya et al., 2000b), in adult mice it can also be localized in other parts of the neurons plasma membrane, including dendritic, somatic, and axonal membranes (Mironov et al., 2003). These findings point to a broader

physiological role for PrP^C in adult life than simply a synaptic one. Indeed, besides synapse formation and function, PrP^C was shown to influence several cellular processes in the nervous system, e.g., neuronal survival, intercellular contacts, and signaling, and maintenance of myelin fibers (reviewed in (Aguzzi et al., 2008)). These results can indeed support the hypothesis for distinct temporal functions for PrP^C as being supposedly involved in circuit formation and refinement during neuronal development, and in other functions in adult life once the correct neuronal circuits have been formed.

The *Prnp*$^{0/0}$ mice revealed no overt phenotype (Büeler et al., 1992; Manson et al., 1994), thus PrP^C proved not to be essential for the normal development and survival of the animal. However, phenomena of developmental plasticity and genetic compensation may mask the phenotype of PrP^C deficient mice (Steele et al., 2007). A gene expression profile analysis was undertaken in order to analyze the potential influence of PrP^C on the CNS gene expression profile during neuronal postnatal development. To this aim wildtype (*Prnp*$^{+/+}$) and *Prnp*$^{0/0}$ mice were investigated at two different developmental stages: in neonatal animals (postnatal day 4.5, P4.5) and in adult animals (3 months old). As the hippocampus was identified as the region with the earliest and highest expression of PrP^C during neuronal development, I decided to focus my analysis on hippocampal mRNAs from the perspective that the deficiency of PrP^C, such as in *Prnp*$^{0/0}$ animals, may be more detrimental in brain regions requiring high levels of expression of the protein during development (*i.e.*, the hippocampus), rather than in regions with a lower physiological expression.

The absence of PrP^C affected several biological pathways, the most representative being cell signaling, cell-cell communication and transduction processes, calcium homeostasis, nervous system development, synaptic transmission and cell adhesion. However, there was only a moderate alteration of the gene expression profile between

wildtype and *Prnp*$^{0\backslash0}$ animals. Thus, PrP^C expression or absence in general does not bring about an extremely drastic alteration in gene expression profile, and produces moderately altered gene expression levels during neuronal development, leading to the conclusion that the lack of PrP^C is not compensated by a strong overexpression of (an)other specific gene(s) rescuing PrP^C function. This finding suggests that PrP^C performs more than just one function in the CNS, supporting the hypothesis of a pleiotropic role for the protein.

Indeed real-time RT-PCR data for some selected genes support the stability of the transcriptome in the hippocampus of *Prnp*$^{0/0}$ mice, and point at possible influences due to the deficiency of PrP^C in cellular mechanisms other than gene transcription modification. Moreover, as *Prnp*$^{0/0}$ mice show no gross phenotypical differences in physiological conditions, but reveal stronger phenotypes in stressful or challenging conditions (Criado et al., 2005; Sánchez-Alavez et al., 2007; Sanchez-Alavez et al., 2008; Lobão-Soares et al., 2008), one may also argue that in physiological conditions PrP^C is in a resting/silent state, and that only in a challenging environment PrP^C actual function can be switched on. Thus, it would be interesting to perform new gene expression studies in such conditions, in order to unveil possible influences of PrP^C on the cellular transcriptome.

Down-regulation of PrP^C during prion disease has been proven to reverse spongiosis, to prevent neuronal loss and to rescue early neuronal and cognitive dysfunction (Mallucci et al., 2003, 2007; White et al., 2008). These results are further supportive of a strategy against prion diseases involving a decrease in PrP^C expression levels, suggesting that the manipulation of its levels may conceivably become a useful tool in the treatment and clinical approach to these diseases.

One interesting aspect that arises from this study was the effect of PrP on Tau phosphorylation. The levels of phosphorylated tau were similar in adult wildtype and in

adult *Prnp*$^{0/0}$ mice, whereas the levels of phosphorylated tau were significantly higher in newborn *Prnp*$^{0/0}$ mice if compared to newborn wildtype animals (Figure 19). Besides being highly phosphorylated in AD brain, tau is also highly phosphorylated in normal developing brain, in the window of age of neuritic outgrowth (Kenessey and Yen, 1993; Yu et al., 2009). This is probably occurring in order to keep a high dynamics of microtubule assembly-disassembly during brain development. So, PrP^{C} seems to negatively influence the phosphorylation levels of tau during the first postnatal brain development, while it has no effect on tau phosphorylation in adult brain, when phosphorylation of tau is physiologically at a steady-state. Future studies on other phosphorylation sites on Tau protein are necessary to clarify the involvement of PrP^{C} on the mechanisms regulating Tau phosphorylation. Nevertheless, although as a preliminary result, this finding may in part shed new light on the developmental functions linked to PrP^{C}, and additionally an involvement of PrP^{C} on the regulation of tau phosphorylation could imply a novel correlation between AD and prion biology.

One strong correlation between AD and prion biology is the regulation of the activity of the β-site of APP cleaving enzyme (β-secretase BACE1) by PrP^{C} (Parkin et al., 2007). In fact, PrP^{C} was shown to directly interact with and inhibit BACE1 on the processing of APP, thus lowering the total amount of Aβ peptide (Parkin et al., 2007). One common feature for both PrP^{C} and BACE1 is their involvement in myelin homeostasis. *Prnp*$^{0/0}$ mice expressing PrP deletion mutants show severe CNS and PNS demyelination (Radovanovic et al., 2005; Baumann et al., 2007, 2009; Bremer et al., 2010), and *Prnp*$^{0/0}$ mice manifest a late-onset chronic demyelinating polyneuropathy (Bremer et al. 2010). In this latter case, the demyelination was recovered by expression of axonal PrP^{C}, and not by glial expression. This suggests an axonal trophic support, mediated by PrP^{C} neuronal expression, acting *in trans* to Schwann cells for a physiological myelin homeostasis. Thus, I was prompted to investigate for a neuron-specific key element that

could be regulated by PrP^C. The protease BACE1 is preferentially expressed by neurons (Rossner et al., 2001), and, interestingly, BACE1 null mice show myelin defects in the CNS and the PNS (Willem et al., 2006; Hu et al., 2006). These defects were *bona fide* linked to a lack of processing of NRG1 protein, a BACE1 substrate and key regulator of PNS myelination (Mei and Xiong, 2008; Newbern and Birchmeier, 2010). Thus, I investigated whether, besides regulating BACE1 activity in the cleavage of APP (Parkin et al., 2007), PrP^C could also regulate the cleavage of other BACE1 substrates, *i.e.*, neuregulins. Indeed, $Prnp^{0/0}$ mice turned out to have a defective processing of NRG1. However, this defect in NRG1 processing was time- and tissue- definite. Indeed, a difference in NRG1 processing could be highlighted only in aged $Prnp^{0/0}$ mice compared to their wildtype counterpart, whereas in young animals no difference between the two genotypes could be detected (Figure 22). This finding hints that during the first postnatal development, *i.e.* during the initial PNS myelination process, PrP^C role for neuregulin processing is dispensable, whereas it starts to exert its effect and to be relevant in adult and aged animals. This is suggestive of a physiological role of PrP^C for NRG1 processing during the aging of an animal. Moreover, $Prnp^{0/0}$ mice showed altered NRG1 cleavage only in their PNS, whereas they did not show any difference, if compared to their wildtype counterpart, of NRG1 processing in the CNS (Figure 26). The molecule PrP^C thus seems to fulfill different functions between CNS and PNS, at least for NRG processing and, in turn, possibly for myelin homeostasis.

In order to verify whether PrP^C could directly stimulate the cleavage of NRG1, I took advantage of N2a cells stably over-expressing full-length mouse PrP^C, and identified an increase of NRG1 - N-terminal cleaved fragment both in the cell lysates and in the conditioned medium (Figure 23). This suggests that the cleavage of NRG1, stimulated by PrP^C expression, occurs in intracellular compartments, for example in the endosomal system, and then the cleaved fragment is released in the cell medium, probably through

a subsequent move of the cleaved fragment to the protein secretory pathway. The protease BACE1 is known to cleave its substrate APP in the endosomal pathway, and then the cleaved fragment is released in the extracellular medium *via* the secretory pathway (Koo and Squazzo, 1994; Thinakaran et al., 1996; Tomita et al., 1998; Marlow et al., 2003). This suggests the need of acidic compartments (*i.e.* endosomes and/or late Golgi) for BACE1 activity. This finding hints that BACE1-mediated cleavage of NRG1 may require the same endocytosis/recycling process as for BACE1-mediated APP processing.

I could also identify altered processing of NRG3 in *Prnp*$^{0/0}$ mice. NRG3 is another member of the neuregulin family, possesses a similar structural organization to NRG1, and also activates ErbB receptor (Zhang et al., 1997). Like NRG1, NRG3 is also substrate of BACE1, and after proteolytical cleavage it was proposed to bind Schwann cells ErbB receptors (Hu et al., 2008). I could detect a difference in processing also for NRG3 only in the PNS of *Prnp*$^{0/0}$ mice, and not in the CNS if compared to wildtype animals (Figure 24, 26). Hence, PrP^{C} can stimulate the processing of neuregulins only in the PNS and not in the CNS.

I also investigated whether two intracellular signaling pathways, *i.e.* ERK and Fyn kinases, linked both to PrP^{C} and neuregulins signaling, could be altered in the sciatic nerves of *Prnp*$^{0/0}$ mice, but no difference from their wildtype counterpart in the activation of these two signaling cascades could be detected (Figure 25). This suggests that other signaling pathways may be affected by the lack of PrP^{C} and the defective neuregulin processing. Further studies need to investigate other intracellular cascades related to both PrP^{C} and neuregulin signaling (for example, the PI3K pathway).

The age-dependent effect of PrP^{C} on neuregulin processing may be associated to different cellular mechanisms. Lipid rafts are dynamic and highly ordered sterol- and

sphingolipid-enriched domains that can concentrate selected subsets of proteins and serve as a platform for cellular processes, including cell signaling, protein sorting and trafficking, and extracellular/membrane protein proteolysis (Simons and Toomre, 2000; Ledesma et al., 2003; Helms and Zurzolo, 2004; Hancock, 2006). Rafts are continuously endocytosed from cellular plasma membrane *via* the endocytic pathway, and either recycled back to the plasma membrane or returned to the Golgi apparatus (Puri et al., 1999; Mukherjee and Maxfield, 2000). Neuregulin (Frenzel and Falls, 2001), PrP^{C} (Vey et al., 1996) and BACE1 (Riddell et al., 2001) are all enriched in lipid rafts domains. Moreover, targeting BACE1 lumenal domain to lipid rafts by the addition of a glycophosphatidylinositol anchor was shown to increase BACE1-mediated APP processing (Cordy et al., 2003). This hints at lipid rafts as functional compartment for BACE1 activity. Besides, PrP^{C} was shown to exert its regulation on BACE1-mediated APP cleavage only when correctly localized to lipid rafts domain (Parkin et al., 2007). Although from these experiments a direct functional link between PrP^{C} and the regulation of BACE1 cannot be drawn, nevertheless these findings suggest that PrP^{C} could physiologically influence also the BACE1-mediated neuregulins cleavage, and this occurring in an endocytosys/secretory pathway-dependent manner. Lipid rafts however do not maintain the same protein and lipid composition: with aging and in pathological condition (like in AD), the ratio between cholesterol, sphingolipid and phospholipid changes (Prinetti et al., 2001; Palestini et al., 2002; Martin et al., 2010). This in turn may affect the affinity of certain proteins for these microdomains. As a consequence of this, the protein composition of the lipid rafts may dramatically change, and this can consequently modify their properties as "signaling scaffolds" during different cellular life stages. Hence, one may suggest that, during early postnatal development, the lack of PrP^{C} in lipid rafts and the specific protein/lipid composition may not destabilize BACE1-mediated NRGs processing, whereas by changing the

biochemical composition of the rafts, *i.e.* with adulthood and aging, the lack of PrP^C could instead destabilize lipid rafts-mediated BACE1-NRGs interaction. This in turn could lead to the observed altered NRG processing. In this perspective, PrP^C may be a crucial key element in lipid rafts protein homeostasis, composition and in physiological signaling processes during lifetime, and particularly during aging.

Moreover, the possible age-dependent influence of PrP^C on BACE1-mediated neuregulin cleavage may be also due to the opposite dynamic expression levels between PrP^C and BACE1 throughout the lifespan of the animal. Indeed, PrP^C levels were shown to increase during postnatal development then reaching a *plateau* of expression in adulthood (Salès et al., 2002), whereas BACE1 levels are high during development and then decrease to a low levels in adult animals (Willem et al., 2006). Thus, PrP influence could be minimal during early development when PrP^C low levels of expression overlap the high levels of BACE1; on the contrary, in adult animals, the minimal expression of BACE1 could be strongly influenced by the high levels of PrP^C. Accordingly, in $Prnp^{0/0}$ mice BACE1 activity may not be affected by the lack of PrP^C in young animals, while on the contrary it can be effectively altered during adulthood and aging of the animals.

The mechanisms responsible for the tissue-dependent influence of PrP^C on neuregulin processing also are not clear and need further investigation. Altered NRGs processing was detected only in the PNS of aged $Prnp^{0/0}$ mice, and not in their CNS. This can suggest that some compensatory mechanism for neuregulin processing may occur in the CNS, whereas it is not effective in the PNS.

Pharmacological inhibition of BACE1 in adult mice brain was shown to induce significant Aβ-peptide lowering, but it was without any major effect on brain NRG1 processing (Sankaranarayanan et al., 2008). The same study suggests differences in BACE1-mediated NRG1 processing only in early development in the brain, as aged (2-

years-old) BACE1 null mice show identical full-length NRG1 and NRG-NTF levels to their wildtype counterpart. Therefore, BACE1 inhibition in the brain showed to have an effective impact on the lowering of APP processing, and no alteration on NRG1 processing. Similarly, PrP^C was shown to inhibit BACE1-mediated APP processing in the brain (Parkin et al., 2007), whereas I could not detect any role for PrP^C on NRG1 processing in the CNS of aged mice (Figure 26). These independent findings are suggestive of a different PrP^C influence on BACE1 processing activity between the CNS and the PNS.

Taken together, these findings are suggestive of the occurrence of different age-dependent and tissue-dependent cellular mechanisms for the regulation of neuregulins processing. Future studies on NRGs processing and cleavage are necessary to describe a correct spatial and dynamic frame of neuregulins processing and biological action.

In summary, my study points at PrP^C as a positive regulator of NRGs processing. This effect was manifest as age-dependent (only in aged, but not in young mice) and tissue-dependent (only in the PNS, but not in the CNS). The results obtained suggest that PrP^C could exert different functions, during development and aging, between the CNS and the PNS, at least as regards neuregulin processing and possibly myelin homeostasis. In turn, this finding could shed new light on the etiology of the peripheral demyelinating neuropathy affecting aged mice null for the PrP (Bremer et al., 2010).

Conclusive remarks

During my Ph.D. work I have focused on some biological features of the PrP. I could highlight a specific developmental pattern of expression of PrP^C. I revealed regional differences in the expression of PrP^C, with the earliest expression of the protein in the hippocampus, thalamic, and hypothalamic regions, as well as in specific white matter fiber tracts which are part of the thalamolimbic system. Then I have analyzed PrP^C influence on hippocampal transcriptome during development, and could evidence that PrP^C does not dramatically influence the genetic expression profile. Finally I could show that PrP^C influences the cleavage of NRG1 and NRG3 in the PNS of the mouse. *Prnp*$^{0/0}$ mice, in fact, show a defective processing of neuregulins. This effect was manifest as age-dependent (only in aged, but not in young mice) and tissue-dependent (only in the PNS, but not in the CNS), thus suggesting that PrP^C exerts different functions during development and aging, between the CNS and the PNS. This finding could be of interest for peripheral demyeliating diseases, especially during aging.

Appendix

Table 3: UP IN WT Second messengers signaling pathway genes

Gene Symbol	Gene Name	Affymetrix Probe ID	*Prnp*+\+ mice adults *vs* newborns logFC	*Prnp*+\+ mice adults *vs* newborns adj.P.Val	*Prnp*0\0 mice adults *vs* newborns logFC	*Prnp*0\0 mice adults *vs* newborns adj.P.Val	logFCwt-logFCko	FCwt-Fcko
cAMP-mediated signaling pathway genes								
Pde1a	phosphodiesterase 1A, calmodulin-dependent	1449298_a_at	0,70	0,00343722	-0,32	0,128165555	1,03	2,037355647
Adcy8	adenylate cyclase 8	1418754_at	1,00	4,05E-06	0,18	0,192060092	0,82	1,767303424
Akap2	A kinase (PRKA) anchor protein 2	1449168_a_at	0,59	8,35E-05	-0,02	0,830368376	0,62	1,53182338
Camk2d	calcium/calmodulin-dependent protein kinase II, delta	1427763_a_at	0,76	3,87E-06	0,29	0,011049627	0,47	1,383651588
Camk1d	calcium/calmodulin-dependent protein kinase ID	1452050_at	0,64	3,91E-06	0,20	0,03420276	0,44	1,360526393
Rgs7	regulator of G protein signaling 7	1450659_at	0,59	1,61E-06	0,28	0,001817011	0,32	1,245975896
Adrb1	adrenergic receptor, beta 1	1423420_at	0,78	6,58E-05	0,47	0,003577575	0,30	1,231867475
Adora2b	adenosine A2b receptor	1450214_at	0,76	7,01E-07	0,53	3,04E-05	0,23	1,176787817
Ppp3cb	protein phosphatase 3, catalytic subunit, beta isoform	1427468_at	0,69	1,51E-06	0,55	1,74E-05	0,15	1,106729834
RAR activation genes								
Ppargc1a	peroxisome proliferative activated receptor, gamma, coactivator 1 alpha	1460336_at	0,79	0,00388043	-0,29	0,231477564	1,08	2,116132115
Snw1	SNW domain containing 1	1429003_at	0,66	0,00488683	-0,16	0,440089608	0,82	1,770291739
Adcy8	adenylate cyclase 8	1418754_at	1,00	4,05E-06	0,18	0,192060092	0,82	1,767303424
Nrip1	nuclear receptor interacting protein 1	1418469_at	0,64	0,01491063	-0,13	0,588336221	0,77	1,701656948
Smarca2	SWI/SNF related, matrix associated, actin dependent regulator of chromatin	1452333_at	0,97	6,86E-06	0,36	0,018100975	0,61	1,5270052
Ccnh	cyclin H	1418585_at	0,76	2,36E-05	0,31	0,021527262	0,45	1,368294741
Prkcb	protein kinase C, beta	1423478_at	0,81	6,34E-09	0,44	4,58E-06	0,38	1,297099292
Map2k4	mitogen-activated protein kinase kinase 4	1426233_at	0,66	0,00034219	0,46	0,004863923	0,20	1,146070398
NRF2-mediated response genes								
Dnajc3	DnaJ (Hsp40) homolog, subfamily C, member 3	1449373_at	0,60	0,00574597	0,21	0,27509332	0,39	1,310548916
Prkcb	protein kinase C, beta	1423478_at	0,81	6,34E-09	0,44	4,58E-06	0,38	1,297099292
Dnajc5	DnaJ (Hsp40) homolog, subfamily C, member 5	1448851_a_at	0,62	0,00047429	0,30	0,043648971	0,32	1,248550146
Dnajb4	DnaJ (Hsp40) homolog, subfamily B, member 4	1431734_a_at	0,67	4,13E-05	0,39	0,003540784	0,28	1,211553527
Gclc	glutamate-cysteine ligase, catalytic subunit	1424296_at	0,68	0,00024461	0,42	0,008480347	0,26	1,196536697
Dnajb9	DnaJ (Hsp40) homolog, subfamily B, member 9	1417191_at	0,67	1,90E-07	0,43	1,89E-05	0,24	1,179841088
Map2k4	mitogen-activated protein kinase kinase 4	1426233_at	0,66	0,00034219	0,46	0,004863923	0,20	1,146070398
Gsta3	glutathione S-transferase, alpha 3	1423437_at	0,68	3,84E-07	0,50	1,01E-05	0,18	1,135383217
Calcium signaling genes								
Trpc5	transient receptor potential cation channel, subfamily C, member 5	1422048_at	0,67	0,00079189	-0,11	0,520967392	0,78	1,713935648
Camk1d	calcium/calmodulin-dependent protein kinase ID	1426389_at	0,64	0,00196497	-0,01	0,951174261	0,65	1,572277582
Camk2d	calcium/calmodulin-dependent protein kinase II, delta	1427763_a_at	0,76	3,87E-06	0,29	0,011049627	0,47	1,383651588
Tnnc1	troponin C, cardiac/slow skeletal	1418370_at	0,72	3,60E-07	0,47	2,88E-05	0,25	1,189559751
Mef2d	myocyte enhancer factor 2D	1434487_at	0,68	6,87E-08	0,44	6,50E-06	0,24	1,179876899
Gria2	glutamate receptor, ionotropic, AMPA2 (alpha 2)	1421970_a_at	0,59	7,14E-07	0,39	4,98E-05	0,20	1,149104479
Rap2b	RAP2B, member of RAS oncogene family	1417915_at	0,67	2,35E-05	0,50	0,000383759	0,18	1,130810925
Ppp3cb	protein phosphatase 3, catalytic subunit, beta isoform	1427468_at	0,69	1,51E-06	0,55	1,74E-05	0,15	1,106729834

Table 4: UP IN WT Ras/Rab and protein kinases family

Gene Symbol	Gene Name	Affymetrix Probe ID	*Prnp*+\+ mice adults *vs* newborns logFC	*Prnp*+\+ mice adults *vs* newborns adj.P.Val	*Prnp*0\0 mice adults *vs* newborns logFC	*Prnp*0\0 mice adults *vs* newborns adj.P.Val	logFCwt-logFCko	FCwt-Fcko
Arhgap5	Rho GTPase activating protein 5	1423194_at	0,77	0,001044	-0,40	0,049549	1,17	2,255236769
Rab27b	RAB27b, member RAS oncogene family	1417215_at	0,87	5,87E-06	0,20	0,115518	0,67	1,58893703
Camk1d	calcium/calmodulin-dependent protein kinase ID	1426389_at	0,64	0,001965	-0,01	0,951174	0,65	1,572277582
Rab3c	RAB3C, member RAS oncogene family	1432432_a_at	0,98	7,39E-06	0,33	0,029045	0,65	1,567467414
Ripk5	receptor interacting protein kinase 5	1436300_at	1,13	6,34E-07	0,57	0,000509	0,57	1,480651624
Speg	SPEG complex locus	1451886_at	0,64	1,30E-06	0,15	0,068561	0,49	1,407844265
Galk2	galactokinase 2	1438642_at	0,90	9,77E-05	0,41	0,025751	0,49	1,404770105
Camk2d	calcium/calmodulin-dependent protein kinase II, delta	1427763_a_at	0,76	3,87E-06	0,29	0,01105	0,47	1,383651588
Rab6	RAB6, member RAS oncogene family	1448304_a_at	0,81	9,05E-07	0,43	0,000445	0,38	1,304173995
Prkcb	protein kinase C, beta	1423478_at	0,81	6,34E-09	0,44	4,58E-06	0,38	1,297099292
Prkg2	protein kinase, cGMP-dependent, type II	1421354_at	0,62	1,29E-06	0,29	0,001599	0,33	1,259400875
Stk3	serine/threonine kinase 3 (Ste20, yeast homolog)	1418513_at	0,61	0,000336	0,28	0,046631	0,33	1,256843162
Nkiras1	NFKB inhibitor interacting Ras-like protein 1	1428503_a_at	0,89	1,93E-08	0,56	2,49E-06	0,32	1,25225101
Uhmk1	U2AF homology motif (UHM) kinase 1	1433737_at	0,73	1,53E-08	0,47	1,90E-06	0,26	1,200921892
Clk1	CDC-like kinase 1	1426124_a_at	0,67	0,000536	0,42	0,014785	0,26	1,197107378
Hspa4l	heat shock protein 4 like	1449010_at	0,77	1,47E-07	0,56	4,02E-06	0,21	1,152953201
Map2k4	mitogen-activated protein kinase kinase 4	1426233_at	0,66	0,000342	0,46	0,004864	0,20	1,146070398
Rab38	Rab38, member of RAS oncogene family	1417700_at	0,67	2,01E-06	0,48	5,89E-05	0,19	1,143822098
Rasl11b	RAS-like, family 11, member B	1423854_a_at	0,74	2,64E-08	0,56	5,98E-07	0,19	1,137437521
Rap2b	RAP2B, member of RAS oncogene family	1417915_at	0,67	2,35E-05	0,50	0,000384	0,18	1,130810925
Rps6kl1	ribosomal protein S6 kinase-like 1	1426466_s_at	0,71	2,32E-07	0,56	3,02E-06	0,15	1,111197203

Table 5: UP IN WT genes involved in synaptic transmission

Gene Symbol	Gene Name	Affymetrix Probe ID	*Prnp*+\+ mice adults *vs* newborns logFC	*Prnp*+\+ mice adults *vs* newborns adj.P.Val	*Prnp*0\0 mice adults *vs* newborns logFC	*Prnp*0\0 mice adults *vs* newborns adj.P.Val	logFCwt-logFCko	FCwt-FCko
Prnp	prion protein	1416130_at	1,40	6,50E-10	0,53	1,91E-05	0,87	1,82991913
Trpc5	transient receptor potential cation channel, subfamily C, member 5	1422048_at	0,67	0,000791895	-0,11	0,520967392	0,78	1,713935648
Slc12a2	solute carrier family 12, member 2	1448780_at	0,97	1,08E-05	0,27	0,077447849	0,70	1,626000228
Cacna1a	calcium channel, voltage-dependent, P/Q type, alpha 1A subunit	1450510_a_at	0,64	0,000143879	-0,04	0,753785463	0,68	1,606632935
Kcnh1	potassium voltage-gated channel, subfamily H (eag-related), member 1	1418414_at	1,08	2,10E-05	0,58	0,004021213	0,50	1,416582165
Kcnc3	potassium voltage gated channel, Shaw-related subfamily, member 3	1421980_at	0,92	2,69E-06	0,48	0,00108657	0,44	1,355132073
Homer1	homer homolog 1 (Drosophila)	1425710_a_at	0,85	8,03E-05	0,45	0,009621392	0,40	1,315322162
Pcdhb3	protocadherin beta 3	1420429_at	0,61	0,00021915	0,23	0,07704405	0,38	1,300147603
Grid1	glutamate receptor, ionotropic, delta 1	1421569_at	0,63	4,85E-06	0,29	0,004350477	0,34	1,268836078
Dnajc5	DnaJ (Hsp40) homolog, subfamily C, member 5	1448851_a_at	0,62	0,000474294	0,30	0,043648971	0,32	1,248550146
Gabrb1	gamma-aminobutyric acid (GABA-A) receptor, subunit beta 1	1419719_at	0,61	7,29E-07	0,33	0,000289125	0,28	1,211726832
Sypl	synaptophysin-like protein	1422879_at	0,82	0,000140664	0,56	0,00307437	0,26	1,200845841
Slc24a3	solute carrier family 24 (sodium/potassium/calcium exchanger), member 3	1424308_at	0,74	1,56E-06	0,50	7,72E-05	0,24	1,181561822
Glrb	glycine receptor, beta subunit	1422504_at	0,81	5,13E-07	0,58	1,83E-05	0,24	1,179309955
Glrb	glycine receptor, beta subunit	1422504_at	0,81	5,13E-07	0,58	1,83E-05	0,24	1,179309955
Apoe	apolipoprotein E	1432466_a_at	0,61	4,45E-07	0,37	6,06E-05	0,23	1,175089934
Kcnj11	potassium inwardly rectifying channel, subfamily J, member 11	1450515_at	0,78	2,61E-08	0,56	9,15E-07	0,22	1,163544051
Gria2	glutamate receptor, ionotropic, AMPA2 (alpha 2)	1421970_a_at	0,59	7,14E-07	0,39	4,98E-05	0,20	1,149104479
Gria2	glutamate receptor, ionotropic, AMPA2 (alpha 2)	1421970_a_at	0,59	7,14E-07	0,39	4,98E-05	0,20	1,149104479
Vdac1	voltage-dependent anion channel 1	1415998_at	0,64	2,90E-07	0,49	4,62E-06	0,15	1,106684801

Table 6 UP IN WT: chaperone-mediated protein folding

Gene Symbol	Gene Name	Affymetrix Probe ID	*Prnp*+\+ mice adults *vs* newborns logFC	*Prnp*+\+ mice adults *vs* newborns adj.P.Val	*Prnp*0\0 mice adults *vs* newborns logFC	*Prnp*0\0 mice adults *vs* newborns adj.P.Val	logFCwt-logFCko	FCwt-FCko
Sacs	sacsin	1423010_at	0,75	2,78E-05	0,37	0,008652	0,39	1,306753064
Pfdn2	prefoldin 2	1421950_at	0,87	4,83E-05	0,52	0,003196	0,35	1,270771243
Dnajc5	DnaJ (Hsp40) homolog, subfamily C, member 5	1448851_a_at	0,62	0,00047429	0,30	0,043649	0,32	1,248550146
Dnajb4	DnaJ (Hsp40) homolog, subfamily B, member 4	1431734_a_at	0,67	4,13E-05	0,39	0,003541	0,28	1,211553527
Dnajb9	DnaJ (Hsp40) homolog, subfamily B, member 9	1417191_at	0,67	1,90E-07	0,43	1,89E-05	0,24	1,179841088

Table 7: UP IN WT Genes involved in the ubiquitin-proteasomal system

Gene Symbol	Gene Name	Affymetrix Probe ID	*Prnp*+\+ mice adults *vs* newborns logFC	*Prnp*+\+ mice adults *vs* newborns adj.P.Val	*Prnp*0\0 mice adults *vs* newborns logFC	*Prnp*0\0 mice adults *vs* newborns adj.P.Val	logFCwt-logFCko	FCwt-Fcko
Parp3	poly (ADP-ribose) polymerase family, member 3	1451969_s_at	0,76	3,92E-06	0,31	0,007251978	0,45	1,364520344
Ptplb	protein tyrosine phosphatase-like, member b	1449342_at	0,71	1,23E-06	0,33	0,001483656	0,38	1,303313496
Brcc3	BRCA1/BRCA2-containing complex, subunit 3	1452128_a_at	0,85	2,18E-07	0,56	1,52E-05	0,28	1,216517669
Fbxo9	f-box protein 9	1432211_a_at	0,68	6,45E-06	0,51	0,000108046	0,17	1,126217074
Wdsub1	WD repeat, SAM and U-box domain containing 1	1453113_at	0,71	1,06E-06	0,54	1,70E-05	0,17	1,123274455
Rnf19a	ring finger protein 19A	1417509_at	0,73	2,42E-06	0,57	3,30E-05	0,17	1,123234137

Table 8: UP IN KO Cytosolic signaling pathway genes

Gene Symbol	Gene Name	Affymetrix Probe ID	*Prnp*0\0 mice adults *vs* newborns logFC	*Prnp*0\0 mice adults *vs* newborns adj.P.Val	*Prnp*+\+ mice adults *vs* newborns logFC	*Prnp*+\+ mice adults *vs* newborns adj.P.Val	logFCko-logFCwt	FCko-FCwt
Grk6	G protein-coupled receptor kinase 6	1450480_a_at	0,80	6,96E-06	0,36	0,005486454	0,43	1,35
Prkci	protein kinase C, iota	1448695_at	0,75	2,50E-05	0,36	0,009501212	0,39	1,31
Ephb6	Eph receptor B6	1418051_at	0,63	9,38E-08	0,25	0,000727304	0,38	1,30
Cdk5	cyclin-dependent kinase 5	1450674_at	0,74	5,25E-07	0,41	0,000185785	0,33	1,26
Fgfr1	fibroblast growth factor receptor 1	1425911_a_at	0,62	0,000144627	0,32	0,015912045	0,29	1,23
Mapk3	mitogen-activated protein kinase 3	1427060_at	0,61	3,78E-07	0,36	7,50E-05	0,25	1,19
Map2k7	mitogen-activated protein kinase kinase 7	1425512_at	0,76	5,09E-08	0,55	1,55E-06	0,21	1,16
Pcsk6	proprotein convertase subtilisin/kexin type 6	1426981_at	0,59	1,09E-05	0,39	0,000492405	0,20	1,15
Npr2	natriuretic peptide receptor 2	1427191_at	0,61	1,15E-05	0,43	0,000302524	0,18	1,13
Prkaca	protein kinase, cAMP dependent, catalytic, alpha	1450519_a_at	0,73	4,77E-07	0,56	7,45E-06	0,17	1,13
Csnk1d	casein kinase 1, delta	1449932_at	0,69	7,94E-06	0,53	0,000106485	0,16	1,12
Mark4	MAP/microtubule affinity-regulating kinase 4	1456618_at	0,62	1,77E-06	0,46	3,07E-05	0,15	1,11
Kit	kit oncogene	1415900_a_at	0,66	3,57E-05	0,51	0,00033623	0,14	1,10
Rps6kb2	ribosomal protein S6 kinase, polypeptide 2	1422268_a_at	0,69	9,88E-06	0,56	7,68E-05	0,13	1,10

Table 9: UP IN KO Cell death signaling genes

Gene Symbol	Gene Name	Affymetrix Probe ID	*Prnp*0\0 mice adults *vs* newborns logFC	*Prnp*0\0 mice adults *vs* newborns adj.P.Val	*Prnp*+\+ mice adults *vs* newborns logFC	*Prnp*+\+ mice adults *vs* newborns adj.P.Val	logFCko-logFCwt	FCko-FCwt
Lcn2	lipocalin 2	1427747_a_at	3,18	5,88E-08	0,11	0,70348076	3,07	8,40
Msn	moesin	1450379_at	0,72	0,000813217	0,00	0,992469718	0,72	1,65
S100a9	S100 calcium binding protein A9 (calgranulin B)	1448756_at	0,83	7,83E-06	0,16	0,198828943	0,67	1,60
Ucp2	uncoupling protein 2 (mitochondrial, proton carrier)	1448188_at	0,70	1,81E-05	0,13	0,262803022	0,57	1,49
Hist1h1c	histone cluster 1, H1c	1416101_a_at	0,84	1,13E-05	0,32	0,020286042	0,52	1,44
Clic4	chloride intracellular channel 4 (mitochondrial)	1423392_at	0,94	8,15E-09	0,44	1,89E-05	0,50	1,41
Atrx	alpha thalassemia/mental retardation syndrome X-linked homolog (human)	1420948_s_at	0,92	0,000294673	0,50	0,02122656	0,43	1,34
Gfra1	glial cell line derived neurotrophic factor family receptor alpha 1	1450440_at	0,99	9,06E-06	0,58	0,00109835	0,41	1,33
Ube2m	ubiquitin-conjugating enzyme E2M (UBC12 homolog, yeast)	1424345_s_at	0,80	2,76E-07	0,40	0,00025689	0,40	1,32
Prkci	protein kinase C, iota	1448695_at	0,75	2,50E-05	0,36	0,009501212	0,39	1,31
Casd1	CAS1 domain containing 1	1427463_at	0,69	3,40E-05	0,30	0,019200853	0,39	1,31
Ephb6	Eph receptor B6	1418051_at	0,63	9,38E-08	0,25	0,000727304	0,38	1,30
Grin2b	glutamate receptor, ionotropic, NMDA2B (epsilon 2)	1422223_at	0,65	0,000363825	0,27	0,069909634	0,38	1,30
Cdk5r1	cyclin-dependent kinase 5, regulatory subunit 1 (p35)	1421123_at	0,81	1,89E-06	0,43	0,000557868	0,38	1,30
Cyb5r3	cytochrome b5 reductase 3	1425329_a_at	0,61	2,48E-06	0,25	0,005557657	0,36	1,28
Gmfb	glia maturation factor, beta	1431686_a_at	0,70	3,22E-05	0,34	0,008838898	0,35	1,28
Ccnl2	cyclin L2	1453740_a_at	0,71	0,00040049	0,36	0,03472801	0,35	1,28
Hnrnpc	heterogeneous nuclear ribonucleoprotein C	1418693_at	0,60	2,18E-07	0,25	0,000906484	0,35	1,27
Cdk5	cyclin-dependent kinase 5	1450674_at	0,74	5,25E-07	0,41	0,000185785	0,33	1,26
Clcn7	chloride channel 7	1450408_at	0,61	4,87E-06	0,33	0,001474505	0,29	1,22
Stxbp1	syntaxin binding protein 1	1420506_a_at	0,83	1,63E-07	0,57	8,31E-06	0,27	1,20
E2f4	E2F transcription factor 4	1451480_at	0,62	7,37E-07	0,36	0,000170641	0,26	1,20
Tmem173	transmembrane protein 173	1427911_at	0,78	8,14E-08	0,52	5,60E-06	0,26	1,20
Cd14	CD14 antigen	1417268_at	0,82	8,72E-07	0,56	3,78E-05	0,26	1,20
Mapk3	mitogen-activated protein kinase 3	1427060_at	0,61	3,78E-07	0,36	7,50E-05	0,25	1,19
Hras1	Harvey rat sarcoma virus oncogene 1	1422407_s_at	0,68	1,22E-07	0,45	7,80E-06	0,23	1,17
Fcgr1	Fc receptor, IgG, high affinity I	1417876_at	0,64	0,000205429	0,42	0,005577579	0,22	1,17
Tgm2	transglutaminase 2, C polypeptide	1417500_a_at	0,78	2,70E-06	0,56	7,30E-05	0,22	1,17
Map2k7	mitogen-activated protein kinase kinase 7	1425512_at	0,76	5,09E-08	0,55	1,55E-06	0,21	1,16
Men1	multiple endocrine neoplasia 1	1416348_at	0,66	8,05E-06	0,46	0,000267707	0,21	1,15
Ikbkg	inhibitor of kappaB kinase gamma	1450161_at	0,59	5,31E-05	0,39	0,001748575	0,20	1,15
Herpud1	homocysteine-inducible, ER stress-inducible, ubiquitin-like domain member 1	1435626_a_at	0,69	1,27E-06	0,49	3,86E-05	0,20	1,15
Psen1	presenilin 1	1450399_at	0,77	3,08E-07	0,58	6,11E-06	0,20	1,15
Smpd1	sphingomyelin phosphodiesterase 1, acid lysosomal	1448621_a_at	0,64	2,21E-06	0,45	6,61E-05	0,19	1,14
Cables1	Cdk5 and Abl enzyme substrate 1	1422477_at	0,75	1,52E-05	0,56	0,000224665	0,19	1,14
Wdr85	WD40 repeat domain 85	1429220_at	0,63	1,17E-06	0,44	3,77E-05	0,19	1,14
Ppp5c	protein phosphatase 5, catalytic subunit	1424115_at	0,70	1,41E-06	0,52	2,94E-05	0,18	1,14
Soat1	sterol O-acyltransferase 1	1417697_at	0,65	2,34E-05	0,46	0,000483641	0,18	1,14
Plcg2	phospholipase C, gamma 2	1426926_at	0,67	1,80E-05	0,49	0,000328846	0,18	1,13
Oaz1	ornithine decarboxylase antizyme 1	1428868_a_at	0,73	2,88E-08	0,56	4,98E-07	0,18	1,13
Prkaca	protein kinase, cAMP dependent, catalytic, alpha	1450519_a_at	0,73	4,77E-07	0,56	7,45E-06	0,17	1,13
Cttn	cortactin	1421315_s_at	0,63	1,72E-05	0,46	0,000321282	0,17	1,13
Nck2	non-catalytic region of tyrosine kinase adaptor protein 2	1416797_at	0,74	9,25E-06	0,57	0,000109504	0,17	1,12
Apoc3	apolipoprotein C-III	1418278_at	0,68	2,87E-06	0,52	4,08E-05	0,16	1,12
Cdc37	cell division cycle 37 homolog (S. cerevisiae)	1416819_at	0,68	3,47E-08	0,52	5,28E-07	0,16	1,12
Kit	kit oncogene	1415900_a_at	0,66	3,57E-05	0,51	0,00033623	0,14	1,10
Rad51l3	RAD51-like 3 (S. cerevisiae)	1425944_a_at	0,68	1,88E-08	0,53	2,13E-07	0,14	1,10
Dvl2	dishevelled 2, dsh homolog (Drosophila)	1417207_at	0,64	0,000124177	0,50	0,001062285	0,14	1,10
Hmox2	heme oxygenase (decycling) 2	1416399_a_at	0,63	2,43E-08	0,49	3,04E-07	0,14	1,10
Sod2	superoxide dismutase 2, mitochondrial	1417194_at	0,62	7,15E-06	0,49	7,59E-05	0,14	1,10
Rps6kb2	ribosomal protein S6 kinase, polypeptide 2	1422268_a_at	0,69	9,88E-06	0,56	7,68E-05	0,13	1,10

Table 10: UP IN KO Neuregulin pathway genes

Gene Symbol	Gene Name	Affymetrix Probe ID	*Prnp*0\0 mice adults *vs* newborns logFC	*Prnp*0\0 mice adults *vs* newborns adj.P.Val	*Prnp*+\+ mice adults *vs* newborns logFC	*Prnp*+\+ mice adults *vs* newborns adj.P.Val	logFCko-logFCwt	FCko-FCwt
Prkci	protein kinase C, iota	1448695_at	0,75	2,50E-05	0,36	0,009501212	0,39	1,31
Cdk5r1	cyclin-dependent kinase 5, regulatory subunit 1 (p35)	1421123_at	0,81	1,89E-06	0,43	0,000657868	0,38	1,30
Cdk5	cyclin-dependent kinase 5	1450674_at	0,74	5,25E-07	0,41	0,000185785	0,33	1,26
Mapk3	mitogen-activated protein kinase 3	1427060_at	0,61	3,78E-07	0,36	7,50E-05	0,25	1,19
Hras1	Harvey rat sarcoma virus oncogene 1	1422407_s_at	0,68	1,22E-07	0,45	7,80E-06	0,23	1,17
Crkl	v-crk sarcoma virus CT10 oncogene homolog (avian)-like	1421954_at	0,59	0,000345546	0,39	0,0069595	0,20	1,15
Psen1	presenilin 1	1450399_at	0,77	3,08E-07	0,58	6,11E-06	0,20	1,15
Plcg2	phospholipase C, gamma 2	1426926_at	0,67	1,80E-05	0,49	0,000328846	0,18	1,13
Rps6kb2	ribosomal protein S6 kinase, polypeptide 2	1422268_a_at	0,69	9,88E-06	0,56	7,68E-05	0,13	1,10

Table 11: UP IN KO Synaptic plasticity genes

Gene Symbol	GeneName	Affymetrix Probe ID	*Prnp*0\0 mice adults *vs* newborns logFC	*Prnp*0\0 mice adults *vs* newborns adj.P.Val	*Prnp*+\+ mice adults *vs* newborns logFC	*Prnp*+\+ mice adults *vs* newborns adj.P.Val	logFCko-logFCwt	FCko-FCwt
Grin2b	glutamate receptor, ionotropic, NMDA2B (epsilon 2)	1422223_at	0,65	0,000363825	0,27	0,069909634	0,38	1,30
Cdk5	cyclin-dependent kinase 5	1450674_at	0,74	5,25E-07	0,41	0,000185785	0,33	1,26
Hras1	Harvey rat sarcoma virus oncogene 1	1422407_s_at	0,68	1,22E-07	0,45	7,80E-06	0,23	1,17
Psen1	presenilin 1	1450399_at	0,77	3,08E-07	0,58	6,11E-06	0,20	1,15
Prkaca	protein kinase, cAMP dependent, catalytic, alpha	1450519_a_at	0,73	4,77E-07	0,56	7,45E-06	0,17	1,13
Kit	kit oncogene	1415900_a_at	0,66	3,57E-05	0,51	0,00033623	0,14	1,10
Gipc1	GIPC PDZ domain containing family, member 1	1422763_at	0,59	2,61E-06	0,45	3,24E-05	0,13	1,10

Table 12: UP IN KO Chloride channel-related genes

Gene Symbol	Gene Name	Affymetrix Probe ID	*Prnp*0\0 mice adults *vs* newborns logFC	*Prnp*0\0 mice adults *vs* newborns adj.P.Val	*Prnp*+\+ mice adults *vs* newborns logFC	*Prnp*+\+ mice adults *vs* newborns adj.P.Val	logFCko-logFCwt	FCko-FCwt
Clic4	chloride intracellular channel 4 (mitochondrial)	1423392_at	0,94	8,15E-09	0,44	1,89E-05	0,50	1,41
Clcn7	chloride channel 7	1450408_at	0,61	4,87E-06	0,33	0,001475	0,29	1,22
Clcn6	chloride channel 6	1422314_at	0,74	8,30E-06	0,48	0,00048	0,26	1,20
Clcnka	chloride channel Ka	1455677_s_at	0,70	6,02E-06	0,47	0,000257	0,23	1,17
Kcnd1	potassium voltage-gated channel, Shal-related family, member 1	1421538_at	0,59	9,96E-05	0,41	0,001911	0,18	1,13

Table 13: UP IN KO Cell adhesion, Neurite outgrowth and Axon guidance genes

Gene Symbol	Gene Name	Affymetrix Probe ID	*Prnp*0\0 mice adults *vs* newborns logFC	*Prnp*0\0 mice adults *vs* newborns adj.P.Val	*Prnp*+\+ mice adults *vs* newborns logFC	*Prnp*+\+ mice adults *vs* newborns adj.P.Val	logFCko-logFCwt	FCko-FCwt
CELL ADHESION								
S100a9	S100 calcium binding protein A9 (calgranulin B)	1448756_at	0,83	7,83E-06	0,16	0,198828943	0,67	1,60
Gfra1	glial cell line derived neurotrophic factor family receptor alpha 1	1450440_at	0,99	9,06E-06	0,58	0,00109835	0,41	1,33
Gpnmb	glycoprotein (transmembrane) nmb	1448303_at	0,73	0,00031634	0,33	0,048167101	0,40	1,32
Cdk5r1	cyclin-dependent kinase 5, regulatory subunit 1 (p35)	1421123_at	0,81	1,89E-06	0,43	0,000657868	0,38	1,30
Jam3	junction adhesion molecule 3	1423503_at	0,69	2,25E-08	0,33	3,95E-05	0,36	1,28
Tnxb	tenascin XB	1450798_at	0,77	2,04E-06	0,45	0,000345233	0,32	1,25
Fgfr1	fibroblast growth factor receptor 1	1425911_a_at	0,62	0,000144627	0,32	0,015912045	0,29	1,23
Csf3r	colony stimulating factor 3 receptor (granulocyte)	1418806_at	0,77	2,23E-06	0,53	8,33E-05	0,24	1,18
Hras1	Harvey rat sarcoma virus oncogene 1	1422407_s_at	0,68	1,22E-07	0,45	7,80E-06	0,23	1,17
Tgm2	transglutaminase 2, C polypeptide	1417500_a_at	0,78	2,70E-06	0,56	7,30E-05	0,22	1,17
Vav3	vav 3 oncogene	1417123_at	0,66	2,88E-05	0,44	0,000917923	0,21	1,16
Crkl	v-crk sarcoma virus CT10 oncogene homolog (avian)-like	1421954_at	0,59	0,000345546	0,39	0,0069595	0,20	1,15
Psen1	presenilin 1	1450399_at	0,77	3,08E-07	0,58	6,11E-06	0,20	1,15
Plcg2	phospholipase C, gamma 2	1426926_at	0,67	1,80E-05	0,49	0,000328846	0,18	1,13
Apoc3	apolipoprotein C-III	1418278_at	0,68	2,87E-06	0,52	4,08E-05	0,16	1,12
Epas1	endothelial PAS domain protein 1	1449888_at	0,68	5,10E-06	0,54	5,28E-05	0,15	1,11
Kit	kit oncogene	1415900_a_at	0,66	3,57E-05	0,51	0,00033623	0,14	1,10
NEURITE OUTGROWTH								
Gfra1	glial cell line derived neurotrophic factor family receptor alpha 1	1450440_at	0,99	9,06E-06	0,58	0,00109835	0,41	1,33
Cdk5r1	cyclin-dependent kinase 5, regulatory subunit 1 (p35)	1421123_at	0,81	1,89E-06	0,43	0,000657868	0,38	1,30
Cdk5	cyclin-dependent kinase 5	1450674_at	0,74	5,25E-07	0,41	0,000185785	0,33	1,26
Fgfr1	fibroblast growth factor receptor 1	1425911_a_at	0,62	0,000144627	0,32	0,015912045	0,29	1,23
Mapk3	mitogen-activated protein kinase 3	1427060_at	0,61	3,78E-07	0,36	7,50E-05	0,25	1,19
Hras1	Harvey rat sarcoma virus oncogene 1	1422407_s_at	0,68	1,22E-07	0,45	7,80E-06	0,23	1,17
Tgm2	transglutaminase 2, C polypeptide	1417500_a_at	0,78	2,70E-06	0,56	7,30E-05	0,22	1,17
Vav3	vav 3 oncogene	1417123_at	0,66	2,88E-05	0,44	0,000917923	0,21	1,16
Cables1	Cdk5 and Abl enzyme substrate 1	1422477_at	0,75	1,52E-05	0,56	0,000224665	0,19	1,14
Prkaca	protein kinase, cAMP dependent, catalytic, alpha	1450519_a_at	0,73	4,77E-07	0,56	7,45E-06	0,17	1,13
Nck2	non-catalytic region of tyrosine kinase adaptor protein 2	1416797_at	0,74	9,25E-06	0,57	0,000109504	0,17	1,12
Kit	kit oncogene	1415900_a_at	0,66	3,57E-05	0,51	0,00033623	0,14	1,10
AXON GUIDANCE								
Klf5c	kinesin family member 5C	1450804_at	0,88	0,000387999	0,44	0,033764559	0,44	1,35
Cdk5r1	cyclin-dependent kinase 5, regulatory subunit 1 (p35)	1421123_at	0,81	1,89E-06	0,43	0,000657868	0,38	1,30
Cdk5	cyclin-dependent kinase 5	1450674_at	0,74	5,25E-07	0,41	0,000185785	0,33	1,26
Mapk3	mitogen-activated protein kinase 3	1427060_at	0,61	3,78E-07	0,36	7,50E-05	0,25	1,19
Galns	galactosamine (N-acetyl)-6-sulfate sulfatase	1448744_at	0,67	4,83E-07	0,44	3,84E-05	0,24	1,18
Hras1	Harvey rat sarcoma virus oncogene 1	1422407_s_at	0,68	1,22E-07	0,45	7,80E-06	0,23	1,17

Table 14: UP IN KO Calcium homeostasis genes

Gene Symbol	Gene Name	Affymetrix Probe ID	*Prnp*0/0 mice adults *vs* newborns logFC	*Prnp*0/0 mice adults *vs* newborns adj.P.Val	*Prnp*+/+ mice adults *vs* newborns logFC	*Prnp*+/+ mice adults *vs* newborns adj.P.Val	logFCko-logFCwt	FCko-FCwt
S100a9	S100 calcium binding protein A9 (calgranulin B)	1448756_at	0,83	7,83E-06	0,16	0,198828943	0,67	1,60
Cant1	calcium activated nucleotidase 1	1421476_a_at	1,02	2,74E-07	0,50	0,00028859	0,52	1,43
Grk6	G protein-coupled receptor kinase 6	1450480_a_at	0,80	6,96E-06	0,36	0,005486454	0,43	1,35
Slc27a1	solute carrier family 27 (fatty acid transporter), member 1	1422811_at	0,85	1,83E-06	0,42	0,001217698	0,43	1,35
Gna14	guanine nucleotide binding protein, alpha 14	1420385_at	0,83	2,07E-05	0,44	0,004277527	0,39	1,31
Grin2b	glutamate receptor, ionotropic, NMDA2B (epsilon 2)	1422223_at	0,65	0,000363825	0,27	0,069909634	0,38	1,30
Casq2	calsequestrin 2	1422529_s_at	0,59	2,30E-06	0,32	0,000716576	0,27	1,21
Kcnip3	Kv channel interacting protein 3, calsenilin	1449129_a_at	0,62	5,71E-06	0,39	0,000489463	0,24	1,18
Fcgr1	Fc receptor, IgG, high affinity I	1417876_at	0,64	0,000205429	0,42	0,005577579	0,22	1,17
Vav3	vav 3 oncogene	1417123_at	0,66	2,88E-05	0,44	0,000917923	0,21	1,16
Herpud1	homocysteine-inducible, ER stress-inducible, ubiquitin-like domain member 1	1435626_a_at	0,69	1,27E-06	0,49	3,86E-05	0,20	1,15
Psen1	presenilin 1	1450399_at	0,77	3,08E-07	0,58	6,11E-06	0,20	1,15
Psen1	presenilin 1	1450399_at	0,77	3,08E-07	0,58	6,11E-06	0,20	1,15
Plcg2	phospholipase C, gamma 2	1426926_at	0,67	1,80E-05	0,49	0,000328846	0,18	1,13
Prkaca	protein kinase, cAMP dependent, catalytic, alpha	1450519_a_at	0,73	4,77E-07	0,56	7,45E-06	0,17	1,13
Prkaca	protein kinase, cAMP dependent, catalytic, alpha	1450519_a_at	0,73	4,77E-07	0,56	7,45E-06	0,17	1,13
Apoc3	apolipoprotein C-III	1418278_at	0,68	2,87E-06	0,52	4,08E-05	0,16	1,12

Table 15: DOWN IN WT Carbohydrate and small molecules metabolism genes

Gene Symbol	Gene Name	Affymetrix Probe ID	*Prnp*+/+ mice adults *vs* newborns logFC	*Prnp*+/+ mice adults *vs* newborns adj.P.Val	*Prnp*0/0 mice adults *vs* newborns logFC	*Prnp*0/0 mice adults *vs* newborns adj.P.Val	logFCwt-logFCko	FCwt-FCko	Inverse
TRASFERASE ACTIVITY									
Ugt1a6a	UDP glucuronosyltransferase 1 family, polypeptide A6A	1426260_a_at	-0,97	1,12E-06	-0,56	0,000258452	-0,42	0,75	-1,33
Ergic3	ERGIC and golgi 3	1456745_x_at	-0,61	4,26E-07	-0,24	0,002389004	-0,37	0,77	-1,29
Rtn2	reticulon 2 (Z-band associated protein)	1419056_at	-0,63	6,49E-07	-0,33	0,000370246	-0,30	0,81	-1,23
Ugt1a6a	UDP glucuronosyltransferase 1 family, polypeptide A6A	1426261_s_at	-0,62	0,000120767	-0,40	0,003792723	-0,22	0,86	-1,16
Yif1a	Yip1 interacting factor homolog A (S. cerevisiae)	1423939_a_at	-0,59	0,000415099	-0,42	0,005027184	-0,17	0,89	-1,12
B4galt2	betaGlcNAc beta 1,4- galactosyltransferase, polypeptide 2	1418080_at	-0,65	6,27E-05	-0,50	0,000607547	-0,15	0,90	-1,11
Mfng	MFNG O-fucosylpeptide 3-beta-N-acetylglucosaminyltransferase	1416992_at	-0,62	5,72E-05	-0,48	0,000593454	-0,14	0,90	-1,11
NUCLEOSIDE TRIPHOSPHATASE ACTIVITY									
Rfc2	replication factor C (activator 1) 2	1417503_at	-0,60	2,37E-07	-0,26	0,000907235	-0,35	0,79	-1,27
Atad3a	ATPase family, AAA domain containing 3A	1456541_x_at	-0,86	2,26E-07	-0,57	1,56E-05	-0,29	0,82	-1,22
Ruvbl2	RuvB-like protein 2	1422482_at	-0,63	4,08E-07	-0,39	5,76E-05	-0,24	0,85	-1,18
Fancm	Fanconi anemia, complementation group M	1447935_at	-0,69	3,16E-06	-0,52	5,41E-05	-0,17	0,89	-1,13
Ddx18	DEAD (Asp-Glu-Ala-Asp) box polypeptide 18	1416070_a_at	-0,63	3,28E-07	-0,47	6,96E-06	-0,16	0,90	-1,12
Eif4a3	eukaryotic translation initiation factor 4A, isoform 3	1417242_at	-0,60	5,86E-08	-0,47	9,55E-07	-0,14	0,91	-1,10
N-LINKED GLYCOSYLATION ACTIVITY									
Rasip1	Ras interacting protein 1	1428016_a_at	-0,86	0,000177427	-0,41	0,026155371	-0,44	0,74	-1,36
St8sia1	ST8 alpha-N-acetyl-neuraminide alpha-2,8-sialyltransferase 1	1419695_at	-0,74	7,37E-06	-0,45	0,000691033	-0,29	0,82	-1,22
Tmem123	transmembrane protein 123	1417222_a_at	-0,68	0,000177734	-0,52	0,001708381	-0,17	0,89	-1,12
Mfng	MFNG O-fucosylpeptide 3-beta-N-acetylglucosaminyltransferase	1416992_at	-0,62	5,72E-05	-0,48	0,000593454	-0,14	0,90	-1,11

Table 16: DOWN IN KO Embryonic and central nervous system development

Gene Symbol	Gene Name	Affymetrix Probe ID	*Prnp*0/0 mice adults *vs* newborns logFC	*Prnp*0/0 mice adults *vs* newborns adj.P.Val	*Prnp*+/+ mice adults *vs* newborns logFC	*Prnp*+/+ mice adults *vs* newborns adj.P.Val	logFCko-logFCwt	FCko-FCwt	Inverse
EMBRYONICI DEVELOPMENT AND DIFFERENTIATION									
Tbx18	T-box18	1449871_at	-0,98	1,02E-07	-0,05	0,616338954	-0,93	0,53	-1,90
Ctcf	CCCTC-binding factor	1449042_at	-1,47	0,000235306	-0,54	0,089216744	-0,92	0,53	-1,90
Lims1	LIM and senescent cell antigen-like domains 1	1418230_a_at	-1,42	6,16E-05	-0,52	0,053619799	-0,90	0,54	-1,87
Lims1	LIM and senescent cell antigen-like domains 1	1418230_a_at	-1,42	6,16E-05	-0,52	0,053619799	-0,90	0,54	-1,87
Ncor1	nuclear receptor co-repressor 1	1423201_at	-0,70	0,00035368	0,20	0,211155329	-0,90	0,54	-1,86
Elf5	E74-like factor 5	1419555_at	-0,97	2,88E-05	-0,08	0,609067014	-0,89	0,54	-1,85
Ptn	pleiotrophin	1416211_a_at	-0,64	0,020079883	0,20	0,44946573	-0,83	0,56	-1,78
Ndel1	nuclear distribution gene E-like homolog 1 (A. nidulans)	1424893_at	-0,98	3,38E-05	-0,20	0,243280992	-0,79	0,58	-1,72
Gsk3b	glycogen synthase kinase 3 beta	1451020_at	-0,76	0,000176525	-0,09	0,555566071	-0,66	0,63	-1,58
Fst	follistatin	1421365_at	-0,60	0,000267985	0,03	0,846070323	-0,63	0,65	-1,55
Igf2	insulin-like growth factor 2	1448152_at	-1,05	8,53E-06	-0,42	0,012936336	-0,63	0,65	-1,54
Epha4	Eph receptor A4	1421929_at	-0,90	0,00456601	-0,28	0,322484798	-0,62	0,65	-1,54
Pf4	platelet factor 4	1448995_at	-0,95	1,88E-09	-0,35	5,48E-05	-0,60	0,66	-1,51
Thra	thyroid hormone receptor alpha	1426997_at	-0,82	9,26E-08	-0,30	0,001263504	-0,52	0,70	-1,43
Ebf1	early B-cell factor 1	1416301_a_at	-0,67	0,001144064	-0,21	0,224200396	-0,46	0,73	-1,37
Sp1	trans-acting transcription factor 1	1418180_at	-0,90	1,28E-07	-0,45	0,000141672	-0,45	0,73	-1,37
Dnase2a	deoxyribonuclease II alpha	1448986_x_at	-0,63	3,24E-06	-0,19	0,034155093	-0,44	0,74	-1,36
Ttc3	tetratricopeptide repeat domain 3	1416482_at	-0,69	0,028583842	-0,25	0,401800704	-0,44	0,74	-1,36
Ahr	aryl-hydrocarbon receptor	1422631_at	-0,66	3,71E-06	-0,24	0,01457469	-0,42	0,75	-1,34
Serpinf1	serine (or cysteine) peptidase inhibitor, clade F, member 1	1416168_at	-0,69	0,002765178	-0,28	0,159655436	-0,41	0,75	-1,32
S100a4	S100 calcium binding protein A4	1424542_at	-0,73	0,007298816	-0,33	0,182539055	-0,40	0,76	-1,32
Hbegf	heparin-binding EGF-like growth factor	1418350_at	-0,83	9,78E-05	-0,43	0,013212471	-0,40	0,76	-1,32
Hbegf	heparin-binding EGF-like growth factor	1418350_at	-0,83	9,78E-05	-0,43	0,013212471	-0,40	0,76	-1,32
Foxc1	forkhead box C1	1419486_at	-0,72	6,86E-06	-0,33	0,005185632	-0,39	0,76	-1,31
Pdgfrb	platelet derived growth factor receptor, beta polypeptide	1436970_a_at	-0,91	1,27E-05	-0,57	0,000894478	-0,34	0,79	-1,27
Hmgb1	high mobility group box 1	1448235_s_at	-0,64	0,013496053	-0,29	0,217745763	-0,34	0,79	-1,27
Tceb3	transcription elongation factor B (SIII), polypeptide 3	1450676_at	-0,72	0,000177821	-0,40	0,013267685	-0,32	0,80	-1,25
Ikzf4	IKAROS family zinc finger 4	1438274_at	-0,77	8,80E-07	-0,46	0,000152166	-0,32	0,80	-1,24
Nab1	Ngfi-A binding protein 1	1417624_at	-0,63	2,40E-06	-0,33	0,001058991	-0,31	0,81	-1,24
Ednrb	endothelin receptor type B	1423594_a_at	-0,88	0,015183628	-0,58	0,089247167	-0,29	0,82	-1,23
Acaca	acetyl-Coenzyme A carboxylase alpha	1427595_at	-0,68	1,23E-08	-0,40	3,15E-06	-0,28	0,82	-1,22
Mll5	myeloid/lymphoid or mixed-lineage leukemia 5	1434704_at	-0,62	3,71E-06	-0,35	0,00086709	-0,28	0,82	-1,21
Smarca1	SWI/SNF related, matrix associated, subfamily a, member 1	1460292_a_at	-0,77	3,63E-07	-0,49	3,30E-05	-0,28	0,82	-1,21
Id4	inhibitor of DNA binding 4	1438441_at	-0,76	0,002196679	-0,49	0,030261617	-0,28	0,83	-1,21
Mapk1	mitogen-activated protein kinase 1	1419568_at	-0,71	0,000188062	-0,44	0,007317988	-0,27	0,83	-1,21
Sox6	SRY-box containing gene 6	1427677_a_at	-0,79	1,09E-05	-0,53	0,000441649	-0,26	0,84	-1,20
Fcgr2b	Fc receptor, IgG, low affinity IIb	1435477_s_at	-0,70	0,000280161	-0,44	0,00841968	-0,26	0,84	-1,20
Nfkbia	nuclear factor of kappa light polypeptide gene enhancer in B-cells inhibitor, alpha	1420089_at	-0,78	6,08E-05	-0,52	0,001750237	-0,25	0,84	-1,19
Lcp2	lymphocyte cytosolic protein 2	1418641_at	-0,78	6,92E-07	-0,54	2,84E-05	-0,24	0,85	-1,18
Snrk	SNF related kinase	1425678_a_at	-0,60	7,81E-07	-0,37	8,75E-05	-0,23	0,85	-1,17
Elavl2	ELAV (embryonic lethal, abnormal vision, Drosophila)-like 2 (Hu antigen B)	1421883_at	-0,69	5,44E-07	-0,46	3,12E-05	-0,23	0,85	-1,17
Acvr2b	activin receptor IIB	1419140_at	-0,76	3,10E-06	-0,56	5,67E-05	-0,19	0,87	-1,14
Xrcc4	X-ray repair complementing defective repair in Chinese hamster cells 4	1424602_s_at	-0,78	6,51E-06	-0,58	0,000102361	-0,19	0,87	-1,14
Tox	thymocyte selection-associated high mobility group box	1425484_at	-0,60	2,57E-06	-0,42	8,70E-05	-0,18	0,88	-1,13
Erbb2ip	Erbb2 interacting protein	1439079_a_at	-0,64	2,15E-05	-0,49	0,000243356	-0,15	0,90	-1,11
NERVOUS SYSTEM DEVELOPMENT AND FUNCTION									
Prkg1	protein kinase, cGMP-dependent, type I	1449876_at	-1,04	4,56E-05	-0,19	0,312627103	-0,86	0,55	-1,81
Bptf	bromodomain PHD finger transcription factor	1427310_at	-0,69	9,01E-05	0,14	0,299189128	-0,82	0,57	-1,77
Ndel1	nuclear distribution gene E-like homolog 1 (A. nidulans)	1424893_at	-0,98	3,38E-05	-0,20	0,243280992	-0,79	0,58	-1,72
Kif3a	kinesin family member 3A	1420375_at	-1,02	1,04E-05	-0,27	0,082545304	-0,74	0,60	-1,67
Zeb2	zinc finger E-box binding homeobox 2	1422748_at	-0,94	0,000352913	-0,34	0,114142493	-0,61	0,66	-1,52
Il1rapl2	interleukin 1 receptor accessory protein-like 2	1420462_at	-0,72	4,79E-05	-0,23	0,080268644	-0,49	0,71	-1,40
Dmd	dystrophin, muscular dystrophy	1430320_at	-0,83	0,004701373	-0,34	0,18996692	-0,49	0,71	-1,40
Klhl1	kelch-like 1 (Drosophila)	1449241_at	-0,59	1,33E-06	-0,10	0,157004978	-0,48	0,72	-1,40
Cacna1a	calcium channel, voltage-dependent, P/Q type, alpha 1A subunit	1459996_at	-0,81	2,00E-05	-0,37	0,010845328	-0,44	0,74	-1,36
Odz2	odd Oz/ten-m homolog 2 (Drosophila)	1420718_at	-0,72	2,57E-06	-0,45	0,000249232	-0,28	0,83	-1,21
Pard3	par-3 (partitioning defective 3) homolog (C. elegans)	1434775_at	-0,76	3,17E-06	-0,49	0,000220505	-0,27	0,83	-1,21
Nrp2	neuropilin 2	1426528_at	-0,71	1,95E-07	-0,51	6,31E-06	-0,20	0,87	-1,15
Jarid2	jumonji, AT rich interactive domain 2	1422698_s_at	-0,59	4,61E-07	-0,40	2,43E-05	-0,19	0,88	-1,14

Table 17: DOWN IN KO Cadherin genes

Gene Symbol	Gene Name	Affymetrix Probe ID	*Prnp*0\0 mice adults *vs* newborns logFC	*Prnp*0\0 mice adults *vs* newborns adj.P.Val	*Prnp*+\+ mice adults *vs* newborns logFC	*Prnp*+\+ mice adults *vs* newborns adj.P.Val	logFCko-logFCwt	FCko-FCwt	Inverse
Cdh8	cadherin 8	1422052_at	-0,72	0,002921425	-0,13	0,531260225	-0,59	0,67	-1,50
Pcdhb21	protocadherin beta 21	1420422_at	-0,81	6,51E-05	-0,23	0,129119004	-0,58	0,67	-1,50
Pcdh21	protocadherin 21	1418304_at	-0,83	1,67E-06	-0,53	0,000126602	-0,30	0,81	-1,23
Cdh10	cadherin 10	1425092_at	-0,60	2,87E-06	-0,39	0,000193968	-0,21	0,86	-1,16
Cdh13	cadherin 13	1423551_at	-0,62	4,06E-06	-0,47	5,57E-05	-0,15	0,90	-1,11

Table 18: DOWN IN KO Transition metal ions binding genes

Gene Symbol	Gene Name	Affymetrix Probe ID	*Prnp*0\0 mice adults *vs* newborns logFC	*Prnp*0\0 mice adults *vs* newborns adj.P.Val	*Prnp*+\+ mice adults *vs* newborns logFC	*Prnp*+\+ mice adults *vs* newborns adj.P.Val	logFCko-logFCwt	FCko-FCwt	Inverse
Zfp207	zinc finger protein 207	1423546_at	-1,43	3,87E-05	-0,33	0,187875091	-1,10	0,47	-2,14
Rbm5	RNA binding motif protein 5	1456262_at	-1,05	0,005247743	-0,09	0,791728207	-0,96	0,51	-1,95
Zfp292	zinc finger protein 292	1449515_at	-0,93	0,000235531	-0,02	0,91971782	-0,91	0,53	-1,88
Osr1	odd-skipped related 1 (Drosophila)	1449350_at	-0,83	0,00135992	0,02	0,937267908	-0,85	0,56	-1,80
Rspry1	ring finger and SPRY domain containing 1	1424134_at	-0,86	5,01E-06	-0,33	0,01285019	-0,53	0,69	-1,45
Zmym5	zinc finger, MYM-type 5	1425577_at	-0,80	1,52E-06	-0,28	0,009989372	-0,51	0,70	-1,43
Zcchc14	zinc finger, CCHC domain containing 14	1418170_a_at	-0,75	0,000123271	-0,30	0,048655443	-0,44	0,73	-1,36
Ttc3	tetratricopeptide repeat domain 3	1416482_at	-0,69	0,028583842	-0,25	0,401800704	-0,44	0,74	-1,36
Tiparp	TCDD-inducible poly(ADP-ribose) polymerase	1452160_at	-0,85	0,001062027	-0,49	0,031080483	-0,36	0,78	-1,28
March7	membrane-associated ring finger (C3HC4) 7	1436893_a_at	-0,78	0,00033344	-0,42	0,020643837	-0,35	0,78	-1,28
Dnajc24	DnaJ (Hsp40) homolog, subfamily C, member 24	1451389_at	-0,80	0,000144769	-0,47	0,008569902	-0,33	0,79	-1,26
Mobkl1b	MOB1, Mps One Binder kinase activator-like 1B (yeast)	1423782_at	-0,69	8,49E-07	-0,39	0,000221739	-0,30	0,81	-1,23
Zfp644	zinc finger protein 644	1449691_at	-0,74	0,000130287	-0,44	0,007199209	-0,30	0,81	-1,23
Mll5	myeloid/lymphoid or mixed-lineage leukemia 5	1427236_a_at	-0,70	9,86E-05	-0,48	0,002423528	-0,23	0,85	-1,17
Zc3h14	zinc finger CCCH type containing 14	1426999_at	-0,59	3,70E-06	-0,37	0,00031143	-0,22	0,86	-1,16
Zfp7	zinc finger protein 7	1451323_at	-0,72	2,97E-06	-0,51	8,46E-05	-0,21	0,86	-1,16
Rbm26	RNA binding motif protein 26	1426420_at	-0,71	2,19E-06	-0,55	3,03E-05	-0,17	0,89	-1,12

Table 19: DOWN IN KO Ubiquitin system genes

Gene Symbol	Gene Name	Affymetrix Probe ID	*Prnp*0\0 mice adults *vs* newborns logFC	*Prnp*0\0 mice adults *vs* newborns adj.P.Val	*Prnp*+\+ mice adults *vs* newborns logFC	*Prnp*+\+ mice adults *vs* newborns adj.P.Val	logFCko-logFCwt	FCko-FCwt	Inverse
Usp48	ubiquitin specific peptidase 48	1419277_at	-0,98	0,003432504	0,07	0,811381387	-1,06	0,48	-2,08
Topors	topoisomerase I binding, arginine/serine-rich	1417754_at	-1,30	1,70E-05	-0,34	0,110708616	-0,96	0,51	-1,95
Usp1	ubiquitin specific peptdiase 1	1423674_at	-0,73	0,001107754	0,04	0,82376519	-0,77	0,58	-1,71
Cbll1	Casitas B-lineage lymphoma-like 1	1437203_at	-0,66	6,64E-06	-0,21	0,039639058	-0,45	0,73	-1,37
Tiparp	TCDD-inducible poly(ADP-ribose) polymerase	1452160_at	-0,85	0,001062027	-0,49	0,031080483	-0,36	0,78	-1,28
Ttll3	tubulin tyrosine ligase-like family, member 3	1421219_at	-0,87	0,000488703	-0,52	0,016978342	-0,35	0,78	-1,28
March7	membrane-associated ring finger (C3HC4) 7	1436893_a_at	-0,78	0,00033344	-0,42	0,020643837	-0,35	0,78	-1,28
Psma7	proteasome (prosome, macropain) subunit, alpha type 7	1423568_at	-0,76	2,69E-07	-0,47	3,68E-05	-0,29	0,82	-1,23
Usp34	ubiquitin specific peptidase 34	1434393_at	-0,68	0,000135267	-0,43	0,004828925	-0,25	0,84	-1,19
Ube2v2	ubiquitin-conjugating enzyme E2 variant 2	1417983_a_at	-0,70	2,01E-06	-0,51	4,81E-05	-0,19	0,87	-1,14
Usp52	ubiquitin specific peptidase 52	1426700_a_at	-0,65	6,75E-06	-0,46	0,000169491	-0,19	0,88	-1,14
Rnf19b	ring finger protein 19B	1435226_at	-0,60	1,22E-07	-0,46	2,04E-06	-0,14	0,91	-1,10

Table 20: Comparison between adult PrPC-deficient mice and adult wildtype mice

Gene Symbol	Gene Name	Affymetrix Probe ID	logFC	P.Value	adj.P.Val
UPREGULATED GENES					
Lcn2	lipocalin 2	1427747_a_at	3,042086394	1,77E-06	0,001610054
Lrg1	leucine-rich alpha-2-glycoprotein 1	1417290_at	1,363082416	1,06E-05	0,006010402
S100a8	S100 calcium binding protein A8 (calgranulin A)	1419394_s_at	0,958961501	2,26E-05	0,010581718
Thyn1	thymocyte nuclear protein 1	1438769_a_at	0,888054795	8,79E-10	1,44E-05
Jam3	junction adhesion molecule 3	1423503_at	0,837661922	3,97E-09	2,17E-05
Jag1	jagged 1	1421106_at	0,831844509	5,36E-06	0,003445852
S100a9	S100 calcium binding protein A9 (calgranulin B)	1448756_at	0,830281228	2,94E-07	0,000402128
Vps26b	vacuolar protein sorting 26 homolog B (yeast)	1428247_at	0,824895488	7,99E-08	0,000130975
Atpbd4	ATP binding domain 4	1426548_a_at	0,79966703	4,13E-07	0,000504171
Ch25h	cholesterol 25-hydroxylase	1449227_at	0,790814051	0,000441622	0,049573562
Vps26b	vacuolar protein sorting 26 homolog B (yeast)	1428246_at	0,775831892	6,21E-08	0,000113076
Atp1b2	ATPase, Na+/K+ transporting, beta 2 polypeptide	1422009_at	0,769106642	0,000210063	0,038682902
Fos	FBJ osteosarcoma oncogene	1423100_at	0,744253846	0,000364782	0,044796979
Thyn1	thymocyte nuclear protein 1	1438480_a_at	0,716924595	1,06E-08	3,49E-05
Thyn1	thymocyte nuclear protein 1	1460007_at	0,678223452	5,67E-08	0,000113076
Nol1	nucleolar protein 1	1424019_at	0,675043709	5,18E-08	0,000113076
C1qc	complement component 1, q subcomponent, C chain	1449401_at	0,66376915	0,00036627	0,044796979
C1qb	complement component 1, q subcomponent, beta polypeptide	1417063_at	0,654273776	7,90E-05	0,025591492
C1qb	complement component 1, q subcomponent, beta polypeptide	1437726_x_at	0,652039167	0,000221868	0,038682902
Hspa8	heat shock protein 8	1431182_at	0,63386946	5,47E-06	0,003445852
Adm	adrenomedullin	1416077_at	0,522121938	0,000361084	0,044796979
Icam1	intercellular adhesion molecule 1	1424067_at	0,50892784	9,47E-05	0,02820437
Ier3	immediate early response 3	1419647_a_at	0,50599963	5,25E-05	0,018307809
Mobp	myelin-associated oligodendrocytic basic protein	1450088_a_at	0,491041601	2,10E-06	0,001815417
Scgb3a1	secretoglobin, family 3A, member 1	1419699_at	0,490566961	0,000217175	0,038682902
Pygm	muscle glycogen phosphorylase	1448602_at	0,470286427	1,40E-06	0,001349558
Vamp1	vesicle-associated membrane protein 1	1421862_a_at	0,45270583	0,000289626	0,04186476
Dtd1	D-tyrosyl-tRNA deacylase 1 homolog (S. cerevisiae)	1451040_at	0,451872952	7,37E-07	0,000754462
Mobp	myelin-associated oligodendrocytic basic protein	1421010_at	0,450019651	5,45E-06	0,003445852
Cxcl1	chemokine (C-X-C motif) ligand 1	1419209_at	0,412719612	0,000106996	0,029542727
Tgm2	transglutaminase 2, C polypeptide	1417500_a_at	0,41247099	7,89E-05	0,025591492
Aqr	aquarius	1433497_at	0,411895479	2,22E-05	0,010581718
Cd14	CD14 antigen	1417268_at	0,409225151	0,000203458	0,038682902
Acad8	acyl-Coenzyme A dehydrogenase family, member 8	1419262_at	0,407421568	4,23E-06	0,003014221
Acad8	acyl-Coenzyme A dehydrogenase family, member 8	1419261_at	0,391226508	2,35E-05	0,01064284
Ids	iduronate 2-sulfatase	1434751_at	0,390392582	0,000289351	0,04186476
Acly	ATP citrate lyase	1425326_at	0,377147111	0,000249684	0,040515591
Cds2	CDP-diacylglycerol synthase (phosphatidate cytidylyltransferase) 2	1454891_at	0,374788054	7,96E-05	0,025591492
Cd24a	CD24a antigen	1416034_at	0,364618698	2,96E-05	0,012138916
Ly6a	lymphocyte antigen 6 complex, locus A	1417185_at	0,358297731	0,000347196	0,044036006
Stard4	StAR-related lipid transfer (START) domain containing 4	1429239_a_at	0,346689699	0,000116527	0,030147811
Hist2h3c1	histone cluster 2, H3c1	1460314_s_at	0,341662774	0,000376628	0,045386477
Sparc	secreted acidic cysteine rich glycoprotein	1448392_at	0,323315434	0,000107022	0,029542727
Vamp1	vesicle-associated membrane protein 1	1421863_at	0,322330361	0,000212532	0,038682902
Sdccag3	serologically defined colon cancer antigen 3	1431760_a_at	0,318665844	0,000117729	0,030147811
Mal	myelin and lymphocyte protein, T-cell differentiation protein	1417275_at	0,316075923	0,000176167	0,038300993
Pm20d1	peptidase M20 domain containing 1	1426876_at	0,316007641	0,000296081	0,04186476
Clic4	chloride intracellular channel 4 (mitochondrial)	1423392_at	0,30054744	0,000231352	0,039016916
Cnp	2',3'-cyclic nucleotide 3' phosphodiesterase	1449296_a_at	0,299610517	0,000239714	0,039286655
Cln8	ceroid-lipofuscinosis, neuronal 8	1448456_at	0,294241936	0,000341424	0,044036006
Mobp	myelin-associated oligodendrocytic basic protein	1433785_at	0,291548221	4,87E-05	0,017366037
Tfrc	transferrin receptor	1422966_a_at	0,290985745	0,000351075	0,044036006
Cdr2	cerebellar degeneration-related 2	1417430_at	0,289413894	9,24E-05	0,028040584
Phf12	PHD finger protein 12	1434922_at	0,286803525	6,20E-05	0,021155318
Lcat	lecithin cholesterol acyltransferase	1417043_at	0,286386147	0,000169464	0,037531765
Mal	myelin and lymphocyte protein, T-cell differentiation protein	1432558_a_at	0,278512578	0,00032655	0,044036006
Gadd45b	growth arrest and DNA-damage-inducible 45 beta	1450971_at	0,278068629	0,000167785	0,037531765
Atp6v0a1	ATPase, H+ transporting, lysosomal V0 subunit A1	1425227_a_at	0,277977396	0,000286282	0,04186476
Sparc	secreted acidic cysteine rich glycoprotein	1416589_at	0,272305263	2,88E-05	0,012118843
Tlcd1	TLC domain containing 1	1426616_at	0,271658848	0,000233306	0,039016916
Casq1	calsequestrin 1	1422598_at	0,268661957	0,000419997	0,047800963
Mkrn1	makorin, ring finger protein, 1	1455504_a_at	0,266659348	4,24E-05	0,015797578
Tubb2a-ps2	tubulin, beta 2a, pseudogene 2	1449682_s_at	0,260251142	0,000215501	0,038682902
Cds2	CDP-diacylglycerol synthase (phosphatidate cytidylyltransferase) 2	1438957_x_at	0,258930968	0,00026893	0,04186476
Ttyh1	tweety homolog 1 (Drosophila)	1422694_at	0,258663351	8,22E-05	0,025898849
Tfrc	transferrin receptor	AFFX-TransRecMur/X57349_3_at	0,254127808	2,40E-05	0,01064284
Tspan2	tetraspanin 2	1432417_a_at	0,247810451	0,000287563	0,04186476
Ly6c1	lymphocyte antigen 6 complex, locus C1	1421571_a_at	0,246618147	0,000309593	0,042999312
Gusb	glucuronidase, beta	1430332_a_at	0,243832933	0,000413168	0,047534263
Snx5	sorting nexin 5	1448791_at	0,243140944	0,000108712	0,029542727
Ptpra	protein tyrosine phosphatase, receptor type, A	1425340_a_at	0,23679769	0,000111761	0,029542727
Gpt	glutamic pyruvic transaminase, soluble	1426502_s_at	0,233887169	0,000403605	0,046912584
Rnaseh2c	ribonuclease H2, subunit C	1417427_at	0,226816247	0,000225616	0,038922321
Glrx	glutaredoxin	1416593_at	0,225298255	0,000216435	0,038682902
Rnf167	ring finger protein 167	1430527_a_at	0,221776544	0,00022878	0,039016916
Sertad1	SERTA domain containing 1	1417406_at	0,22127276	0,000206819	0,038682902
Pfn1	profilin 1	1449018_at	0,210308044	0,00012385	0,031227308
Gdpd3	glycerophosphodiester phosphodiesterase domain containing 3	1449526_a_at	0,20662577	0,000285873	0,04186476
2900086B20Rik	RIKEN cDNA 2900086B20 gene	1435788_at	0,206399538	0,000351987	0,044036006
Ndufaf1	NADH dehydrogenase (ubiquinone) 1 alpha subcomplex, assembly factor 1	1423711_at	0,205580487	0,000220604	0,038682902
Plekhb1	pleckstrin homology domain containing, family B (evectins) member 1	1416178_a_at	0,191112	0,00018855	0,038682902
Cds2	CDP-diacylglycerol synthase (phosphatidate cytidylyltransferase) 2	1434256_s_at	0,189068067	0,000401021	0,046912584
Hnrnpa1	heterogeneous nuclear ribonucleoprotein A1	1430019_a_at	0,175252288	0,000280392	0,04186476
DOWNREGULATED GENES					
Xlr4b	X-linked lymphocyte-regulated 4B	1449347_a_at	-1,797792188	0,0002903	0,04186476
Crnkl1	Crn, crooked neck-like 1 (Drosophila)	1420849_at	-1,009867181	0,000282289	0,04186476
5830428H23Rik	RIKEN cDNA 5830428H23 gene	1438465_at	-0,968929991	0,000349586	0,044036006
Prnp	prion protein	1416130_at	-0,847854653	0,000238653	0,039286655
Xrn2	5'-3' exoribonuclease 2	1422843_at	-0,748488636	0,000392085	0,046229314
Sfrs12	splicing factor, arginine/serine-rich 12	1427136_s_at	-0,630030804	0,00018904	0,038682902
Snx5	sorting nexin 5	1417648_s_at	-0,629852349	0,000183127	0,038682902
Ddb2	damage specific DNA binding protein 2	1425706_a_at	-0,622653149	0,000143029	0,034399877
Ddb2	damage specific DNA binding protein 2	1436680_s_at	-0,610921288	0,000150663	0,035274426
Zmym6	zinc finger, MYM-type 6	1438685_at	-0,606757073	0,000335547	0,044036006

Acin1	apoptotic chromatin condensation inducer 1	1416568_a_at	-0,592988999	0,000265663	0,04186476
BC024479	cDNA sequence BC024479	1426232_at	-0,538238294	0,000343473	0,044036006
Sfi1	Sfi1 homolog, spindle assembly associated (yeast)	1435353_a_at	-0,534369202	9,94E-05	0,029080099
LOC433466	hypothetical protein LOC433466	1425045_at	-0,531371896	4,75E-05	0,017294407
Sntb2	syntrophin, basic 2	1420372_at	-0,525113722	0,000200751	0,038682902
1110007M04Rik	RIKEN cDNA 1110007M04 gene	1427997_at	-0,523773935	0,00015878	0,036651309
Slc6a20a	solute carrier family 6 (neurotransmitter transporter), member 20A	1427221_at	-0,492446277	4,04E-05	0,01575744
2410005O16Rik	RIKEN cDNA 2410005O16 gene	1438034_at	-0,48226182	1,55E-05	0,008475997
Ivd	isovaleryl coenzyme A dehydrogenase	1449001_at	-0,477394667	2,86E-05	0,012118843
Prkg1	protein kinase, cGMP-dependent, type I	1449876_at	-0,453446843	0,000131019	0,032534337
4933439C20Rik	RIKEN cDNA 4933439C20 gene	1434975_x_at	-0,442720982	4,15E-05	0,015797578
Hsp90b1	heat shock protein 90, beta (Grp94), member 1	1438040_a_at	-0,423266993	0,000144828	0,034399877
Usp1	ubiquitin specific peptdiase 1	1423674_at	-0,41631314	0,000101992	0,029325408
Ralbp1	ralA binding protein 1	1417248_at	-0,413232579	7,06E-06	0,004286073
Chrna5	cholinergic receptor, nicotinic, alpha polypeptide 5	1427401_at	-0,410649333	2,89E-06	0,002371133
Zc3h11a	zinc finger CCCH type containing 11A	1426360_at	-0,410422225	0,000436357	0,049320396
Tubd1	tubulin, delta 1	1421748_a_at	-0,400286149	0,000166931	0,037531765
Rexo4	REX4, RNA exonuclease 4 homolog (S. cerevisiae)	1434113_a_at	-0,399513656	0,000349275	0,044036006
Rock1	Rho-associated coiled-coil containing protein kinase 1	1460729_at	-0,398683664	0,000316557	0,04359712
Cdc7	cell division cycle 7 (S. cerevisiae)	1426002_a_at	-0,397980797	0,000133904	0,032754627
Psrc1	proline/serine-rich coiled-coil 1	1417323_at	-0,397018017	0,000210025	0,038682902
Gabra2	gamma-aminobutyric acid (GABA-A) receptor, subunit alpha 2	1421738_at	-0,376080121	0,000384626	0,045678505
4933439C20Rik	RIKEN cDNA 4933439C20 gene	1436944_x_at	-0,375476383	0,000328451	0,044036006
Cpxm1	carboxypeptidase X 1 (M14 family)	1448901_at	-0,374979223	3,67E-05	0,014679349
Nts	neurotensin	1422860_at	-0,351601932	0,000296315	0,04186476
Obfc2a	oligonucleotide/oligosaccharide-binding fold containing 2A	1452203_at	-0,346221461	1,98E-05	0,009817
Dusp11	dual specificity phosphatase 11 (RNA/RNP complex 1-interacting)	1452594_at	-0,341730208	0,000216166	0,038682902
4933439C20Rik	RIKEN cDNA 4933439C20 gene	1439070_x_at	-0,337986446	0,00020096	0,038682902
Prnp	prion protein	1448233_at	-0,337322895	0,000192175	0,038682902
Slc25a28	solute carrier family 25, member 28	1424776_a_at	-0,324449323	0,000278896	0,04186476
Rexo4	REX4, RNA exonuclease 4 homolog (S. cerevisiae)	1434114_at	-0,323818017	0,000414754	0,047534263
Tial1	Tia1 cytotoxic granule-associated RNA binding protein-like 1	1421148_a_at	-0,320397349	8,46E-05	0,026151402
Lipc	lipase, hepatic	1419560_at	-0,315982862	0,000111729	0,029542727
Chuk	conserved helix-loop-helix ubiquitous kinase	1451383_a_at	-0,309124494	0,000335346	0,044036006
Htr1f	5-hydroxytryptamine (serotonin) receptor 1F	1450548_at	-0,300758849	3,72E-06	0,002771153
Unc13b	unc-13 homolog B (C. elegans)	1417757_at	-0,300684325	0,000369696	0,044881051
Sgcb	sarcoglycan, beta (dystrophin-associated glycoprotein)	1419667_at	-0,291658337	0,000294044	0,04186476
Rbm26	RNA binding motif protein 26	1426420_at	-0,290522408	1,75E-05	0,009276311
Spg11	spastic paraplegia 11	1426451_at	-0,281121502	0,000305953	0,042856968
Lin7b	lin-7 homolog B (C. elegans)	1439239_at	-0,269238376	3,68E-06	0,002771153
Setd6	SET domain containing 6	1428798_s_at	-0,261083701	0,00034066	0,044036006
Map3k7ip2	mitogen-activated protein kinase kinase kinase 7 interacting protein 2	1451003_at	-0,257824713	8,30E-06	0,004857619
Eml5	echinoderm microtubule associated protein like 5	1427484_at	-0,255861633	0,000195321	0,038682902
Mmaa	methylmalonic aciduria (cobalamin deficiency) type A	1417857_at	-0,246215159	6,17E-08	0,000113076
Tial1	Tia1 cytotoxic granule-associated RNA binding protein-like 1	1455675_a_at	-0,2370288	4,31E-07	0,000504171
Trim39	tripartite motif-containing 39	1418851_at	-0,230940948	9,46E-08	0,000140964
Pltp	phospholipid transfer protein	1456424_s_at	-0,230544868	5,94E-07	0,000648947
Ash1l	ash1 (absent, small, or homeotic)-like (Drosophila)	1450071_at	-0,211116306	0,000383066	0,045678505
Cryl1	crystallin, lambda 1	1430681_at	-0,209753241	1,84E-05	0,009427636
Ars2	arsenate resistance protein 2	1417655_a_at	-0,190874409	3,76E-09	2,17E-05
Birc2	baculoviral IAP repeat-containing 2	1418854_at	-0,183895961	0,000177612	0,038300993
Myo9a	myosin IXa	1436307_at	-0,178424904	1,07E-08	3,49E-05
Exdl2	exonuclease 3''-5'' domain-like 2	1449075_at	-0,177383604	0,000264288	0,04186476

Table 21: Alzheimer's Disease (AD) related genes

			*Prnp*0/0 mice adults *vs* newborns		*Prnp*+/+ mice adults *vs* newborns				
Gene Symbol	Gene Name	Affymetrix Probe ID	logFC	adj.P.Val	logFC	adj.P.Val	logFCko-logFCwt	FCko-FCwt	
UP IN *Prnp*0/0 MICE									
Ch25h	cholesterol 25-hydroxylase	1449227_at	0,62	0,00062483	-0,34	0,029901277	0,96	1,95	
S100a9	S100 calcium binding protein A9 (calgranulin B)	1448756_at	0,83	7,83E-06	0,16	0,198828943	0,67	1,60	
Kcnip3	Kv channel interacting protein 3, calsenilin	1418544_at	0,69	3,43E-06	0,28	0,007997032	0,41	1,33	
Grin2b	glutamate receptor, ionotropic, NMDA2B (epsilon 2)	1422223_at	0,65	0,000363825	0,27	0,069909634	0,38	1,30	
Cdk5r1	cyclin-dependent kinase 5, regulatory subunit 1 (p35)	1421123_at	0,81	1,89E-06	0,43	0,000657868	0,38	1,30	
Tspo	translocator protein	1416695_at	0,76	2,31E-05	0,39	0,005828016	0,37	1,29	
Cdk5	cyclin-dependent kinase 5	1450674_at	0,74	5,25E-07	0,41	0,000185785	0,33	1,26	
Mapk3	mitogen-activated protein kinase 3	1427060_at	0,61	3,78E-07	0,36	7,50E-05	0,25	1,19	
Csf3r	colony stimulating factor 3 receptor (granulocyte)	1418806_at	0,77	2,23E-06	0,53	8,33E-05	0,24	1,18	
Tgm2	transglutaminase 2, C polypeptide	1417500_a_at	0,78	2,70E-06	0,56	7,30E-05	0,22	1,17	
Psen1	presenilin 1	1450399_at	0,77	3,08E-07	0,58	6,11E-06	0,20	1,15	
Ppp5c	protein phosphatase 5, catalytic subunit	1424115_at	0,70	1,41E-06	0,52	2,94E-05	0,18	1,14	
Soat1	sterol O-acyltransferase 1	1417697_at	0,65	2,34E-05	0,46	0,000483641	0,18	1,14	
Prkaca	protein kinase, cAMP dependent, catalytic, alpha	1450519_a_at	0,73	4,77E-07	0,56	7,45E-06	0,17	1,13	
Csnk1d	casein kinase 1, delta	1449932_at	0,69	7,94E-06	0,53	0,000106485	0,16	1,12	
Apoc3	apolipoprotein C-III	1418278_at	0,68	2,87E-06	0,52	4,08E-05	0,16	1,12	
Hmox2	heme oxygenase (decycling) 2	1416399_a_at	0,63	2,43E-08	0,49	3,04E-07	0,14	1,10	
Sod2	superoxide dismutase 2, mitochondrial	1417194_at	0,62	7,15E-06	0,49	7,59E-05	0,14	1,10	
DOWN IN *Prnp*0/0 MICE							logFCko-logFCwt	FCko-FCwt	Inverse
Ppig	peptidyl-prolyl isomerase G (cyclophilin G)	1436505_at	-1,21	8,45E-05	-0,13	0,581312036	-1,08	0,47	-2,12
Ptn	pleiotrophin	1416211_a_at	-0,64	0,020079883	0,20	0,44946573	-0,83	0,56	-1,78
Bptf	bromodomain PHD finger transcription factor	1427310_at	-0,69	9,01E-05	0,14	0,299189128	-0,82	0,57	-1,77
Gsk3b	glycogen synthase kinase 3 beta	1451020_at	-0,76	0,000176525	-0,09	0,555566071	-0,66	0,63	-1,58
F13a1	coagulation factor XIII, A1 subunit	1448929_at	-0,66	0,000106586	-0,09	0,472404936	-0,57	0,67	-1,49
Anxa6	annexin A6	1429247_at	-0,73	7,96E-05	-0,18	0,187249622	-0,55	0,69	-1,46
Casp1	caspase 1	1449265_at	-0,67	2,88E-05	-0,20	0,081069078	-0,47	0,72	-1,38
Tm2d1	TM2 domain containing 1	1451996_at	-0,98	5,89E-05	-0,57	0,005001846	-0,42	0,75	-1,34
Serpinf1	serine (or cysteine) peptidase inhibitor, clade F, member 1	1416168_at	-0,69	0,002765178	-0,28	0,159655436	-0,41	0,75	-1,32
Eif2s1	eukaryotic translation initiation factor 2, subunit 1 alpha	1420491_at	-0,76	0,00047305	-0,44	0,019784268	-0,32	0,80	-1,25
Mapk1	mitogen-activated protein kinase 1	1419568_at	-0,71	0,000188062	-0,44	0,007317988	-0,27	0,83	-1,21
Nfkbia	nuclear factor of kappa light polypeptide gene enhancer in B-cells inhibitor, alpha	1420089_at	-0,78	6,08E-05	-0,52	0,001750237	-0,25	0,84	-1,19

Table Legends

Table 3. UP IN WT: Second messengers signaling pathway genes. Significantly up-regulated genes during hippocampal development only in *Prnp*$^{+/+}$ mice but not in *Prnp*$^{0/0}$ mice are listed. This gene group comprises cAMP-mediated signaling pathway genes, RAR-activation genes, NRF2-mediated response genes and calcium signaling related genes. Genes are sorted in a descending order according to the difference in fold change values (column L) between *Prnp*$^{+/+}$ developmental expression value (WT adults *vs* WT newborns, column E) and *Prnp*$^{0/0}$ developmental expression value (KO adults *vs* KO newborns, column H).

Table 4. UP IN WT: Second messengers signaling pathway genes (2). Up-regulated genes only in *Prnp*$^{+/+}$ mice during hippocampal development. These genes belong to the Ras/Rab and protein kinases family. Genes are sorted in a descending order according to the difference in fold change values (column L) between *Prnp*$^{+/+}$ developmental expression value (WT adults *vs* WT newborns, column E) and *Prnp*$^{0/0}$ developmental expression value (KO adults *vs* KO newborns, column H).

Table 5. UP IN WT: Synaptic transmission genes. Significantly up-regulated genes during hippocampal development only in *Prnp*$^{+/+}$ related to synaptic function, such as ionic transporters, ionic channels and receptor subunits. Genes are sorted in a descending order according to the difference in fold change values between *Prnp*$^{+/+}$ developmental expression value and *Prnp*$^{0/0}$ developmental expression value.

Table 6. UP IN WT: Chaperone-mediated protein folding. Significantly up-regulated genes during hippocampal development only in *Prnp*$^{+/+}$ related to chaperone-mediated protein folding. Genes are sorted in a descending order according to the difference in fold change values between *Prnp*$^{+/+}$ developmental expression value and *Prnp*$^{0/0}$ developmental expression value.

Table 7. UP IN WT: Genes involved in the ubiquitin-proteasomal system. Up-regulated genes only in *Prnp*$^{+/+}$ mice during hippocampal development related to the ubiquitin-proteasomal system (UPS) function. Genes are sorted in a descending order

according to the difference in fold change values between *Prnp*$^{+/+}$ developmental expression value and *Prnp*$^{0/0}$ developmental expression value.

Table 8. UP IN KO: Cytosolic signaling pathway genes. Significantly up-regulated genes during hippocampal development only in *Prnp*$^{0/0}$ mice but not in *Prnp*$^{+/+}$ mice are listed. This gene group comprises cytosolic signaling pathway genes such as kinases. Genes are sorted in a descending order according to the difference in fold change values between *Prnp*$^{0/0}$ developmental expression value and *Prnp*$^{+/+}$ developmental expression value.

Table 9. UP IN KO: Cell death signaling genes. Significantly up-regulated genes during hippocampal development only in *Prnp*$^{0/0}$ mice related to cell death mechanisms. Genes are sorted in a descending order according to the difference in fold change values between *Prnp*$^{0/0}$ developmental expression value and *Prnp*$^{+/+}$ developmental expression value.

Table 10. UP IN KO: Neuregulin pathway genes. Up-regulated genes only in *Prnp*$^{0/0}$ mice during hippocampal development related to neuregulin signaling. Genes are sorted in a descending order according to the difference in fold change values between *Prnp*$^{0/0}$ developmental expression value and *Prnp*$^{+/+}$ developmental expression value.

Table 11. UP IN KO: Synaptic plasticity genes. Significantly up-regulated genes during hippocampal development only in *Prnp*$^{0/0}$ mice related to synaptic plasticity mechanisms. Genes are sorted in a descending order according to the difference in fold change values between *Prnp*$^{0/0}$ developmental expression value and *Prnp*$^{+/+}$ developmental expression value.

Table 12. UP IN KO: Chloride channel-related genes. These genes represent members of potassium and chloride channel subunits that are significantly up-regulated during hippocampal development only in *Prnp*$^{0/0}$ mice. Genes are sorted in a descending order according to the difference in fold change values between *Prnp*$^{0/0}$ developmental expression value and *Prnp*$^{+/+}$ developmental expression value.

Table 13. UP IN KO: Cell adhesion, neurite outgrowth and axon guidance genes. Significantly up-regulated genes during hippocampal development only in *Prnp*$^{0/0}$ mice related to activity mediated by cell-to-cell interaction, such as cell adhesion, neurite outgrowth and axon guidance. Genes are sorted in a descending order according to the difference in fold change values between *Prnp*$^{0/0}$ developmental expression value and *Prnp*$^{+/+}$ developmental expression value.

Table 14. UP IN KO: Calcium homeostasis genes. Developmentally up-regulated genes related to calcium homeostasis were detected in *Prnp*$^{0/0}$ mice. Genes are sorted in a descending order according to the difference in fold change values between *Prnp*$^{0/0}$ developmental expression value and *Prnp*$^{+/+}$ developmental expression value.

Table 15. DOWN IN WT: Carbohydrate and small molecule metabolism genes. Genes belonging to the metabolism of carbohydrate and of small molecules (such as nucleotides) were identified as uniquely down-regulated during neuronal development in *Prnp*$^{+/+}$ mice. Genes are sorted in a descending order according to the inverse of the difference in fold change values between *Prnp*$^{+/+}$ developmental expression value and *Prnp*$^{0/0}$ developmental expression value.

Table 16. DOWN IN KO: Embryonic and central nervous system development. These genes are down-regulated exclusively in *Prnp*$^{0/0}$ mice during neuronal development, whereas not in *Prnp*$^{+/+}$ mice, and are involved in embryonic development and differentiation, and nervous system development and function. Genes are sorted in a descending order according to the inverse of the difference in fold change values between *Prnp*$^{0/0}$ developmental expression value and *Prnp*$^{+/+}$ developmental expression value.

Table 17. DOWN IN KO: Cadherin genes. Developmentally down-regulated genes of cadherin family were detected in *Prnp*$^{0/0}$ mice. Genes are sorted in a descending order according to the inverse of the difference in fold change values between *Prnp*$^{0/0}$ developmental expression value and *Prnp*$^{+/+}$ developmental expression value.

Table 18. DOWN IN KO: Transition metal ion binding genes. Significantly down-regulated genes during hippocampal development only in *Prnp*$^{0/0}$ mice related to

transition metal ion binding. Genes are sorted in a descending order according to the inverse of the difference in fold change values between *Prnp*$^{0/0}$ developmental expression value and *Prnp*$^{+/+}$ developmental expression value.

Table 19. DOWN IN KO: Ubiquitin system genes. Significantly down-regulated genes during hippocampal development only in *Prnp*$^{0/0}$ related to the ubiquitin system function. Genes are sorted in a descending order according to the inverse of the difference in fold change values between *Prnp*$^{0/0}$ developmental expression value and *Prnp*$^{+/+}$ developmental expression value.

Table 20. Comparison between adult wildtype and adult PrP^{C}-deficient mice. Adult *Prnp*$^{0/0}$ and *Prnp*$^{+/+}$ mice gene expression profiles were compared. Listed are genes significantly up- or down-regulated in PrP^{C}-deficient mice *vs* their wildtype counterpart. Genes are sorted according to descending fold change values.

Table 21. Alzheimer's Disease (AD)-related genes. *Prnp*$^{0/0}$ adult mice were compared to young animals, and significantly deregulated genes were subjected to GeneCards® GeneALaCart Beta software (http://www.genecards.org/), in order to identify AD-related genes. Listed are AD-related genes significantly up- or down-regulated in PrP^{C}-deficient mice during neuronal development. Genes are sorted in a descending order according to the difference in fold change values.

References

Aguzzi A, Montrasio F, Kaeser PS (2001) Prions: health scare and biological challenge. Nat. Rev. Mol. Cell Biol 2:118-126

Aguzzi A, Baumann F, Bremer J (2008) The prion's elusive reason for being. Annu. Rev. Neurosci 31:439-477

Aguzzi A, Calella AM (2009) Prions: protein aggregation and infectious diseases. Physiol. Rev 89:1105-1152

Aguzzi A, Heikenwalder M, Miele G (2004) Progress and problems in the biology, diagnostics, and therapeutics of prion diseases. J. Clin. Invest 114:153-160

Aguzzi A, O'Connor T (2010) Protein aggregation diseases: pathogenicity and therapeutic perspectives. Nat Rev Drug Discov 9:237-248

Alper T, Cramp WA, Haig DA, Clarke MC (1967) Does the agent of scrapie replicate without nucleic acid? Nature 214:764-766

Alper T, Haig DA, Clarke MC (1966) The exceptionally small size of the scrapie agent. Biochem. Biophys. Res. Commun 22:278-284

Atarashi R, Nishida N, Shigematsu K, Goto S, Kondo T, Sakaguchi S, Katamine S (2003) Deletion of N-terminal residues 23-88 from prion protein (PrP) abrogates the potential to rescue PrP-deficient mice from PrP-like protein/doppel-induced Neurodegeneration. J. Biol. Chem 278:28944-28949

Balducci C, Beeg M, Stravalaci M, Bastone A, Sclip A, Biasini E, Tapella L, Colombo L, Manzoni C, Borsello T, Chiesa R, Gobbi M, Salmona M, Forloni G (2010) Synthetic amyloid-beta oligomers impair long-term memory independently of cellular prion protein. Proc. Natl. Acad. Sci. U.S.A 107:2295-2300

Baumann F, Pahnke J, Radovanovic I, Rülicke T, Bremer J, Tolnay M, Aguzzi A (2009) Functionally relevant domains of the prion protein identified in vivo. PLoS ONE 4:e6707

Baumann F, Tolnay M, Brabeck C, Pahnke J, Kloz U, Niemann HH, Heikenwalder M, Rülicke T, Bürkle A, Aguzzi A (2007) Lethal recessive myelin toxicity of prion protein lacking its central domain. EMBO J 26:538-547

Behrens A, Genoud N, Naumann H, Rülicke T, Janett F, Heppner FL, Ledermann B, Aguzzi A (2002) Absence of the prion protein homologue Doppel causes male sterility. EMBO J 21:3652-3658

Bertram L, McQueen MB, Mullin K, Blacker D, Tanzi RE (2007) Systematic meta-analyses of Alzheimer disease genetic association studies: the AlzGene database. Nat. Genet 39:17-23

Bertrand S, Lacaille JC (2001) Unitary synaptic currents between lacunosum-moleculare interneurones and pyramidal cells in rat hippocampus. J. Physiol. (Lond.) 532:369-384

Birchmeier C (2009) ErbB receptors and the development of the nervous system. Exp. Cell Res 315:611-618

Bjarnadottir M, Misner DL, Haverfield-Gross S, Bruun S, Helgason VG, Stefansson H, Sigmundsson A, Firth DR, Nielsen B, Stefansdottir R, Novak TJ, Stefansson K, Gurney ME, Andresson T (2007) Neuregulin1 (NRG1) signaling through Fyn modulates NMDA receptor phosphorylation: differential synaptic function in NRG1+/- knock-outs compared with wild-type mice. J. Neurosci 27:4519-4529

Bolton DC, McKinley MP, Prusiner SB (1982) Identification of a protein that purifies with the scrapie prion. Science 218:1309-1311

Borchelt DR, Koliatsos VE, Guarnieri M, Pardo CA, Sisodia SS, Price DL (1994) Rapid anterograde axonal transport of the cellular prion glycoprotein in the peripheral and central nervous systems. J. Biol. Chem 269:14711-14714

Bounhar Y, Zhang Y, Goodyer CG, LeBlanc A (2001) Prion protein protects human neurons against Bax-mediated apoptosis. J. Biol. Chem 276:39145-39149

Brandner S, Isenmann S, Raeber A, Fischer M, Sailer A, Kobayashi Y, Marino S, Weissmann C, Aguzzi A (1996) Normal host prion protein necessary for scrapie-induced neurotoxicity. Nature 379:339-343

Bremer J, Baumann F, Tiberi C, Wessig C, Fischer H, Schwarz P, Steele AD, Toyka KV, Nave K, Weis J, Aguzzi A (2010) Axonal prion protein is required for peripheral myelin maintenance. Nat. Neurosci 13:310-318

Bretteville A, Planel E (2008) Tau aggregates: toxic, inert, or protective species? J. Alzheimers Dis 14:431-436

Brinkmann BG, Agarwal A, Sereda MW, Garratt AN, Müller T, Wende H, Stassart RM, Nawaz S, Humml C, Velanac V, Radyushkin K, Goebbels S, Fischer TM, Franklin RJ, Lai C, Ehrenreich H, Birchmeier C, Schwab MH, Nave KA (2008) Neuregulin-1/ErbB signaling serves distinct functions in myelination of the peripheral and central nervous system. Neuron 59:581-595

Brown DR, Qin K, Herms JW, Madlung A, Manson J, Strome R, Fraser PE, Kruck T, von Bohlen A, Schulz-Schaeffer W, Giese A, Westaway D, Kretzschmar H (1997a) The cellular prion protein binds copper in vivo. Nature 390:684-687

Brown DR, Schmidt B, Kretzschmar HA (1997b) Effects of oxidative stress on prion protein expression in PC12 cells. Int. J. Dev. Neurosci 15:961-972

Büeler H, Aguzzi A, Sailer A, Greiner RA, Autenried P, Aguet M, Weissmann C (1993) Mice devoid of PrP are resistant to scrapie. Cell 73:1339-1347

Büeler H, Fischer M, Lang Y, Bluethmann H, Lipp HP, DeArmond SJ, Prusiner SB, Aguet M, Weissmann C (1992) Normal development and behaviour of mice lacking the neuronal cell-surface PrP protein. Nature 356:577-582

Burns A, Iliffe S (2009) Alzheimer's disease. BMJ 338:b158

Calella AM, Farinelli M, Nuvolone M, Mirante O, Moos R, Falsig J, Mansuy IM, Aguzzi A (2010) Prion protein and Abeta-related synaptic toxicity impairment. EMBO Mol Med 2:306-314

Campana V, Sarnataro D, Zurzolo C (2005) The highways and byways of prion protein trafficking. Trends Cell Biol 15:102-111

Cancellotti E, Wiseman F, Tuzi NL, Baybutt H, Monaghan P, Aitchison L, Simpson J, Manson JC (2005) Altered glycosylated PrP proteins can have different neuronal trafficking in brain but do not acquire scrapie-like properties. J. Biol. Chem 280:42909-42918

Carleton A, Tremblay P, Vincent JD, Lledo PM (2001) Dose-dependent, prion protein (PrP)-mediated facilitation of excitatory synaptic transmission in the mouse hippocampus. Pflugers Arch 442:223-229

Caughey BW, Dong A, Bhat KS, Ernst D, Hayes SF, Caughey WS (1991) Secondary structure analysis of the scrapie-associated protein PrP 27-30 in water by infrared spectroscopy. Biochemistry 30:7672-7680

Caughey B, Baron GS (2006) Prions and their partners in crime. Nature 443:803-810

Charrière-Bertrand C, Nunez J (1992) Regulation of tubulin, Tau and microtubule associated protein 2 expression during mouse brain development. Neurochem. Int 21:535-541

Checler F, Vincent B (2002) Alzheimer's and prion diseases: distinct pathologies, common proteolytic denominators. Trends Neurosci 25:616-620

Chen S, Mangé A, Dong L, Lehmann S, Schachner M (2003) Prion protein as trans-interacting partner for neurons is involved in neurite outgrowth and neuronal survival. Mol. Cell. Neurosci 22:227-233

Chesebro B, Caughey B (1993) Scrapie agent reflication without the prion protein? Curr. Biol 3:696-698

Chesebro B, Trifilo M, Race R, Meade-White K, Teng C, LaCasse R, Raymond L, Favara C, Baron G, Priola S, Caughey B, Masliah E, Oldstone M (2005) Anchorless prion protein results in infectious amyloid disease without clinical scrapie. Science 308:1435-1439

Colling SB, Collinge J, Jefferys JG (1996) Hippocampal slices from prion protein null mice: disrupted Ca(2+)-activated K+ currents. Neurosci. Lett 209:49-52

Collinge J, Whittington MA, Sidle KC, Smith CJ, Palmer MS, Clarke AR, Jefferys JG

(1994) Prion protein is necessary for normal synaptic function. Nature 370:295-297

Collins SJ, Lawson VA, Masters CL (2004) Transmissible spongiform encephalopathies. Lancet 363:51-61

Cordy JM, Hussain I, Dingwall C, Hooper NM, Turner AJ (2003) Exclusively targeting beta-secretase to lipid rafts by GPI-anchor addition up-regulates beta-site processing of the amyloid precursor protein. Proc. Natl. Acad. Sci. U.S.A 100:11735-11740

Criado JR, Sánchez-Alavez M, Conti B, Giacchino JL, Wills DN, Henriksen SJ, Race R, Manson JC, Chesebro B, Oldstone MBA (2005) Mice devoid of prion protein have cognitive deficits that are rescued by reconstitution of PrP in neurons. Neurobiol. Dis 19:255-265

Cunningham C, Deacon R, Wells H, Boche D, Waters S, Diniz CP, Scott H, Rawlins JNP, Perry VH (2003) Synaptic changes characterize early behavioural signs in the ME7 model of murine prion disease. Eur. J. Neurosci 17:2147-2155

Curtis J, Errington M, Bliss T, Voss K, MacLeod N (2003) Age-dependent loss of PTP and LTP in the hippocampus of PrP-null mice. Neurobiol. Dis 13:55-62

Del Bo R, Scarlato M, Ghezzi S, Martinelli-Boneschi F, Fenoglio C, Galimberti G, Galbiati S, Virgilio R, Galimberti D, Ferrarese C, Scarpini E, Bresolin N, Comi GP (2006) Is M129V of PRNP gene associated with Alzheimer's disease? A case-control study and a meta-analysis. Neurobiol. Aging 27:770.e1-770.e5

Deng J, Yu D, Li M (2006a) Formation of the entorhino-hippocampal pathway: a tracing study in vitro and in vivo. Neurosci Bull 22:305-314

Deng J, Yu D, Li M (2006b) Formation of the entorhino-hippocampal pathway: a tracing study in vitro and in vivo. Neurosci Bull 22:305-314

Dennis G, Sherman BT, Hosack DA, Yang J, Gao W, Lane HC, Lempicki RA (2003) DAVID: Database for Annotation, Visualization, and Integrated Discovery. Genome Biol 4:P3

Deriziotis P, Tabrizi SJ (2008) Prions and the proteasome. Biochim. Biophys. Acta 1782:713-722

Dermaut B, Croes EA, Rademakers R, Van den Broeck M, Cruts M, Hofman A, van Duijn CM, Van Broeckhoven C (2003) PRNP Val129 homozygosity increases risk for early-onset Alzheimer's disease. Ann. Neurol 53:409-412

Ehehalt R, Keller P, Haass C, Thiele C, Simons K (2003) Amyloidogenic processing of the Alzheimer beta-amyloid precursor protein depends on lipid rafts. J. Cell Biol 160:113-123

Falls DL (2003) Neuregulins: functions, forms, and signaling strategies. Exp. Cell Res

284:14-30

Ford MJ, Burton LJ, Li H, Graham CH, Frobert Y, Grassi J, Hall SM, Morris RJ (2002) A marked disparity between the expression of prion protein and its message by neurones of the CNS. Neuroscience 111:533-551

Fournier JG, Escaig-Haye F, Billette de Villemeur T, Robain O (1995) Ultrastructural localization of cellular prion protein (PrPc) in synaptic boutons of normal hamster hippocampus. C. R. Acad. Sci. III, Sci. Vie 318:339-344

Frenzel KE, Falls DL (2001) Neuregulin-1 proteins in rat brain and transfected cells are localized to lipid rafts. J. Neurochem 77:1-12

Friauf E, Shatz CJ (1991) Changing patterns of synaptic input to subplate and cortical plate during development of visual cortex. J. Neurophysiol 66:2059-2071

Galvan C, Camoletto PG, Dotti CG, Aguzzi A, Ledesma MD (2005) Proper axonal distribution of PrP(C) depends on cholesterol-sphingomyelin-enriched membrane domains and is developmentally regulated in hippocampal neurons. Mol. Cell. Neurosci 30:304-315

Garratt AN, Britsch S, Birchmeier C (2000a) Neuregulin, a factor with many functions in the life of a schwann cell. Bioessays 22:987-996

Garratt AN, Voiculescu O, Topilko P, Charnay P, Birchmeier C (2000b) A dual role of erbB2 in myelination and in expansion of the schwann cell precursor pool. J. Cell Biol 148:1035-1046

Gasset M, Baldwin MA, Fletterick RJ, Prusiner SB (1993) Perturbation of the secondary structure of the scrapie prion protein under conditions that alter infectivity. Proc. Natl. Acad. Sci. U.S.A 90:1-5

Gauczynski S, Peyrin JM, Haïk S, Leucht C, Hundt C, Rieger R, Krasemann S, Deslys JP, Dormont D, Lasmézas CI, Weiss S (2001) The 37-kDa/67-kDa laminin receptor acts as the cell-surface receptor for the cellular prion protein. EMBO J 20:5863-5875

Gayrard V, Picard-Hagen N, Grino M, Sauze N, Grandjean C, Galea J, Andreoletti O, Schelcher F, Toutain PL (2000) Major hypercorticism is an endocrine feature of ewes with naturally occurring scrapie. Endocrinology 141:988-994

Ghaemmaghami S, Ullman J, Ahn M, St Martin S, Prusiner SB (2010) Chemical induction of misfolded prion protein conformers in cell culture. J. Biol. Chem 285:10415-10423

Ghosh A, Shatz CJ (1992) Involvement of subplate neurons in the formation of ocular dominance columns. Science 255:1441-1443

Graner E, Mercadante AF, Zanata SM, Forlenza OV, Cabral AL, Veiga SS, Juliano MA, Roesler R, Walz R, Minetti A, Izquierdo I, Martins VR, Brentani RR (2000) Cellular prion protein binds laminin and mediates neuritogenesis.

Brain Res. Mol. Brain Res 76:85-92

Haass C, Selkoe DJ (2007) Soluble protein oligomers in neurodegeneration: lessons from the Alzheimer's amyloid beta-peptide. Nat. Rev. Mol. Cell Biol 8:101-112

Hainfellner JA, Wanschitz J, Jellinger K, Liberski PP, Gullotta F, Budka H (1998) Coexistence of Alzheimer-type neuropathology in Creutzfeldt-Jakob disease. Acta Neuropathol 96:116-122

Hancock JF (2006) Lipid rafts: contentious only from simplistic standpoints. Nat. Rev. Mol. Cell Biol 7:456-462

Hanger DP, Seereeram A, Noble W (2009) Mediators of tau phosphorylation in the pathogenesis of Alzheimer's disease. Expert Rev Neurother 9:1647-1666

Haraguchi T, Fisher S, Olofsson S, Endo T, Groth D, Tarentino A, Borchelt DR, Teplow D, Hood L, Burlingame A (1989) Asparagine-linked glycosylation of the scrapie and cellular prion proteins. Arch. Biochem. Biophys 274:1-13

Helms JB, Zurzolo C (2004) Lipids as targeting signals: lipid rafts and intracellular trafficking. Traffic 5:247-254

Herman JP, Figueiredo H, Mueller NK, Ulrich-Lai Y, Ostrander MM, Choi DC, Cullinan WE (2003) Central mechanisms of stress integration: hierarchical circuitry controlling hypothalamo-pituitary-adrenocortical responsiveness. Front Neuroendocrinol 24:151-180

Herman JP, Ostrander MM, Mueller NK, Figueiredo H (2005) Limbic system mechanisms of stress regulation: hypothalamo-pituitary-adrenocortical axis. Prog. Neuropsychopharmacol. Biol. Psychiatry 29:1201-1213

Hermann B, Seidenberg M, Jones J (2008) The neurobehavioural comorbidities of epilepsy: can a natural history be developed? Lancet Neurol 7:151-160

Herms J, Tings T, Gall S, Madlung A, Giese A, Siebert H, Schürmann P, Windl O, Brose N, Kretzschmar H (1999) Evidence of presynaptic location and function of the prion protein. J. Neurosci 19:8866-8875

Herms JW, Tings T, Dunker S, Kretzschmar HA (2001) Prion protein affects Ca2+-activated K+ currents in cerebellar purkinje cells. Neurobiol. Dis 8:324-330

Hochberg Y, Benjamini Y (1990) More powerful procedures for multiple significance testing. Stat Med 9:811-818

Holbro T, Hynes NE (2004) ErbB receptors: directing key signaling networks throughout life. Annu. Rev. Pharmacol. Toxicol 44:195-217

Hossain S, Fragoso G, Mushynski WE, Almazan G (2010) Regulation of peripheral myelination by Src-like kinases. Exp. Neurol 226:47-57

Hu X, He W, Diaconu C, Tang X, Kidd GJ, Macklin WB, Trapp BD, Yan R (2008) Genetic deletion of BACE1 in mice affects remyelination of sciatic nerves. FASEB J 22:2970-2980

Hu X, Hicks CW, He W, Wong P, Macklin WB, Trapp BD, Yan R (2006) Bace1 modulates myelination in the central and peripheral nervous system. Nat. Neurosci 9:1520-1525

Huang DW, Sherman BT, Lempicki RA (2009) Systematic and integrative analysis of large gene lists using DAVID bioinformatics resources. Nat Protoc 4:44-57

Irizarry RA, Hobbs B, Collin F, Beazer-Barclay YD, Antonellis KJ, Scherf U, Speed TP (2003) Exploration, normalization, and summaries of high density oligonucleotide array probe level data. Biostatistics 4:249-264

Ishikura N, Clever JL, Bouzamondo-Bernstein E, Samayoa E, Prusiner SB, Huang EJ, DeArmond SJ (2005) Notch-1 activation and dendritic atrophy in prion disease. Proc. Natl. Acad. Sci. U.S.A 102:886-891

Jeffrey M, Halliday WG, Bell J, Johnston AR, MacLeod NK, Ingham C, Sayers AR, Brown DA, Fraser JR (2000) Synapse loss associated with abnormal PrP precedes neuronal degeneration in the scrapie-infected murine hippocampus. Neuropathol. Appl. Neurobiol 26:41-54

Jessen KR, Mirsky R (2005) The origin and development of glial cells in peripheral nerves. Nat. Rev. Neurosci 6:671-682

Kanaani J, Prusiner SB, Diacovo J, Baekkeskov S, Legname G (2005) Recombinant prion protein induces rapid polarization and development of synapses in embryonic rat hippocampal neurons in vitro. J. Neurochem 95:1373-1386

Kaneko K, Vey M, Scott M, Pilkuhn S, Cohen FE, Prusiner SB (1997) COOH-terminal sequence of the cellular prion protein directs subcellular trafficking and controls conversion into the scrapie isoform. Proc. Natl. Acad. Sci. U.S.A 94:2333-2338

Kellett KAB, Hooper NM (2009) Prion protein and Alzheimer disease. Prion 3:190-194

Kenessey A, Yen SH (1993) The extent of phosphorylation of fetal tau is comparable to that of PHF-tau from Alzheimer paired helical filaments. Brain Res 629:40-46

Kessels HW, Nguyen LN, Nabavi S, Malinow R (2010) The prion protein as a receptor for amyloid-beta. Nature 466:E3-4; discussion E4-5

Kim B, Lee H, Choi J, Kim J, Choi E, Carp RI, Kim Y (2004) The cellular prion protein (PrPC) prevents apoptotic neuronal cell death and mitochondrial dysfunction induced by serum deprivation. Brain Res. Mol. Brain Res 124:40-50

Klamt F, Dal-Pizzol F, Conte da Frota ML, Walz R, Andrades ME, da Silva EG, Brentani RR, Izquierdo I, Fonseca Moreira JC (2001) Imbalance of antioxidant defense in mice lacking cellular prion protein. Free Radic. Biol. Med 30:1137-1144

Koo EH, Squazzo SL (1994) Evidence that production and release of amyloid beta-protein involves the endocytic pathway. J. Biol. Chem 269:17386-17389

Kraus F, Haenig B, Kispert A (2001) Cloning and expression analysis of the mouse T-box gene Tbx18. Mech. Dev 100:83-86

Krinke G (2000) The laboratory rat. Academic Press.

Laurén J, Gimbel DA, Nygaard HB, Gilbert JW, Strittmatter SM (2009) Cellular prion protein mediates impairment of synaptic plasticity by amyloid-beta oligomers. Nature 457:1128-1132

Lazarini F, Deslys JP, Dormont D (1991) Regulation of the glial fibrillary acidic protein, beta actin and prion protein mRNAs during brain development in mouse. Brain Res. Mol. Brain Res 10:343-346

Le Pichon CE, Firestein S (2008) Expression and localization of the prion protein PrP(C) in the olfactory system of the mouse. J. Comp. Neurol 508:487-499

Leclerc E, Peretz D, Ball H, Solforosi L, Legname G, Safar J, Serban A, Prusiner SB, Burton DR, Williamson RA (2003) Conformation of PrP(C) on the cell surface as probed by antibodies. J. Mol. Biol 326:475-483

Ledesma MD, Da Silva JS, Schevchenko A, Wilm M, Dotti CG (2003) Proteomic characterisation of neuronal sphingolipid-cholesterol microdomains: role in plasminogen activation. Brain Res 987:107-116

Lee Y, Davis M (1997) Role of the hippocampus, the bed nucleus of the stria terminalis, and the amygdala in the excitatory effect of corticotropin-releasing hormone on the acoustic startle reflex. J. Neurosci 17:6434-6446

Lesné S, Koh MT, Kotilinek L, Kayed R, Glabe CG, Yang A, Gallagher M, Ashe KH (2006) A specific amyloid-beta protein assembly in the brain impairs memory. Nature 440:352-357

Li A, Christensen HM, Stewart LR, Roth KA, Chiesa R, Harris DA (2007) Neonatal lethality in transgenic mice expressing prion protein with a deletion of residues 105-125. EMBO J 26:548-558

Lim K, Tan JMM (2007) Role of the ubiquitin proteasome system in Parkinson's disease. BMC Biochem 8 Suppl 1:S13

Linden R, Martins VR, Prado MAM, Cammarota M, Izquierdo I, Brentani RR (2008) Physiology of the prion protein. Physiol. Rev 88:673-728

Lledo PM, Tremblay P, DeArmond SJ, Prusiner SB, Nicoll RA (1996) Mice deficient

for prion protein exhibit normal neuronal excitability and synaptic transmission in the hippocampus. Proc. Natl. Acad. Sci. U.S.A 93:2403-2407

Lobão-Soares B, Walz R, Prediger RDS, Freitas RL, Calvo F, Bianchin MM, Leite JP, Landemberger MC, Coimbra NC (2008) Cellular prion protein modulates defensive attention and innate fear-induced behaviour evoked in transgenic mice submitted to an agonistic encounter with the tropical coral snake Oxyrhopus guibei. Behav. Brain Res 194:129-137

Loeb JA, Susanto ET, Fischbach GD (1998) The neuregulin precursor proARIA is processed to ARIA after expression on the cell surface by a protein kinase C-enhanced mechanism. Mol. Cell. Neurosci 11:77-91

Lopes MH, Hajj GNM, Muras AG, Mancini GL, Castro RMPS, Ribeiro KCB, Brentani RR, Linden R, Martins VR (2005) Interaction of cellular prion and stress-inducible protein 1 promotes neuritogenesis and neuroprotection by distinct signaling pathways. J. Neurosci 25:11330-11339

Maglio LE, Perez MF, Martins VR, Brentani RR, Ramirez OA (2004) Hippocampal synaptic plasticity in mice devoid of cellular prion protein. Brain Res. Mol. Brain Res 131:58-64

Málaga-Trillo E, Solis GP, Schrock Y, Geiss C, Luncz L, Thomanetz V, Stuermer CAO (2009) Regulation of embryonic cell adhesion by the prion protein. PLoS Biol 7:e55

Mallucci GR, Ratté S, Asante EA, Linehan J, Gowland I, Jefferys JGR, Collinge J (2002) Post-natal knockout of prion protein alters hippocampal CA1 properties, but does not result in neurodegeneration. EMBO J 21:202-210

Mallucci G, Collinge J (2004) Update on Creutzfeldt-Jakob disease. Curr. Opin. Neurol 17:641-647

Mallucci G, Dickinson A, Linehan J, Klöhn P, Brandner S, Collinge J (2003) Depleting neuronal PrP in prion infection prevents disease and reverses spongiosis. Science 302:871-874

Mallucci GR, White MD, Farmer M, Dickinson A, Khatun H, Powell AD, Brandner S, Jefferys JGR, Collinge J (2007) Targeting cellular prion protein reverses early cognitive deficits and neurophysiological dysfunction in prion-infected mice. Neuron 53:325-335

Mangé A, Béranger F, Peoc'h K, Onodera T, Frobert Y, Lehmann S (2004) Alpha- and beta- cleavages of the amino-terminus of the cellular prion protein. Biol. Cell 96:125-132

Manson J, West JD, Thomson V, McBride P, Kaufman MH, Hope J (1992) The prion protein gene: a role in mouse embryogenesis? Development 115:117-122

Manson JC, Clarke AR, Hooper ML, Aitchison L, McConnell I, Hope J (1994) 129/Ola mice carrying a null mutation in PrP that abolishes mRNA production

are developmentally normal. Mol. Neurobiol 8:121-127

Marella M, Lehmann S, Grassi J, Chabry J (2002) Filipin prevents pathological prion protein accumulation by reducing endocytosis and inducing cellular PrP release. J. Biol. Chem 277:25457-25464

Marin-Padilla M (1978) Dual origin of the mammalian neocortex and evolution of the cortical plate. Anat. Embryol 152:109-126

Marlow L, Cain M, Pappolla MA, Sambamurti K (2003) Beta-secretase processing of the Alzheimer's amyloid protein precursor (APP). J. Mol. Neurosci 20:233-239

Martin M, Dotti CG, Ledesma MD (2010) Brain cholesterol in normal and pathological aging. Biochim. Biophys. Acta 1801:934-944

Masters CL, Richardson EP (1978) Subacute spongiform encephalopathy (Creutzfeldt-Jakob disease). The nature and progression of spongiform change. Brain 101:333-344

McConnell SK, Ghosh A, Shatz CJ (1989) Subplate neurons pioneer the first axon pathway from the cerebral cortex. Science 245:978-982

McCormick DA, Contreras D (2001) On the cellular and network bases of epileptic seizures. Annu. Rev. Physiol 63:815-846

McLennan NF, Brennan PM, McNeill A, Davies I, Fotheringham A, Rennison KA, Ritchie D, Brannan F, Head MW, Ironside JW, Williams A, Bell JE (2004) Prion protein accumulation and neuroprotection in hypoxic brain damage. Am. J. Pathol 165:227-235

Mei L, Xiong W (2008) Neuregulin 1 in neural development, synaptic plasticity and schizophrenia. Nat. Rev. Neurosci 9:437-452

Meyer G, Soria JM, Martínez-Galán JR, Martín-Clemente B, Fairén A (1998) Different origins and developmental histories of transient neurons in the marginal zone of the fetal and neonatal rat cortex. J. Comp. Neurol 397:493-518

Michailov GV, Sereda MW, Brinkmann BG, Fischer TM, Haug B, Birchmeier C, Role L, Lai C, Schwab MH, Nave K (2004) Axonal neuregulin-1 regulates myelin sheath thickness. Science 304:700-703

Mironov A, Latawiec D, Wille H, Bouzamondo-Bernstein E, Legname G, Williamson RA, Burton D, DeArmond SJ, Prusiner SB, Peters PJ (2003) Cytosolic prion protein in neurons. J. Neurosci 23:7183-7193

Mobley WC, Neve RL, Prusiner SB, McKinley MP (1988) Nerve growth factor increases mRNA levels for the prion protein and the beta-amyloid protein precursor in developing hamster brain. Proc. Natl. Acad. Sci. U.S.A 85:9811-9815

Montagna P, Gambetti P, Cortelli P, Lugaresi E (2003) Familial and sporadic fatal insomnia. Lancet Neurol 2:167-176

Montero JC, Rodríguez-Barrueco R, Yuste L, Juanes PP, Borges J, Esparís-Ogando A, Pandiella A (2007) The extracellular linker of pro-neuregulin-alpha2c is required for efficient sorting and juxtacrine function. Mol. Biol. Cell 18:380-393

Moore DJ, Dawson VL, Dawson TM (2003) Role for the ubiquitin-proteasome system in Parkinson's disease and other neurodegenerative brain amyloidoses. Neuromolecular Med 4:95-108

Moore RC et al. (1999) Ataxia in prion protein (PrP)-deficient mice is associated with upregulation of the novel PrP-like protein doppel. J. Mol. Biol 292:797-817

Moore RC, Mastrangelo P, Bouzamondo E, Heinrich C, Legname G, Prusiner SB, Hood L, Westaway D, DeArmond SJ, Tremblay P (2001) Doppel-induced cerebellar degeneration in transgenic mice. Proc. Natl. Acad. Sci. U.S.A 98:15288-15293

Mouillet-Richard S, Ermonval M, Chebassier C, Laplanche JL, Lehmann S, Launay JM, Kellermann O (2000) Signal transduction through prion protein. Science 289:1925-1928

Mount C, Downton C (2006) Alzheimer disease: progress or profit? Nat. Med 12:780-784

Moya KL, Salès N, Hässig R, Créminon C, Grassi J, Di Giamberardino L (2000a) Immunolocalization of the cellular prion protein in normal brain. Microsc. Res. Tech 50:58-65

Moya KL, Salès N, Hässig R, Créminon C, Grassi J, Di Giamberardino L (2000b) Immunolocalization of the cellular prion protein in normal brain. Microsc. Res. Tech 50:58-65

Moya KL, Hässig R, Créminon C, Laffont I, Di Giamberardino L (2004) Enhanced detection and retrograde axonal transport of PrPc in peripheral nerve. J. Neurochem 88:155-160

Mukherjee S, Maxfield FR (2000) Role of membrane organization and membrane domains in endocytic lipid trafficking. Traffic 1:203-211

Naslavsky N, Stein R, Yanai A, Friedlander G, Taraboulos A (1997) Characterization of detergent-insoluble complexes containing the cellular prion protein and its scrapie isoform. J. Biol. Chem 272:6324-6331

Nave K, Salzer JL (2006) Axonal regulation of myelination by neuregulin 1. Curr. Opin. Neurobiol 16:492-500

Nelson WJ (2008) Regulation of cell-cell adhesion by the cadherin-catenin complex. Biochem. Soc. Trans 36:149-155

Newbern J, Birchmeier C (2010) Nrg1/ErbB signaling networks in Schwann cell development and myelination. Semin Cell Dev Biol Available at: http://www.ncbi.nlm.nih.gov/pubmed/20832498 [Consultato Ottobre 25, 2010].

Nishida N, Tremblay P, Sugimoto T, Shigematsu K, Shirabe S, Petromilli C, Erpel SP, Nakaoke R, Atarashi R, Houtani T, Torchia M, Sakaguchi S, DeArmond SJ, Prusiner SB, Katamine S (1999) A mouse prion protein transgene rescues mice deficient for the prion protein gene from purkinje cell degeneration and demyelination. Lab. Invest 79:689-697

Oesch B, Westaway D, Wälchli M, McKinley MP, Kent SB, Aebersold R, Barry RA, Tempst P, Teplow DB, Hood LE (1985) A cellular gene encodes scrapie PrP 27-30 protein. Cell 40:735-746

Oliveira-Martins JB, Yusa S, Calella AM, Bridel C, Baumann F, Dametto P, Aguzzi A (2010) Unexpected tolerance of alpha-cleavage of the prion protein to sequence variations. PLoS ONE 5:e9107

Olton DS, Walker JA, Gage FH (1978) Hippocampal connections and spatial discrimination. Brain Res 139:295-308

Palestini P, Botto L, Guzzi F, Calvi C, Ravasi D, Masserini M, Pitto M (2002) Developmental changes in the protein composition of sphingolipid- and cholesterol-enriched membrane domains of rat cerebellar granule cells. J. Neurosci. Res 67:729-738

Parkin ET, Watt NT, Hussain I, Eckman EA, Eckman CB, Manson JC, Baybutt HN, Turner AJ, Hooper NM (2007) Cellular prion protein regulates beta-secretase cleavage of the Alzheimer's amyloid precursor protein. Proc. Natl. Acad. Sci. U.S.A 104:11062-11067

Peretz D, Williamson RA, Kaneko K, Vergara J, Leclerc E, Schmitt-Ulms G, Mehlhorn IR, Legname G, Wormald MR, Rudd PM, Dwek RA, Burton DR, Prusiner SB (2001) Antibodies inhibit prion propagation and clear cell cultures of prion infectivity. Nature 412:739-743

Peretz D, Williamson RA, Matsunaga Y, Serban H, Pinilla C, Bastidas RB, Rozenshteyn R, James TL, Houghten RA, Cohen FE, Prusiner SB, Burton DR (1997) A conformational transition at the N terminus of the prion protein features in formation of the scrapie isoform. J. Mol. Biol 273:614-622

Peters PJ, Mironov A, Peretz D, van Donselaar E, Leclerc E, Erpel S, DeArmond SJ, Burton DR, Williamson RA, Vey M, Prusiner SB (2003) Trafficking of prion proteins through a caveolae-mediated endosomal pathway. J. Cell Biol 162:703-717

Prinetti A, Chigorno V, Prioni S, Loberto N, Marano N, Tettamanti G, Sonnino S (2001) Changes in the lipid turnover, composition, and organization, as sphingolipid-enriched membrane domains, in rat cerebellar granule cells

developing in vitro. J. Biol. Chem 276:21136-21145

Prusiner SB (1982) Novel proteinaceous infectious particles cause scrapie. Science 216:136-144

Prusiner SB (1991) Molecular biology of prion diseases. Science 252:1515-1522

Prusiner SB (1992) Natural and experimental prion diseases of humans and animals. Curr. Opin. Neurobiol 2:638-647

Prusiner SB (1994) Biology and genetics of prion diseases. Annu. Rev. Microbiol 48:655-686

Prusiner SB (2001) Shattuck lecture--neurodegenerative diseases and prions. N. Engl. J. Med 344:1516-1526

Prusiner SB, DeArmond SJ (1994) Prion diseases and neurodegeneration. Annu. Rev. Neurosci 17:311-339

Puri V, Watanabe R, Dominguez M, Sun X, Wheatley CL, Marks DL, Pagano RE (1999) Cholesterol modulates membrane traffic along the endocytic pathway in sphingolipid-storage diseases. Nat. Cell Biol 1:386-388

Race B, Meade-White K, Race R, Baumann F, Aguzzi A, Chesebro B (2009) Prion protein on astrocytes or in extracellular fluid impedes neurodegeneration induced by truncated prion protein. Exp. Neurol 217:347-352

Radovanovic I, Braun N, Giger OT, Mertz K, Miele G, Prinz M, Navarro B, Aguzzi A (2005) Truncated prion protein and Doppel are myelinotoxic in the absence of oligodendrocytic PrPC. J. Neurosci 25:4879-4888

Rangel A, Burgaya F, Gavín R, Soriano E, Aguzzi A, Del Río JA (2007) Enhanced susceptibility of Prnp-deficient mice to kainate-induced seizures, neuronal apoptosis, and death: Role of AMPA/kainate receptors. J. Neurosci. Res 85:2741-2755

Riddell DR, Christie G, Hussain I, Dingwall C (2001) Compartmentalization of beta-secretase (Asp2) into low-buoyant density, noncaveolar lipid rafts. Curr. Biol 11:1288-1293

Rieger R, Edenhofer F, Lasmézas CI, Weiss S (1997) The human 37-kDa laminin receptor precursor interacts with the prion protein in eukaryotic cells. Nat. Med 3:1383-1388

Rossi D, Cozzio A, Flechsig E, Klein MA, Rülicke T, Aguzzi A, Weissmann C (2001) Onset of ataxia and Purkinje cell loss in PrP null mice inversely correlated with Dpl level in brain. EMBO J 20:694-702

Rossner S, Apelt J, Schliebs R, Perez-Polo JR, Bigl V (2001) Neuronal and glial beta-secretase (BACE) protein expression in transgenic Tg2576 mice with amyloid plaque pathology. J. Neurosci. Res 64:437-446

Sakaguchi S, Katamine S, Nishida N, Moriuchi R, Shigematsu K, Sugimoto T, Nakatani A, Kataoka Y, Houtani T, Shirabe S, Okada H, Hasegawa S, Miyamoto T, Noda T (1996) Loss of cerebellar Purkinje cells in aged mice homozygous for a disrupted PrP gene. Nature 380:528-531

Salès N, Hässig R, Rodolfo K, Di Giamberardino L, Traiffort E, Ruat M, Frétier P, Moya KL (2002) Developmental expression of the cellular prion protein in elongating axons. Eur. J. Neurosci 15:1163-1177

Sanchez-Alavez M, Criado JR, Klein I, Moroncini G, Conti B (2008) Hypothalamic-pituitary-adrenal axis disregulation in PrPC-null mice. Neuroreport 19:1473-1477

Sánchez-Alavez M, Conti B, Moroncini G, Criado JR (2007) Contributions of neuronal prion protein on sleep recovery and stress response following sleep deprivation. Brain Res 1158:71-80

Sankaranarayanan S, Price EA, Wu G, Crouthamel M, Shi X, Tugusheva K, Tyler KX, Kahana J, Ellis J, Jin L, Steele T, Stachel S, Coburn C, Simon AJ (2008) In vivo beta-secretase 1 inhibition leads to brain Abeta lowering and increased alpha-secretase processing of amyloid precursor protein without effect on neuregulin-1. J. Pharmacol. Exp. Ther 324:957-969

Santuccione A, Sytnyk V, Leshchyns'ka I, Schachner M (2005) Prion protein recruits its neuronal receptor NCAM to lipid rafts to activate p59fyn and to enhance neurite outgrowth. J. Cell Biol 169:341-354

Saper CB (2006) Staying awake for dinner: hypothalamic integration of sleep, feeding, and circadian rhythms. Prog. Brain Res 153:243-252

Sarnataro D, Campana V, Paladino S, Stornaiuolo M, Nitsch L, Zurzolo C (2004) PrP(C) association with lipid rafts in the early secretory pathway stabilizes its cellular conformation. Mol. Biol. Cell 15:4031-4042

Schmitt-Ulms G, Legname G, Baldwin MA, Ball HL, Bradon N, Bosque PJ, Crossin KL, Edelman GM, DeArmond SJ, Cohen FE, Prusiner SB (2001) Binding of neural cell adhesion molecules (N-CAMs) to the cellular prion protein. J. Mol. Biol 314:1209-1225

Schwartz TH, Rabinowitz D, Unni V, Kumar VS, Smetters DK, Tsiola A, Yuste R (1998) Networks of coactive neurons in developing layer 1. Neuron 20:541-552

Schwarze-Eicker K, Keyvani K, Görtz N, Westaway D, Sachser N, Paulus W (2005) Prion protein (PrPc) promotes beta-amyloid plaque formation. Neurobiol. Aging 26:1177-1182

Selkoe DJ (2008) Soluble oligomers of the amyloid beta-protein impair synaptic plasticity and behavior. Behav. Brain Res 192:106-113

Shmerling D, Hegyi I, Fischer M, Blättler T, Brandner S, Götz J, Rülicke T, Flechsig E, Cozzio A, von Mering C, Hangartner C, Aguzzi A, Weissmann C (1998) Expression of amino-terminally truncated PrP in the mouse leading to ataxia and specific cerebellar lesions. Cell 93:203-214

Shyng SL, Heuser JE, Harris DA (1994) A glycolipid-anchored prion protein is endocytosed via clathrin-coated pits. J. Cell Biol 125:1239-1250

Si J, Luo Z, Mei L (1996) Induction of acetylcholine receptor gene expression by ARIA requires activation of mitogen-activated protein kinase. J. Biol. Chem 271:19752-19759

Simons K, Toomre D (2000) Lipid rafts and signal transduction. Nat. Rev. Mol. Cell Biol 1:31-39

Smyth GK (2004) Linear models and empirical bayes methods for assessing differential expression in microarray experiments. Stat Appl Genet Mol Biol 3:Article3

Soto C, Satani N (2010) The intricate mechanisms of neurodegeneration in prion diseases. Trends Mol Med Available at: http://www.ncbi.nlm.nih.gov/pubmed/20889378 [Consultato Ottobre 25, 2010].

Spilman P, Lessard P, Sattavat M, Bush C, Tousseyn T, Huang EJ, Giles K, Golde T, Das P, Fauq A, Prusiner SB, Dearmond SJ (2008) A gamma-secretase inhibitor and quinacrine reduce prions and prevent dendritic degeneration in murine brains. Proc. Natl. Acad. Sci. U.S.A 105:10595-10600

Stahl N, Borchelt DR, Hsiao K, Prusiner SB (1987) Scrapie prion protein contains a phosphatidylinositol glycolipid. Cell 51:229-240

Steele AD, Emsley JG, Ozdinler PH, Lindquist S, Macklis JD (2006) Prion protein (PrPc) positively regulates neural precursor proliferation during developmental and adult mammalian neurogenesis. Proc. Natl. Acad. Sci. U.S.A 103:3416-3421

Steele AD, Lindquist S, Aguzzi A (2007) The prion protein knockout mouse: a phenotype under challenge. Prion 1:83-93

Steinacker P, Hawlik A, Lehnert S, Jahn O, Meier S, Görz E, Braunstein KE, Krzovska M, Schwalenstöcker B, Jesse S, Pröpper C, Böckers T, Ludolph A, Otto M (2010) Neuroprotective function of cellular prion protein in a mouse model of amyotrophic lateral sclerosis. Am. J. Pathol 176:1409-1420

Stöckel J, Safar J, Wallace AC, Cohen FE, Prusiner SB (1998) Prion protein selectively binds copper(II) ions. Biochemistry 37:7185-7193

Sunyach C, Cisse MA, da Costa CA, Vincent B, Checler F (2007) The C-terminal products of cellular prion protein processing, C1 and C2, exert distinct influence on p53-dependent staurosporine-induced caspase-3 activation. J.

Biol. Chem 282:1956-1963

Talora C, Campese AF, Bellavia D, Felli MP, Vacca A, Gulino A, Screpanti I (2008) Notch signaling and diseases: an evolutionary journey from a simple beginning to complex outcomes. Biochim. Biophys. Acta 1782:489-497

Tansey MG, Chu GC, Merlie JP (1996) ARIA/HRG regulates AChR epsilon subunit gene expression at the neuromuscular synapse via activation of phosphatidylinositol 3-kinase and Ras/MAPK pathway. J. Cell Biol 134:465-476

Taraboulos A, Scott M, Semenov A, Avrahami D, Laszlo L, Prusiner SB, Avraham D (1995) Cholesterol depletion and modification of COOH-terminal targeting sequence of the prion protein inhibit formation of the scrapie isoform. J. Cell Biol 129:121-132

Taveggia C, Zanazzi G, Petrylak A, Yano H, Rosenbluth J, Einheber S, Xu X, Esper RM, Loeb JA, Shrager P, Chao MV, Falls DL, Role L, Salzer JL (2005) Neuregulin-1 type III determines the ensheathment fate of axons. Neuron 47:681-694

Taylor DR, Hooper NM (2006) The prion protein and lipid rafts. Mol. Membr. Biol 23:89-99

Taylor DR, Watt NT, Perera WSS, Hooper NM (2005) Assigning functions to distinct regions of the N-terminus of the prion protein that are involved in its copper-stimulated, clathrin-dependent endocytosis. J. Cell. Sci 118:5141-5153

Thinakaran G, Teplow DB, Siman R, Greenberg B, Sisodia SS (1996) Metabolism of the "Swedish" amyloid precursor protein variant in neuro2a (N2a) cells. Evidence that cleavage at the "beta-secretase" site occurs in the golgi apparatus. J. Biol. Chem 271:9390-9397

Tobler I, Gaus SE, Deboer T, Achermann P, Fischer M, Rülicke T, Moser M, Oesch B, McBride PA, Manson JC (1996) Altered circadian activity rhythms and sleep in mice devoid of prion protein. Nature 380:639-642

Tomita S, Kirino Y, Suzuki T (1998) Cleavage of Alzheimer's amyloid precursor protein (APP) by secretases occurs after O-glycosylation of APP in the protein secretory pathway. Identification of intracellular compartments in which APP cleavage occurs without using toxic agents that interfere with protein metabolism. J. Biol. Chem 273:6277-6284

Toni M, Spisni E, Griffoni C, Santi S, Riccio M, Lenaz P, Tomasi V (2006) Cellular prion protein and caveolin-1 interaction in a neuronal cell line precedes Fyn/Erk 1/2 signal transduction. J. Biomed. Biotechnol 2006:69469

Tramontin AD, García-Verdugo JM, Lim DA, Alvarez-Buylla A (2003) Postnatal development of radial glia and the ventricular zone (VZ): a continuum of the neural stem cell compartment. Cereb. Cortex 13:580-587

Tremblay P, Bouzamondo-Bernstein E, Heinrich C, Prusiner SB, DeArmond SJ (2007) Developmental expression of PrP in the post-implantation embryo. Brain Res 1139:60-67

Tsutsui S, Hahn JN, Johnson TA, Ali Z, Jirik FR (2008) Absence of the cellular prion protein exacerbates and prolongs neuroinflammation in experimental autoimmune encephalomyelitis. Am. J. Pathol 173:1029-1041

Ulrich-Lai YM, Herman JP (2009) Neural regulation of endocrine and autonomic stress responses. Nat. Rev. Neurosci 10:397-409

Umemori H, Sato S, Yagi T, Aizawa S, Yamamoto T (1994) Initial events of myelination involve Fyn tyrosine kinase signalling. Nature 367:572-576

Upadhya SC, Hegde AN (2007) Role of the ubiquitin proteasome system in Alzheimer's disease. BMC Biochem 8 Suppl 1:S12

Valjakka A, Vartiainen J, Tuomisto L, Tuomisto JT, Olkkonen H, Airaksinen MM (1998) The fasciculus retroflexus controls the integrity of REM sleep by supporting the generation of hippocampal theta rhythm and rapid eye movements in rats. Brain Res. Bull 47:171-184

Vassar R (2004) BACE1: the beta-secretase enzyme in Alzheimer's disease. J. Mol. Neurosci 23:105-114

Vey M, Pilkuhn S, Wille H, Nixon R, DeArmond SJ, Smart EJ, Anderson RG, Taraboulos A, Prusiner SB (1996) Subcellular colocalization of the cellular and scrapie prion proteins in caveolae-like membranous domains. Proc. Natl. Acad. Sci. U.S.A 93:14945-14949

Vincent B, Sunyach C, Orzechowski H, St George-Hyslop P, Checler F (2009) p53-Dependent transcriptional control of cellular prion by presenilins. J. Neurosci 29:6752-6760

Voigtländer T, Klöppel S, Birner P, Jarius C, Flicker H, Verghese-Nikolakaki S, Sklaviadis T, Guentchev M, Budka H (2001) Marked increase of neuronal prion protein immunoreactivity in Alzheimer's disease and human prion diseases. Acta Neuropathol 101:417-423

Voigtländer T, Unterberger U, Touma C, Palme R, Polster B, Strohschneider M, Dorner S, Budka H (2006) Prominent corticosteroid disturbance in experimental prion disease. Eur. J. Neurosci 23:2723-2730

Walker DL, Toufexis DJ, Davis M (2003) Role of the bed nucleus of the stria terminalis versus the amygdala in fear, stress, and anxiety. Eur. J. Pharmacol 463:199-216

Walsh DM, Klyubin I, Fadeeva JV, Cullen WK, Anwyl R, Wolfe MS, Rowan MJ, Selkoe DJ (2002) Naturally secreted oligomers of amyloid beta protein potently inhibit hippocampal long-term potentiation in vivo. Nature 416:535-539

Walter ED, Stevens DJ, Visconte MP, Millhauser GL (2007) The prion protein is a combined zinc and copper binding protein: Zn2+ alters the distribution of Cu2+ coordination modes. J. Am. Chem. Soc 129:15440-15441

Walz R, Amaral OB, Rockenbach IC, Roesler R, Izquierdo I, Cavalheiro EA, Martins VR, Brentani RR (1999) Increased sensitivity to seizures in mice lacking cellular prion protein. Epilepsia 40:1679-1682

Watt NT, Hooper NM (2005) Reactive oxygen species (ROS)-mediated beta-cleavage of the prion protein in the mechanism of the cellular response to oxidative stress. Biochem. Soc. Trans 33:1123-1125

Whatley BR, Li L, Chin L (2008) The ubiquitin-proteasome system in spongiform degenerative disorders. Biochim. Biophys. Acta 1782:700-712

White AR, Collins SJ, Maher F, Jobling MF, Stewart LR, Thyer JM, Beyreuther K, Masters CL, Cappai R (1999) Prion protein-deficient neurons reveal lower glutathione reductase activity and increased susceptibility to hydrogen peroxide toxicity. Am. J. Pathol 155:1723-1730

White MD, Farmer M, Mirabile I, Brandner S, Collinge J, Mallucci GR (2008) Single treatment with RNAi against prion protein rescues early neuronal dysfunction and prolongs survival in mice with prion disease. Proc. Natl. Acad. Sci. U.S.A 105:10238-10243

Willem M, Garratt AN, Novak B, Citron M, Kaufmann S, Rittger A, DeStrooper B, Saftig P, Birchmeier C, Haass C (2006) Control of peripheral nerve myelination by the beta-secretase BACE1. Science 314:664-666

Williamson RA, Peretz D, Pinilla C, Ball H, Bastidas RB, Rozenshteyn R, Houghten RA, Prusiner SB, Burton DR (1998) Mapping the prion protein using recombinant antibodies. J. Virol 72:9413-9418

Wong BS, Liu T, Li R, Pan T, Petersen RB, Smith MA, Gambetti P, Perry G, Manson JC, Brown DR, Sy MS (2001) Increased levels of oxidative stress markers detected in the brains of mice devoid of prion protein. J. Neurochem 76:565-572

Yokozeki T, Wakatsuki S, Hatsuzawa K, Black RA, Wada I, Sehara-Fujisawa A (2007) Meltrin beta (ADAM19) mediates ectodomain shedding of Neuregulin beta1 in the Golgi apparatus: fluorescence correlation spectroscopic observation of the dynamics of ectodomain shedding in living cells. Genes Cells 12:329-343

Yu Y, Run X, Liang Z, Li Y, Liu F, Liu Y, Iqbal K, Grundke-Iqbal I, Gong C (2009) Developmental regulation of tau phosphorylation, tau kinases, and tau phosphatases. J. Neurochem 108:1480-1494

Zahn R, Liu A, Lührs T, Riek R, von Schroetter C, López García F, Billeter M, Calzolai L, Wider G, Wüthrich K (2000) NMR solution structure of the human prion protein. Proc. Natl. Acad. Sci. U.S.A 97:145-150

Zhang D, Sliwkowski MX, Mark M, Frantz G, Akita R, Sun Y, Hillan K, Crowley C, Brush J, Godowski PJ (1997) Neuregulin-3 (NRG3): a novel neural tissue-enriched protein that binds and activates ErbB4. Proc. Natl. Acad. Sci. U.S.A 94:9562-9567